

**PER- AND POLYFLUOROALKYL SUBSTANCES IN THE ROYAL CANADIAN NAVY**  
**LES SUBSTANCES PER- ET POLYFLUOROALKYLIQUES DANS LA MARINE ROYALE**  
**CANADIENNE**

A Thesis Submitted to the Division of Graduate Studies  
of the Royal Military College of Canada  
by

Linda Marlene Hodgkins, CD  
Lieutenant-Commander

In Partial Fulfillment of the Requirements for the Degree of  
Masters of Applied Science

16 April, 2018

©This thesis may be used within the Department of National Defence but  
copyright for open publication remains the property of the author.

## **Acknowledgements**

I would like to thank my supervisor, Dr. Kela Weber, for providing a learning and working environment where all ideas, no matter how good or bad, were considered, and mistakes were seen as part of the learning process. Your patience and positive outlook made returning to University, fifteen years after earning my undergraduate degree, a little less scary.

I would like to thank Dr. Iris Koch for her thorough review and excellent feedback on my seminar paper, which eventually morphed into Chapter 1 of my thesis.

I am especially thankful to my former shipmates, PO1 (ret'd) Gilles Labrie, CPO2 Tom Gallant and CPO2 Ian McNaughton who either provided me with the information on AFFF onboard ships in the RCN, or pointed me toward the right people to get the information that I required.

I am sincerely thankful to Dr. Ryan Mulligan from Queen's University who kindly offered to work with me for the hydrodynamic modelling study of PFAS transport in Halifax Harbour. Your time and dedication toward teaching me how to use the Delft3D suite of software, and assisting me in formulating the contents of Chapter 3 of my thesis are extremely appreciated.

I would like to thank Dr. Mike Hulley, who taught me how to develop and solve a numerical model in Excel, which eventually became the content of Chapter 4 of my thesis.

Lastly, I would like to acknowledge the amazing support of my husband, Ben, and my children, Benjamin and Nina, who not only took on extra domestic chores to compensate for my being away, but made several other sacrifices in order to allow me the opportunity to fulfill my goal of earning a post graduate degree.

## Abstract

Per- and polyfluoroalkyl substances (PFAS) are essential ingredients used in aqueous film forming foam (AFFF), but are also global environmental contaminants that are ubiquitous in water, soil, sediment, wildlife and humans around the world. For the Royal Canadian Navy (RCN), AFFF is an essential firefighting medium used onboard its warships and submarines to protect areas vulnerable to Class B fires. Effects of AFFF use at land based military installations have been studied and are well documented, but little is known about the consequences of AFFF use at sea. Herein, an investigation was made to identify where PFAS exists in the RCN, with an emphasis on AFFF, what the fate of PFAS from AFFF would be if used AFFF was allowed to wash overboard at sea, and potential methods to reduce or eliminate PFAS from used AFFF entering the environment from RCN use.

The quantities and types of AFFF in the RCN, along with historical usage quantities were determined. Currently, the RCN uses both 6% and 3% AFFF formulas manufactured by Ansul, meeting the US military specification (MIL-F-24385F). These formulations can contain up to 8 kg of PFAS per m<sup>3</sup> of AFFF. In total, RCN vessels carry in excess of 90 m<sup>3</sup> of AFFF. In ten years of fire reports, 1 in 62 fires employed the fitted AFFF system onboard to extinguish the fire. While the RCN does not track quantities of AFFF used or sent overboard, reports from an engine room fire in the early 2000s indicate that AFFF was released overboard. Based on the gathered information, it can be concluded that there is a reasonable chance that RCN use of AFFF at sea could be contributing to the PFAS burden in the environment.

To assess the fate and transport of PFAS from AFFF washed overboard at sea, a hydrodynamic model was used to predict the transport of PFAS released into Halifax Harbour, Nova Scotia for different release locations and differing wind and wave conditions. PFAS transport was simulated as a conservative tracer. Model results indicate that PFAS released in the presence of strong wind and waves will travel farther than PFAS released during a period with little wind and no waves (17.7 – 31.1 km and 15.6 – 21.9 km respectively). After 10 days of simulation, PFAS levels from release sites further into the Harbour remained the most elevated (40,000 – 60,000 pg/L), while PFAS levels from the Outer Harbour release site had decreased to 800 pg/L for a period with little wind and no waves. Regardless of the PFAS release site, after 12 hours, shorelines within the Harbour were affected by PFAS with concentrations ranging from 40,000 to 500,000 pg/L. The methods described here could be applied to PFAS transport in other coastal areas, and the results could be used to shape policies and best practices with respect to AFFF use at sea.

Based on the successful use of granular activated carbon (GAC) to remove PFAS from groundwater, a numerical model was developed to simulate PFAS adsorption to GAC in order to determine the amount of GAC that would be required to remediate PFAS from used AFFF and to investigate the feasibility of its use onboard an RCN vessel. The model considered both bulk flow and hydrodynamic dispersion in one dimension, and adsorption of PFAS to GAC was represented using a retardation factor. The model was calibrated and validated using data from a full scale setup whose purpose was to remove PFAS from groundwater. Validation of the model suggested that the output for PFAS concentration in the effluent was not reliable (Nash-Sutcliffe Efficiency (NSE) of -1.92); however, the quantity of PFAS adsorbed per mass unit of GAC

was more dependable (NSE of 0.31). Adding a safety factor of 3, the model predicts that 795 kg of GAC is required to remove all PFAS from 3.6 m<sup>3</sup> of AFFF. Although this represents a reasonable mass of GAC for use onboard a ship, the feasibility of this method for remediation of PFAS from used AFFF in the RCN could not be determined with any certainty due to model uncertainty. Further work to refine the model is recommended.

## Résumé

Les substances perfluoroalkyliques et polyfluoroalkyliques (SPFA) sont des ingrédients essentiels utilisés dans la fabrication de mousses à formation de pellicules aqueuses (MFPA), mais elles sont également des contaminants environnementaux globaux omniprésents dans l'eau, le sol, les sédiments, la faune et les humains du monde entier. Pour la Marine royale du Canada (MRC), la MFPA est un moyen essentiel de lutte contre les incendies et est utilisée à bord de ses navires de guerre et des sous-marins pour protéger les zones vulnérables aux feux de classe B. Les effets de la MFPA sur les installations militaires terrestres ont été étudiés et sont bien documentés, mais on en sait peu sur les conséquences de l'utilisation de la MFPA en mer. Cette étude a été faite pour localiser les SPFA au travers de la MRC, mettant une emphase particulière sur les SPFA contenus dans la MFPA s'ils sont utilisés en mer, et les méthodes potentielles pour réduire ou éliminer SPFA provenant des MFPA usagées produit par la MRC.

Les quantités et les types de la MFPA dans la MRC, ainsi que les quantités d'utilisation historiques ont été déterminés. Actuellement, la MRC utilise à la fois MFPA à 6% et 3% fabriqué par Ansul et conforme à la spécification militaire américaine (MIL-F-24385F). Ces formulations peuvent contenir jusqu'à 8 kg de SPFA par m<sup>3</sup> de la MFPA. Au total, les navires de la MRC transportent plus de 90 m<sup>3</sup> de la MFPA. Au cours de dix années de rapports sur les incendies, un incendie sur 62 a utilisé le système de la MFPA installé à bord pour éteindre l'incendie. Bien que la MRC ne surveille pas les quantités de la MFPA utilisées ou envoyées à la mer, les rapports d'un incendie dans la salle des machines au début des années 2000 indiquent que la MFPA a été rejetée à la mer. D'après les renseignements recueillis, on peut conclure qu'il y a une chance raisonnable que l'utilisation de la MFPA en mer par la MRC contribue aux SPFA dans l'environnement.

Un modèle hydrodynamique a été utilisé pour prédire le transport de SPFA libéré dans le port d'Halifax, en Nouvelle-Écosse, pour les différents sites de rejet ainsi que différentes conditions de vent et de vagues. Le transport de SPFA a été simulé comme un traceur conservateur. Les résultats du modèle indiquent que les SPFA libérés en présence de vents forts et de vagues se disperseront plus loin que les rejets de SPFA pendant une période où il y a peu de vent et pas de vagues (respectivement 17,7 - 31,1 km et 15,6 - 21,9 km). Au bout de 10 jours de simulation, les niveaux SPFA des sites de rejet situés les plus près du Bassin de Bedford sont restés le plus élevé (40 000 - 60 000 pg / L), tandis que les niveaux SPFA des sites de rejet à l'extérieur du Bassin de Bedford avaient diminué à 800 pg / L pour une période avec peu de vent et pas de vagues. Quel que soit le site de rejet du SPFA, après 12 heures, les rivages dans le port ont été affectés par le SPFA avec des concentrations allant de 40 000 à 500 000 pg / L. Les méthodes décrites ici pourraient être appliquées au transport de SPFA dans d'autres zones côtières, et les résultats pourraient être utilisés pour façonner les politiques ainsi que de meilleures pratiques en ce qui concerne l'utilisation de la MFPA en mer.

Basé sur l'utilisation réussie du charbon actif granulaire (CAG) pour retirer les SPFA des eaux souterraines, un modèle numérique a été développé pour simuler l'adsorption des SPFA au CAG afin de déterminer la quantité de CAG nécessaire pour traiter les SPFA des MFPA usagées et enquêter sur la faisabilité de son utilisation à bord d'un navire de la MRC. Le modèle a pris en compte à la fois le flux massique et la dispersion hydrodynamique dans une dimension, et

l'adsorption de SPFA sur CAG a été représentée en utilisant un facteur de retardement. Le modèle a été calibré et validé à l'aide de données provenant d'une installation à grande échelle dont le but était d'enlever les SPFA des eaux souterraines. La validation du modèle a suggéré que la concentration de SPFA dans l'effluent n'était pas fiable (l'efficacité de Nash-Sutcliffe (NSE) était de -1,92); cependant, la quantité de SPFA adsorbée par unité de masse de CAG était plus fiable (NSE était de 0,31). En ajoutant un facteur de sécurité de 3, le modèle prédit que 795 kg de CAG est nécessaire pour enlever tous les SPFA de 3,6 m<sup>3</sup> de la MFPA. Bien que cela représente une masse raisonnable de CAG à utiliser à bord d'un navire, la faisabilité de cette méthode pour le traitement des SPFA des MFPA usagés de la MRC n'a pu être déterminée avec précision en raison de l'incertitude du modèle. Plus de recherches scientifiques seront nécessaire pour affiner les modèles.

# Table of Contents

<b>ACKNOWLEDGEMENTS</b> .....	<b>I</b>
<b>ABSTRACT</b> .....	<b>II</b>
<b>RÉSUMÉ</b> .....	<b>IV</b>
<b>TABLE OF CONTENTS</b> .....	<b>VI</b>
<b>LIST OF TABLES</b> .....	<b>VIII</b>
<b>LIST OF FIGURES</b> .....	<b>IX</b>
<b>LIST OF SYMBOLS</b> .....	<b>XII</b>
<b>LIST OF ABBREVIATIONS AND ACRONYMS</b> .....	<b>XIV</b>
<b>CHAPTER 1 INTRODUCTION PER-AND POLYFLUOROALKYL SUBSTANCES</b> .....	<b>1</b>
1.1 BACKGROUND .....	1
1.1.1 Definitions.....	1
1.1.2 Properties .....	2
1.1.3 Synthesis.....	4
1.1.4 Types and Uses .....	5
1.1.5 Issues Related to PFAS Use .....	6
1.1.6 Guidelines and Regulations related to PFAS.....	8
1.1.7 Replacements for long chain PFAS .....	10
1.2 PFAS IN THE ENVIRONMENT .....	15
1.2.1 Literature Review.....	15
1.2.2 Sources and Environmental Quantification .....	17
1.2.3 Fate and Transport .....	18
1.2.4 Environmental Recovery, Remediation and Destruction of PFAS.....	19
1.3 KNOWLEDGE GAPS.....	20
1.4 OBJECTIVES OF THESIS .....	21
1.5 THESIS ORGANIZATION.....	21
<b>CHAPTER 2 PER-AND POLYFLUOROALKYL SUBSTANCES IN THE ROYAL CANADIAN NAVY</b> .....	<b>22</b>
2.1 STRUCTURE AND FUNCTIONS OF THE RCN .....	22
2.2 TYPES AND QUANTITIES OF PFAS IN ITEMS USED BY THE RCN .....	22
2.3 PFAS IN AFFF .....	23
2.4 PFAS IN THE ENVIRONMENT AS A RESULT OF AFFF USAGE .....	40
2.5 FLUORINE FREE FOAM (FFF) AS AN ALTERNATIVE TO AFFF.....	46
2.6 SUMMARY AND CONCLUSIONS.....	47
<b>CHAPTER 3 HYDRODYNAMIC MODELLING OF PFAS FATE AND TRANSPORT FROM AFFF IN HALIFAX HARBOUR</b> .....	<b>48</b>
3.1 INTRODUCTION .....	48
3.2 OBSERVATIONS.....	49

3.2.1 Study Area .....	49
3.2.2 Observations in the Three Study Periods .....	51
3.3 MODELLING .....	54
3.3.1 Model Description.....	54
3.3.2 Model Setup.....	55
3.3.3 Modelling Scenarios.....	57
3.4 RESULTS AND DISCUSSION .....	59
3.4.1 Model Calibration .....	59
3.4.2 Model Validation .....	61
3.4.3 PFAS Release.....	63
3.5 SUMMARY AND CONCLUSION .....	75
<b>CHAPTER 4 SIZING OF A GAC BASED PFAS ADSORPTION COLUMN FOR A RCN FRIGATE .....</b>	<b>76</b>
4.1 INTRODUCTION.....	76
4.2 METHODS .....	77
4.2.1 Model Setup.....	77
4.2.2 Governing Equations .....	80
4.2.3 Model Calibration, Sensitivity Analysis.....	82
4.2.4 Application of the Model to a Warship.....	83
4.3 RESULTS AND DISCUSSION .....	84
4.3.1 Model Calibration and Sensitivity Analysis .....	84
4.3.2 Model Validation .....	85
4.3.3 Application of Model to Shipboard Scenario .....	87
4.4 SUMMARY AND CONCLUSION .....	88
<b>CHAPTER 5 PRINCIPLE OUTCOMES AND RECOMMENDATIONS.....</b>	<b>89</b>
5.1 SUMMARY OF MAIN OBJECTIVES .....	89
5.2 PER- AND POLYFLUOROALKYL SUBSTANCES IN THE ROYAL CANADIAN NAVY .....	89
5.3 FATE AND TRANSPORT OF PFAS FROM AFFF IN HALIFAX HARBOUR .....	90
5.4 SIZING OF A GAC BASED PFAS ADSORPTION COLUMN .....	90
5.5 FUTURE RESEARCH AND RECOMMENDATIONS .....	91
REFERENCES .....	92



## List of Tables

Table 1-1: Effect of increasing fluorination on bond length and bond strength (3M 1999b).....	3
Table 1-2: Comparison of properties between a perfluoroalkane and its hydrocarbon analogue (3M 1999b). .....	3
Table 1-3: Federal Environmental Quality Guidelines (FEQGs) for PFOS prescribed by Environment and Climate Change Canada. ....	9
Table 1-4: Drinking Water Screening Values (DWSVs) for select PFAS as provided by Health Canada .....	9
Table 1-5: PFECAs currently used in industry as replacement chemicals for PFOA/APFO .....	11
Table 1-6: PFOS alternative used as mist suppressants in the hard chrome plating industry .....	12
Table 1-7: Types and uses of PFBS related chemicals that have replaced their longer chain homologues .....	14
Table 2-1: A compilation of the types and quantities of PFAS detected in different formulas of AFFF using various methods of detection and analysis. ....	26
Table 2-2: Concentrations of PFAS detected in groundwater at various US Military bases. ....	41
Table 3-1: Hydrographic and meteorological, stations, instruments and data. ....	51
Table 3-2: Nomenclature and units for the system of equations in Delft3D-FLOW. ....	55
Table 3-3: Summary of Model Runs. List of the model runs discussed in this paper, the model scenario that they covered and the model forcing mechanisms that were applied. ....	57
Table 3-4: Nomenclature and Units for Equations [9] through [14]. ....	58
Table 3-5: Sensitivity Analysis Results. A comparison of different values of horizontal eddy viscosity and Chezy coefficient for bottom friction on the modelled average current speed for simulation of YD 256 to 259 in 2014. ....	61
Table 4-1: Distribution Coefficients and Retardation Factors. ....	81
Table 4-2: Model Input Parameters Prior to Calibration .....	82
Table 4-3: Results of Sensitivity Analysis. The values for E and R that are bold were used in the calibrated model. ....	85
Table 4-4: Parameters input into the model for the shipboard application.....	87

## List of Figures

Figure 1-1: PFAS classification hierarchy. An example of the classification hierarchy of per-and polyfluoroalkyl substance adapted from Buck et al. (2011). .....	2
Figure 1-2: Number of peer reviewed PFAS articles published by year. The number of peer reviewed journal articles published by year as determined using the search engines Engineering Village and Web of Science, and the key words AFFF, PFAS, per-and polyfluoroalkyl substances, perfluoroalkyl substance, polyfluoroalkyl substance, perfluorinated compound, and polyfluorinated compound .....	15
Figure 1-3: Types of PFAS studied by year. The types of PFAS researched by year are shown for short chain (C2 – C5) PFCAs and PFSAs (blue), long chain (C6 – C12) PFCAs and PFSAs (red), C13 and greater PFCAs and PFSAs (green), fluorotelomers (purple), sulfonamides (light blue) and others (orange), which include all other types of PFAS that do not fit the other categories provided. ....	16
Figure 1-4: Focus of PFAS research by year. PFAS articles were grouped and quantified according to their focus being either PFAS Environmental Identification/Quantification (red), PFAS Fate/Transport (green), Remediation of PFAS (purple), Other, which includes development of analytical methods, synthesis, determination of chemical and/or physical properties, toxicity studies and pharmacokinetic studies (light blue), and PFAS Review Papers (blue). .....	17
Figure 1-5: Random adsorption compared to mixed hemimicelle formation. In random adsorption (a), molecules of PFAS (black tail and red head group) will individually adsorb to soil wherever a free adsorption site exists, whereas in mixed hemimicelle formation (b), molecules of PFAS will adsorb to soil combined with molecules of non-fluorinated surfactants (grey tail and blue head group). .....	19
Figure 2-1: The purpose of PFAS in AFFF. PFAS in AFFF orients itself so that the hydrophobic tails are away from the water and the hydrophilic heads orient into the water where their slight charge causes them to repel each other, which causes the foam to unfold and spread over the fire. Adapted from Dlugogorski <i>et al.</i> (2002). .....	24
Figure 2-2: Biotransformation products of PFAS from AFFF in soil microcosms. The biotransformation products of 6:2 FtTAoS found in AFFF manufactured by Ansul are shown in a), as adapted from Harding-Marjanovic <i>et al.</i> (2015). The dashed red arrows represent the proposed transformation path. The biotransformation products of PFOAaMS and PFOSAaMS are shown in b) and c) as adapted by Mejia-Avendano <i>et al.</i> (2016). .....	44
Figure 3-1: Location and Layout of Halifax Harbour. Halifax Harbour is located on the southeast coast of Nova Scotia as shown on the inset (b). The layout, bathymetry, location of instruments whose data was used to either force or validate the model (black circles) and the five PFAS release locations used in the model simulation (black squares) are shown in (a). .....	50
Figure 3-2: Data for Modelling Scenarios. Data from Scenario A (a through e) in September 2014 was used to calibrate the model, while data from Scenario B (f through j) in July 2013 and Scenario C (k through o) in March 2014 were used to validate the model. The year days between the black vertical lines were modelled for each of the three scenarios. ....	53
Figure 3-3: Model Calibration Results. Comparison of observed data with model results for tide only forcing (R01), tide + wind forcing (R02), and tide + wind + wave forcing (R03) for a) water level, b) near surface current magnitude, c) significant wave height and d) peak wave period. ....	60

**Figure 3-4: Model Calibration Results for Current Magnitude at all Depths. Comparison of modelled current magnitude,  $|u|$ , in all depth layers for a) tide only forcing, b) tide + wind forcing and c) tide + wind + wave forcing with d) the observed data. .... 60**

**Figure 3-5: Model Validation Results for Scenario B. Modelled versus observed results for a) water level,  $\eta$ , b) near surface current magnitude,  $|u|$ , as well as c) the depth profile of the modelled current magnitude and d) the depth profile of the observed current magnitude. .... 62**

**Figure 3-6: Model Validation Results for Scenario C. Modelled versus observed results for a) water level,  $\eta$ , b) significant wave height,  $H_s$ , c) peak wave period,  $T_p$ , and d) near surface current magnitude,  $|u|$ , as well as the depth profile of e) modelled current magnitude and f) observed current magnitude. .... 63**

**Figure 3-7: Map of Near Surface Current Magnitude. The near surface current magnitude is shown for modelling scenarios B (left) and C (right) at 12 hours following the release of PFAS, which corresponds to YD 191 at 12:00 hrs for Scenario B and YD 85 at 12:00 hrs for Scenario C. .... 64**

**Figure 3-8: PFAS transport in the Near Surface for Release Site 2. Shown is a comparison of PFAS transport from release location 2 at 1 hr, 12 hrs and 47 hrs following the release of PFAS at time,  $T_R$ , for scenarios B and C. The PFAS release location is identified by a black circle, and a magenta contour line has been drawn at 1 pg/L. Note the change in scales between subplots. .... 65**

**Figure 3-9: PFAS transport in the Near Surface for Release Site 3. Shown is a comparison of PFAS transport from release location 3 at 1 hr, 12 hrs and 47 hrs following the release of PFAS at time,  $T_R$ , for scenarios B and C. The PFAS release location is identified by a black circle, and a magenta contour line has been drawn at 1 pg/L. Note the change in scales between subplots. .... 66**

**Figure 3-10: PFAS transport in the Near Surface for Release Site 4. Shown is a comparison of PFAS transport from release location 4 at 1 hr, 12 hrs and 47 hrs following the release of PFAS at time,  $T_R$ , for scenarios B and C. The PFAS release location is identified by a black circle, and a magenta contour line has been drawn at 1 pg/L. Note the change in scales between subplots. .... 67**

**Figure 3-11: PFAS transport in the Near Surface for Release Site 5. Shown is a comparison of PFAS transport from release location 5 at 1 hr, 12 hrs and 47 hrs following the release of PFAS at time,  $T_R$ , for scenarios B and C. The PFAS release location is identified by a black circle, and a magenta contour line has been drawn at 1 pg/L. Note the change in scales between subplots. .... 68**

**Figure 3-12: Comparison of PFAS Transport. A comparison of the distance of PFAS transport along a SW-NE transect at a)  $T_R + 12$  hrs and b)  $T_R + 47$  hrs for PFAS released at locations 1 through 5 in modelling Scenarios A, B and C. Release site 1 was not included at  $T_R + 47$  hrs because the results were questionable due to the loss of PFAS through the model boundary. .... 69**

**Figure 3-13: PFAS concentrations for Scenario B (left) and Scenario C (right) are provided in pg/L at 47 hours after release. The release location is given vertically on the left of each table, and the observation locations are given horizontally at the top of each table. For example, at  $T_R + 47$  hrs, the concentration of PFAS released at PFAS site 5 in Scenario C was less than 1 pg/L at PFAS sites 1 and 2, between 1 and 9 pg/L at PFAS site 3, between 1000 and 9999 pg/L at PFAS site 4 and between 10,000 and 99,999 pg/L at PFAS site 5. The diagonal line represents concentrations that are likely too low due to the PFAS leaving the model through the boundaries. .... 70**

**Figure 3-14: PFAS Transport in the Near Surface after 9.8 Days. Shown is the PFAS transport from release locations 1 through 5 at 9.8 days following the release of PFAS at time,  $T_R$ , for Scenario B.**

The PFAS release location is identified by a black circle, and a magenta contour line has been drawn at 1 pg/L. Note the change in scales between subplots. .... 71

Figure 3-15: PFAS Transport in the Near Surface for Release Site 1. Shown is a comparison of PFAS transport from release location 1 at 1 hr, 12 hrs and 47 hrs following the release of PFAS at time,  $T_R$ , for scenarios A, B and C. The PFAS release location is identified by a black circle, and a magenta contour line has been drawn at 1 pg/L. Note the change in scales between subplots. .... 74

Figure 4-1: Configuration of the GAC System used in Minnesota. The setup consisted of two basins of GAC, with the dimensions shown, in a lead-lag configures. Influent flowed into the lead basin at 1.4 to 1.5 m<sup>3</sup>/min. .... 77

Figure 4-2: Average influent concentrations of individual PFAS into the lead basin. .... 78

Figure 4-3: Observed Data Plots. Effluent concentrations of individual PFAS are shown for the calibration data (a) and validation data (b). The quantities of individual PFAS adsorbed per mass unit of GAC is shown in (c) for the calibration data and (d) for the validation data. Data obtained from Appleman *et al.* (2014). .... 79

Figure 4-4: Plot used to determine  $K_d$ . The effluent concentration of PFAS was plotted against the amount of PFAS adsorbed per kg of GAC for PFHxA, PFOA and PFOS. The partition coefficient  $K_d$  was estimated by the slope of the linear trend line..... 82

Figure 4-5: Model Results Prior to Calibration. The observed (black) and pre-calibrated modelled (red) effluent concentration,  $C_e$ , of PFAS is compared in (a) and the quantity of PFAS adsorbed per kg of GAC is compared in (b). .... 84

Figure 4-6: Calibrated Model Results. The observed (black) and calibrated modelled (red) effluent concentration,  $C_e$ , of PFAS is compared in (a) and the quantity of PFAS adsorbed per kg of GAC is compared in (b). .... 85

Figure 4-7: Validation Model Results. The observed (black) and pre-calibrated modelled (red) effluent concentration,  $C_e$ , of PFAS is compared in (a) and the quantity of PFAS adsorbed per kg of GAC is compared in (b). .... 86

Figure 4-8: Results of Applying Model to Shipboard Scenario. The modelled effluent concentration,  $C_e$ , of PFAS from 3.6 m<sup>3</sup> of AFFF (a) and the quantity of PFAS adsorbed per kg of GAC (b) are shown for an input concentration of 0.48 kg/m<sup>3</sup> ..... 88

## List of Symbols

Symbol	Definition
A	Cross-Sectional Area
c	Chezy Coefficient
C	Mass Concentration
$C_e$	Effluent Concentration
$C_i$	Influent Concentration
$C_O$	Observed Concentration
$\bar{C}_O$	Averaged Observed Concentration
$C_M$	Modelled Concentration
$C_{PFAS}$	Concentration of PFAS
$C_x, C_y, C_\sigma, C_\theta$	Propagation Velocities (subscript indicates direction)
D	Molecular Diffusion
$D_H, D_V$	Horizontal and Vertical Diffusion Coefficients
E	Dispersion Coefficient
f	Coriolis Coefficient
$F_x, F_y$	Horizontal Reynolds Stress
g	Acceleration due to Gravity
h	Water depth
$H_s$	Significant Wave Height
$K_d$	Distribution Coefficient
$M_{AFFF}$	Mass of AFFF
$M_{GAC}$	Mass of GAC
$M_{PFAS}$	Mass of PFAS
$M_x, M_y$	External Sources and Sinks of Momentum
n	Number of Data Points
N	Action Density
$P_x, P_y$	Horizontal Pressure Terms
q	Adsorption Rate
Q	Flow
R	Retardation Factor
S	Source and Sink terms
t	time
$T_p$	Peak Wave Period
$T_R$	PFAS Release Time
u, v, w	Eulerian Velocity Components/ Current Speed
$ u_{avg} $	Magnitude of the Averaged Current
$u_{dir}$	Current Direction
U, V	Generalized Lagrangian Mean Velocity Components/ Wind Speed
$\bar{U}, \bar{V}$	Depth Averaged Generalized Lagrangian Mean Velocity Components
$U_{dir}$	Wind Direction
V	Volume
$V_T$	Total Volume
$w_i$	Mass fraction
x, y, z	Cartesian Coordinates

$\alpha$	Dispersivity Constant
$\Delta t$	Time Step
$\Delta x$	Distance Step
$\zeta$	Water Surface Elevation Above Reference Datum
$\eta$	Water Level
$\theta$	Wave Direction
$\nu_H, \nu_V$	Horizontal and Vertical Kinematic Viscosity
$\rho_{AFFF}$	Density of AFFF
$\rho_{bed}$	Bed Density
$\rho_{carbon}$	Density of Carbon
$\rho_0$	Reference Density of Water
$\sigma$	Scaled Vertical Coordinates
$\tau_b$	Bed Shear Stress
$\phi$	Porosity
$\omega$	Vertical Velocity Component in a $\sigma$ Coordinate System
$^\circ$	Degrees
%	Percent
$\Sigma$	Sum of

---

## List of Abbreviations and Acronyms

Abbreviation	Definition
ADCP	Acoustic Doppler Current Profiler
AFFF	Aqueous Film Forming Foam
APFN	Ammonium Perfluorononanoate
APFO	Ammonium Perfluorooctanoate
C	Carbon
CFFM	Canadian Forces Fire Marshall
CHS	Canadian Hydrographic Service
CPF	Canadian Patrol Frigate
DCTF	Damage Control Training Facility
DWSV	Drinking Water Screening Values
ECF	Electrochemical Fluorination
ECHA	European Chemicals Agency
F	Fluorine
FAB-MS	Fast atom bombardment mass spectrometry
FEQG	Federal Environmental Quality Guidelines
FFF	Fluorine Free Foam
FT	Fluorotelomers
FTAC	Fluorotelomer Acrylate
FtB	Fluorotelomer Betaine
FTCA	Fluorotelomer Carboxylic Acid
FTI	Fluorotelomer Iodide
FTICR	Fourier Transform Ion Cyclotron Resonance
FTO	Fluorotelomer Olefin
FTOH	Fluorotelomer Alcohol
FTMAC	Fluorotelomer Methacrylate
FtS	Fluorotelomer Sulfonate
FTSA	Fluorotelomer Sulfonic Acid
FtSaAm	Fluorotelomer Sulfonamido Amine
FtSaB	Fluorotelomer Sulfonamido Betaine
FtTAoS	Fluorotelomer Thioamido Sulfonate
FtTHN	Fluorotelomer Thio Hydroxy Ammonium
GAC	Granular Activated Carbon
H	Hydrogen
HPLC	High Performance Liquid Chromatography
I	Iodine
KMD	Kendrick Mass Defect
LC	Liquid Chromatography
LOD	Limit of Detection
LVI	Large volume injection
MARLANT	Maritime Forces Atlantic
MARPAC	Maritime Forces Pacific
MCDV	Maritime Coastal Defence Vessel
MCH	Methylcyclohexane

MS	Mass Spectrometry
MWD	Mean Wave Direction
N	Nitrogen
N	North
N/A	Not Applicable
NAPL	Non-Aqueous Phase Liquids
ND	Not Detected
NE	Northeast
NEtFOSA	N-Ethyl Perfluorooctane Sulfonamide
NEtFOSAA	N-Ethyl Perfluorooctane Sulfonamidoacetate
NEtFOSE	N-Ethyl Perfluorooctane Sulfonamidoethanol
NMeFBSA	N-Methyl Perfluorobutane Sulfonamide
NMeFBSAC	N-Methyl Perfluorobutane Sulfonamidoethyl Acrylate
NMeFBSSE	N-Methyl Perfluorobutane Sulfonamidoethanol
NMeFOSA	N-Methyl Perfluorooctane Sulfonamide
NMeFOSAA	N-Methyl Perfluorooctane Sulfonamidoacetate
NMeFOSE	N-Methyl Perfluorooctane Sulfonamidoethanol
NMR	Nuclear Magnetic Resonance
NRL	Naval Research Laboratory
NSE	Nash-Sutcliffe Efficiency
NW	Northwest
O	Oxygen
PFAA	Perfluoroalkyl Acid
PFAS	Per- and Poly Fluoroalkyl Substance
PFBA	Perfluorobutanoic Acid or Perfluorobutanoate
PFBS	Perfluorobutane Sulfonic Acid or Sulfonate
PFBSaAm	Perfluorobutane Sulfonamido Amine
PFBSaAmA	Perfluorobutane Sulfonamide Amino Carboxylate
PFCA	Perfluoroalkyl Carboxylic Acid or Carboxylates
PFDA	Perfluorodecanoic Acid or Perfluorodecanoate
PFDoA	Perfluorododecanoic Acid or Perfluorododecanoate
PFDS	Perfluorodecane Sulfonic Acid or Sulfonate
PFECA	Perfluoroalkyl and Polyfluoroalkyl Ether Carboxylic Acid or Carboxylate
PFEtS	Perfluoroethane Sulfonic Acid or Sulfonate
PFHpA	Perfluoroheptanoic Acid or Perfluoroheptanoate
PFHpSaAm	Perfluoroheptane Sulfonamido Amine
PFHpSaAmA	Perfluoroheptane Sulfonamide Amino Carboxylate
PFHpS	Perfluoroheptane Sulfonic Acid or Sulfonate
PFHxA	Perfluorohexanoic Acid or Perfluorohexanoate
PFHxSaAm	Perfluorohexane Sulfonamido Amine
PFHxSaAmA	Perfluorohexane Sulfonamide Amino Carboxylate
PFHxS	Perfluorohexane Sulfonic Acid or Sulfonate
PFNA	Perfluorononanoic Acid or Perfluorononanoate
PFNS	Perfluorononane Sulfonic Acid or Sulfonate
PFOA	Perfluorooctanoic Acid or Perfluorooctanoate



PFOS	Perfluorooctane Sulfonic Acid or Sulfonate
PFOSaAm	Perfluorooctane Sulfonamido Amine
PFOSaAmA	Perfluorooctane Sulfonamide Amino Carboxylate
PFPeA	Perfluoropentanoic Acid or Perfluoropentanoate
PFPeSaAm	Perfluoropentane Sulfonamido Amine
PFPeSaAmA	Perfluoropentane Sulfonamide Amino Carboxylate
PFPeS	Perfluoropentane Sulfonic Acid or Sulfonate
PFPPrS	Perfluoropropane Sulfonic Acid or Sulfonate
PFSA	Perfluoroalkyl Sulfonic Acid
PFUdA	Perfluoroundecanoic Acid or Perfluoroundecanoate
POSF	Perfluorooctanesulfonyl Fluoride
ppb	Parts per billion
ppm	Parts per million
ppt	Parts per trillion
QTOF	Quadrupole-time-of-flight
RCN	Royal Canadian Navy
RMSE	Root-Mean-Square-Error
S	Sulfur
SDS	Sodium Decyl Sulfate
SE	Southeast
SW	Southwest
TCE	Trichloroethylene
UCMR	Unregulated Contaminant Monitoring Rule
US EPA	United States Environmental Protection Agency
V	Volts
W	West
YD	Year Day

---

## **Chapter 1 Introduction Per-and Polyfluoroalkyl Substances**

### **1.1 Background**

#### **1.1.1 Definitions**

Perfluoroalkyl and polyfluoroalkyl substances (PFAS) are aliphatic compounds containing a fluorinated carbon backbone (Knepper and Lange 2011). In a perfluoroalkyl substance, all of the carbon atoms are fluorinated, except those carbon associated with a functional group such as a carboxylic acid (-COOH). A polyfluoroalkyl substance will have at least one carbon that is not fully fluorinated (Knepper and Lange 2011).

There are two main categories of PFAS; polymers and non-polymers. Groups of polymers that are considered PFAS include: fluoropolymers, which have a carbon backbone with fluorine directly attached; perfluoropolyethers, which have a carbon and oxygen backbone with fluorine atoms directly attached to the carbon; and side-chain fluorinated polymers, which have fluorinated side chains attached to variable backbones (Buck et al. 2011). The non-polymer category of PFAS includes two groups: perfluoroalkyl substances and polyfluoroalkyl substances. Each of these groups consists of different families. Families of PFAS can sometimes be broken down into sub-families, as is the case for perfluoroalkyl acids (PFAAs), which include perfluoroalkyl carboxylic acids, sulfonic acids, sulfinic acids, phosphonic acids and phosphinic acids (Buck et al. 2011). The hierarchy associated with select categories, groups, families and sub-families of PFAS is depicted in Figure 1-1.

PFAS are often grouped into “long chain” or “short chain” categories when being discussed. In general, a long chain PFAS will contain 7 or more perfluorinated carbons. One exception is perfluoroalkyl sulfonic acids, in which case 6 or more perfluorinated carbons are considered long chain (Buck et al. 2011).

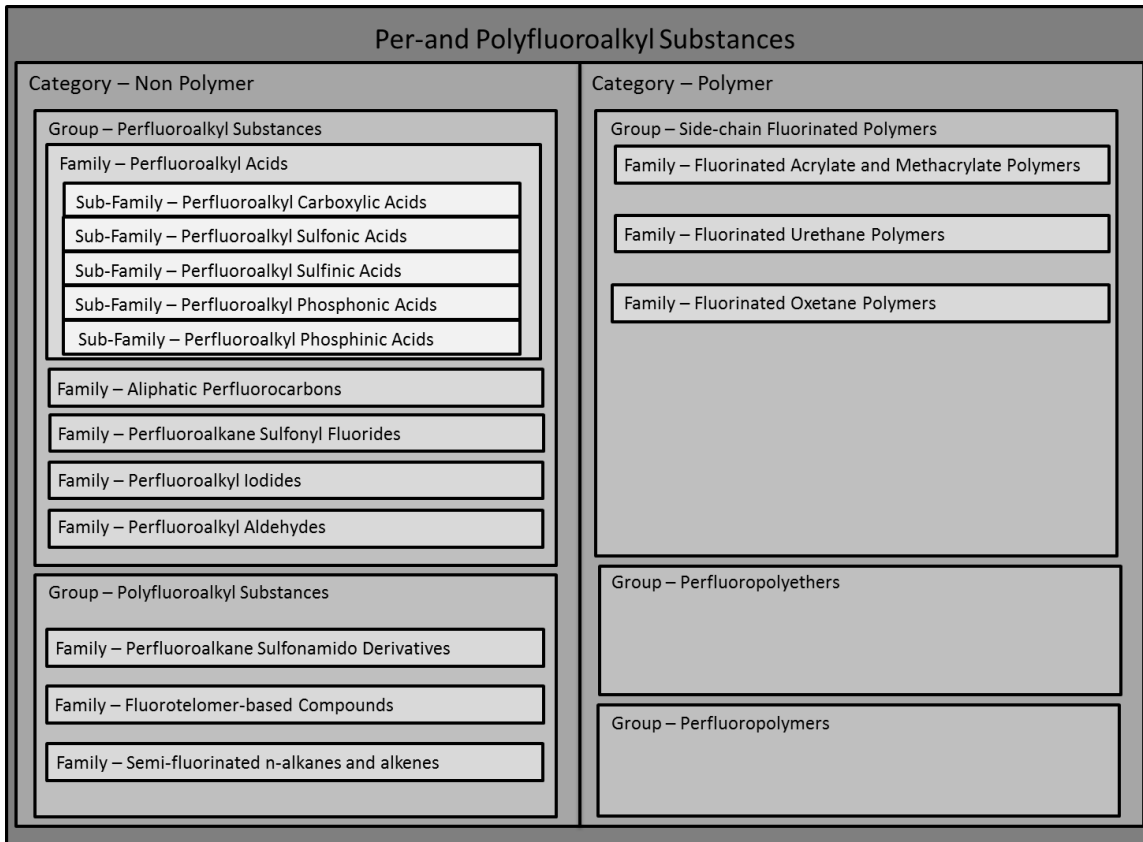


**Figure 1-1: PFAS classification hierarchy. An example of the classification hierarchy of per-and polyfluoroalkyl substance adapted from Buck et al. (2011).**

### 1.1.2 Properties

Elemental fluorine has strong electronegative properties, and can therefore form strong bonds with electropositive atoms. Fluorinated hydrocarbon molecules are not naturally occurring due to the energy required to bond the carbon and the fluorine atoms together. The bond strength of a C-F bond is approximately 460 kJ/mol. With increasing fluorination, the bond strength increases and the bond length decreases, as summarized in Table 1-1 (3M 1999b).

Table 1-1: Effect of increasing fluorination on bond length and bond strength (3M 1999b).

Structure	C-F Bond Length (pm)	C-F Bond Strength (kJ/mol)
$\text{H}_3\text{C} - \text{F}$	138.5	447.7
$\begin{array}{c} \text{F} \\   \\ \text{H}_2\text{C} - \text{F} \end{array}$	135.8	458.6
$\begin{array}{c} \text{F} \\   \\ \text{HC} - \text{F} \\   \\ \text{F} \end{array}$	133.2	479.5
$\begin{array}{c} \text{F} \\   \\ \text{F} - \text{C} - \text{F} \\   \\ \text{F} \end{array}$	131.7	485.3

Fluorine has a high ionization potential (1681 kJ/mol; energy required to remove a single electron from the outer shell), and low polarizability (ease of distortion of the electron cloud by an electric field). Consequently, fluorochemicals have low boiling points relative to their molecular weight, extremely low surface tension (tendency for molecules at the surface of a liquid to form a cohesive force) and low refractive index (ratio of the velocity of light in a vacuum to the velocity of light in a specific medium) when compared to their hydrocarbon analogues as summarized in Table 1-2 for perfluorooctane and octane (3M 1999b).

Table 1-2: Comparison of properties between a perfluoroalkane and its hydrocarbon analogue (3M 1999b).

Property (Units)	Perfluorooctane ( $\text{C}_8\text{F}_{18}$ )	Octane ( $\text{C}_8\text{H}_{18}$ )
Molecular Weight (g/mol)	438	114
Boiling Point ( $^{\circ}\text{C}$ )	97	125
Refractive Index ( $N_D^{20}$ )	1.280	1.3975
Surface Tension (N/m)	0.015	0.0218

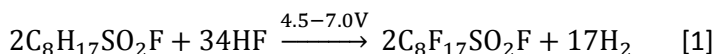
Perfluoroalkanes are both hydrophobic and oleophobic. When the perfluorinated chain, sometimes referred to as a “tail”, is attached to a hydrophilic functional group, often referred to as the “head”, the resulting molecule will be more water soluble and have surfactant-like properties (3M 1999b). Fluorinated surfactants are able to lower surface tension at very low

concentrations, which make them useful agents for wetting, leveling, dispersing, emulsifying or foaming (Knepper and Lange 2011). When a perfluorinated tail is attached to an oleophilic head group, the resulting molecule will become oil soluble (3M 1999b). Some fluorinated surfactants will have a spacer between the perfluorinated tail and the functional head group. The spacer is an organic group, typically nitrogen, oxygen, sulfur or hydrocarbons, which provides distance between the hydrophobic/oleophobic tail and the hydrophilic head of the molecule. This helps to optimize intermolecular and intramolecular interactions. Nitrogen (N), oxygen (O) and sulfur (S) spacers are able to impart greater hydrophilicity than a hydrocarbon spacer (Knepper and Lange 2011).

### 1.1.3 Synthesis

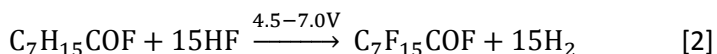
There are two main methods of synthesizing PFAS; electrochemical fluorination (ECF) and telomerization. The former was developed by Dr. Simons from Penn State University, and the intellectual property was licensed to the 3M Company in 1945 (3M 1999b). The latter was developed and patented by William E. Hanford and Robert M. Joyce Jr. from the E.I. du Pont de Nemours & Company in 1948 (Hanford and Joyce 1948).

In ECF, a starting feedstock, such as a hydrocarbon sulfonyl fluoride, is dispersed in liquid, anhydrous hydrogen fluoride. An electric current below 8 volts (V) is passed through the solution, which causes the hydrogen atoms on the molecule to be replaced with fluorine. While the predominant product will have the same carbon skeleton as that which was used in the feedstock solution, fragmentation and rearrangement of the carbon skeleton can also occur. This can result in the formation of cleaved, branched and cyclic structures (3M 1999b). An example is depicted in Reaction [1], where the starting feedstock is 1-octanesulfonyl fluoride ( $C_8H_{17}SO_2F$ ). The resulting fluorinated chemical is perfluorooctanesulfonyl fluoride (POSF,  $C_8F_{17}SO_2F$ ) (3M 1999b).



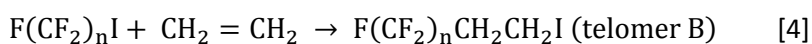
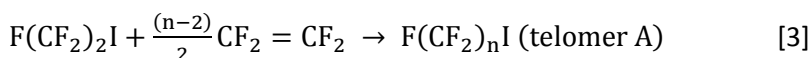
Reaction [1] yields approximately 35-40% straight chain POSF, about 7% higher and lower straight chain homologs, 18-20% branched chain perfluoroalkylsulfonyl fluorides with various chain lengths, 20-25% straight-chain, branched and cyclic perfluoroalkanes and ethers and 10-15% "tars" and other by-products (3M 1999b). POSF is an intermediate material used to manufacture perfluorooctane sulfonic acid (PFOS) and other POSF derivatives (Knepper and Lange 2011).

The ECF process can also be used to create perfluoroalkanoic acid fluorides. An example is provided in Reaction [2] where octanoyl fluoride ( $C_7H_{15}COF$ ) is converted to perfluorooctanoyl fluoride ( $C_7F_{15}COF$ ) (Knepper and Lange 2011).



When using the ECF process to create perfluoroalkanoic acid fluorides, the yields will range between 10% for pentafluorooctanoyl fluoride to approximately 80% for acetyl fluoride (Pabon and Corpart 2002).

Telomerization is a process that consists of reacting a molecule called a telogen with a compound called a taxogen to form a product called a telomer (Hanford and Joyce 1948). When employed for the manufacture of perfluoroalkyl substances, the telogen is a perfluoroethyl iodide, such as pentafluoroethyl iodide (C<sub>2</sub>F<sub>5</sub>I), the taxogen is tetrafluoroethylene (CF<sub>2</sub>=CF<sub>2</sub>), and the resulting telomer is a perfluoroalkyl iodide (C<sub>n</sub>F<sub>2n+1</sub>I, telomer A). The perfluoroalkyl iodide can then be reacted with ethylene (CH<sub>2</sub>=CH<sub>2</sub>) to yield an n:2 fluorotelomer iodide (C<sub>n</sub>F<sub>2n+1</sub>CH<sub>2</sub>CH<sub>2</sub>I, telomer B), which can then be converted to corresponding fluorotelomer alcohols, thiols and sulfonyl chlorides, all of which can be used as intermediates for fluorinated surfactants (Pabon and Corpart 2002; Buck et al. 2011). The production of telomer A and telomer B is shown in Reactions [3] and [4].



#### 1.1.4 Types and Uses

There are many types of PFAS being used in commercial and industrial applications and products. An overview of some of the more common groups, families and sub-families is provided here.

Perfluoroalkyl carboxylic acids (PFCAs) are fluorinated surfactants that have the chemical formula C<sub>n</sub>F<sub>2n+1</sub>COOH or C<sub>n</sub>F<sub>2n+1</sub>COO<sup>-</sup>. They belong to the PFAA family and are manufactured by both ECF and telomerisation (Prevedouros et al. 2006). Historically, perfluorooctanoic acid (PFOA) and its salts have been the most widely used PFCA, although perfluorononanoic acid (PFNA) has also been substantially used. In their ammonium salt forms, ammonium perfluorooctanoate (APFO) and ammonium perfluorononanoate (APFN) have both been used as processing aids in the manufacturing of fluoropolymers (Prevedouros et al. 2006). PFCAs can be formed from both biotic (biodegradation) and abiotic (hydrolysis, photolysis or oxidation) degradation of other fluorinated compounds referred to as precursors. Examples of precursors that are known to transform into PFCAs in the environment include a number of fluorotelomers (alcohols, acrylates, iodides and olefins), N-alkyl perfluoroalkane sulfonamides and sulfonidoethanols, as well as polyfluoroalkyl phosphates (Buck et al. 2011). PFOA is one of the most frequently detected PFAS in humans and wildlife (Kannan 2011).

Perfluoroalkyl sulfonic acids (PFSAs) are fluorinated surfactants that have the chemical formula C<sub>n</sub>F<sub>2n+1</sub>SO<sub>3</sub>H or C<sub>n</sub>F<sub>2n+1</sub>SO<sub>3</sub><sup>-</sup>. They also belong to the PFAA family and are manufactured using the ECF process (Buck et al. 2011). Historically, PFOS and its salts were the most widely used type of PFSA. Other PFSAs that were also frequently used included perfluorohexane sulfonic acid (PFHxS) and perfluorodecane sulfonic acid (PFDS). Today, perfluorobutane sulfonic acid (PFBS) is also used (Martin et al. 2010). Uses of PFSAs include surfactants and mist suppression agents in chrome plating (Knepper and Lange 2011). PFSAs can also form in the environment due to degradation of PFSA precursors. The following are examples of known PFOS pre-cursors that are either intentionally manufactured, or are by-products created during the manufacturing process: POSF; N-methyl and N-ethyl perfluorooctane sulfonamide (NMeFOSA and NEtFOSA); N-methyl and N-ethyl perfluorooctane sulfonamidoethanol (NMeFOSE and NEtFOSE); and N-methyl and N-ethyl perfluorooctane sulfonamidoacetate (NMeFOSAA and NEtFOSAA) (Martin et

al. 2010). PFOS is also one of the most frequently detected PFAS in humans and wildlife around the world (Kannan 2011).

Another common family of PFAS are Fluorotelomers (FTs), which are PFAS products that are manufactured using the telomerization process. They consist of a fluorinated carbon tail with “n” carbons where  $6 \leq n \leq 16$ , a hydrocarbon spacer group with “m” carbons where  $m \geq 1$ , and a functional head group (Buck et al. 2011). In naming FTs, the convention is to proceed the name with the numbers of fluorinated carbons and hydrocarbons in the form of “n:m”. Some common fluorotelomer-based compounds include: n:2 fluorotelomer iodides (FTI); n:2 fluorotelomer olefins (FTOs); n:2 fluorotelomer alcohols (FTOH); n:2 fluorotelomer acrylates and methacrylates (FTACs and FTMACs); n:2 fluorotelomer sulfonic acids (FTSAs); n:2 fluorotelomer carboxylic acids (FTCAs); and n:3 fluorotelomer sulfonamide alkyl betaines (Wang et al. 2013). Fluorotelomers have multiple applications including: raw materials used for surfactants and surface protection products; telomers in the telomerization process; mist suppression agents in metal plating; and as a key ingredient in aqueous film forming foam (Wang et al. 2013). They can also exist as intermediate degradation products in the environment (Buck et al. 2011).

Another family of PFAS are known as perfluoroalkane sulfonamido derivatives. Sub-families included in this family are: N-alkyl perfluoroalkane sulfonamides ( $C_nF_{2n+1}SO_2NHC_mH_{2m+1}$  where  $m = 1, 2, 4$ ); N-alkyl perfluoroalkane sulfonamidoethanols ( $C_nF_{2n+1}SO_2NC_mH_{2m+1}CH_2CH_2OH$  where  $m = 0, 1, 2, 4$ ); N-alkyl perfluoroalkane sulfonamidoethyl acrylates ( $C_nF_{2n+1}SO_2NC_mH_{2m+1}CH_2CH_2OC(O)CH=CH_2$  where  $m = 1, 2, 4$ ) and methacrylates ( $C_nF_{2n+1}SO_2NC_mH_{2m+1}CH_2CH_2OC(O)C(CH_3)=CH_2$  where  $m = 1, 2, 4$ ); and N-alkyl perfluoroalkane sulfonamido acetic acids ( $C_nF_{2n+1}SO_2NC_mH_{2m+1}CH_2COOH$  where  $m = 0, 1, 2, 4$ ) (Buck et al. 2011). These compounds are used as raw materials for surfactant and surface protection products, but can also be formed as an intermediate transformation product in the environment as a result of degradation of other fluorinated substances (Buck et al. 2011).

### 1.1.5 Issues Related to PFAS Use

PFAS has been detected in humans and wildlife around the world, with the most frequently detected PFASs being PFOS and PFOA (Kannan 2011). Research has shown that PFASs are persistent in the environment, can bioaccumulate, and can have adverse effects on both humans and wildlife (Ahrens 2011).

One of the first studies linking the detection of organic fluorine in human serum to a common type of PFAS used in commercial applications was that of Guy et al. (1976). Organic fluorine was detected in the serum of 106 humans living in five cities in the USA in concentrations ranging from 0.1 to 6.8  $\mu\text{mol/L}$ . Using Nuclear Magnetic Resonance (NMR) Spectroscopic analysis, the peaks from the serum analysis were compared to that of PFOA. Although the results were not identical, there were enough similarities to suggest that the organic fluorine present in the human serum samples could potentially be PFOA. It was suggested that the differences in the two peaks could be due to branching.

As a result of the findings of Guy et al. (1976), the 3M Company, which at that time manufactured PFOS and PFOA, along with other POSF-based chemicals, implemented a voluntary medical surveillance program for workers in their fluorochemical production facilities

(3M 1999a). At the 3M Company's Decatur, Alabama facility, which began producing POSF based chemicals in the early 1950s, the average levels of organic fluorine for workers that had six or more measurements taken ranged between 2.5 to 6.5 ppm from 1981 to 1992. It was not until the early 1990's that specific fluorochemical compounds could be detected as a result of the introduction of high performance liquid chromatography-mass spectrometry (HPLC-MS) technology (3M 1999a). Levels of PFOS in serum of the Decatur workers measured in 1995 and 1997 ranged from 0.25 to 12.83 ppm and 0.10 to 9.93 ppm respectively, with mean PFOS levels of 2.44 ppm in 1995 and 1.96 ppm in 1997 (Olsen et al. 1999). In 1998, PFOS was detected in six pooled blood samples obtained from two commercial sources in the US at concentrations ranging from 26 to 45 parts per billion (ppb) (3M 1999a). A separate analysis of eighteen US pooled blood bank samples found that all samples contained PFOS ranging from 9 to 56 ppb, and one-third of the samples contained PFOA with concentrations up to 22 ppb (3M 1999a).

In 2001, PFOS was first identified in birds, mammals, fish, turtles and frogs from both remote and urbanized locations (Giesy and Kannan 2001; Kannan et al. 2001; Kannan et al. 2001). It is believed that the main route of exposure for PFAS for both humans and wildlife is through food and water intake. In a review paper on dietary exposure to PFAS, Domingo (2012) reported on several studies throughout Europe, North America and Asia that found positive correlations between elevated PFAS levels detected in human serum and dietary intake of fish and sea food products from contaminated waters, and food from packaging containing PFAS, such as fast food and popcorn. PFAS contaminated drinking water has also been linked to high levels of PFAS in humans who consume it (Gyllenhammar et al. 2015).

In addition to detection of PFAS in serum, PFAS can also be found in different organs of the body. To determine metabolism and distribution of different PFASs in humans, tissues from the liver, kidney, brain, lung and bone have been obtained from cadavers and analyzed for 21 different PFAS. PFOA was quantifiable in 55 % of bone samples (mean 60.2 ng/g wet weight), 42 % of lung samples (mean 29.2 ng/g wet weight), 45 % of liver samples (mean 13.6 ng/g wet weight), and 95 % of kidney samples (mean 2.0 ng/g wet weight) (Perez et al. 2013). PFOS has been found most prevalently in the liver (90% detection, mean 102 ng/g wet weight), but was also detected in 89% of lung samples at a mean concentration of 29.1 ng/g wet weight, and in 45% of kidney samples at a mean concentration of 75.6 ng/g wet weight (Perez et al. 2013).

Both PFOS and PFOA are eliminated from the body through urine. Zhang et al. (2013) determined that branched isomers of PFOS and PFOA were more preferentially excreted when compared to their linear isomers. PFOS and PFOA are also eliminated from women through breast milk and cord serum. Thomsen et al. (2010) quantified both PFOS and PFOA in breast milk samples monthly for 10 Norwegian woman from approximately 2 weeks after giving birth until 12 months. By the end of the twelve month period, the concentration of PFOA in the breast milk had decreased by 93.6% and the concentration of PFOS had decreased by 37.3% suggesting that lactation was one way in which women excrete PFOS and PFOA from their bodies (Thomsen et al. 2010). Apelberg et al. (2007), analyzed the cord blood from 299 newborns in Baltimore, Maryland who were born between 2004 and 2005. PFOS was detected in 99% of samples, and PFOA in 100% of the cord blood samples. The geometric mean concentrations were determined to be 4.9 ng/mL for PFOS and 1.6 ng/mL for PFOA (Apelberg et al. 2007).



For humans with elevated levels of PFAS in their blood, it can take years for the PFAS to be eliminated from their systems. In a half-life determination study of former residents of Little Hocking, Ohio and Lubeck, West Virginia who were exposed to PFOA through contaminated drinking water from DuPont's Washington Works Facility, the elimination half-life of PFOA was estimated to average 2.9 years for the residents of Little Hocking, and 8.5 years for the residents of Lubeck. The half-life estimates were based on the decline of PFOA in serum levels since the original C8 Health Project, which took place between 2005 and 2006 as part of the outcome of a class action lawsuit against DuPont for contaminating drinking water supplies by allowing PFOA to be released into the Ohio River (Seals et al. 2011). A similar study was conducted involving residents in Arnsberg Germany who were exposed to drinking water contaminated with PFOA, and subsequently had serum levels of PFOA that were between 4 and 8 times higher than that of the general population. A follow-up study was conducted two years after a charcoal filter was installed to reduce the PFOA concentrations in the drinking water. Serum concentrations of PFOA had declined by 39% in the women and children and by 26% in the men. The geometric mean half-life for PFOA in plasma was estimated to be 3.26 years (Brede et al. 2010). The mean serum elimination half-life for PFOS in three retired 3M chemical workers who were followed for 5.5 years after retirement was determined to be 1428 days or 3.91 years (3M 1999a).

Many human health effects have been associated with PFAS exposure. As part of the settlement in the class action lawsuit against DuPont for contaminating drinking water supplies with PFOA in communities near their Washington Works Facility, an independent science panel was established to determine whether or not there was a probable link between PFOA exposure and human diseases in the communities affected (Chemours 2017). The panel concluded that there was a probable link between PFOA exposure and the following diseases: kidney cancer, testicular cancer, ulcerative colitis, thyroid disease, diagnosed high cholesterol and pregnancy induced hypertension (C8 Science Panel 2017). PFAS has also been linked to a suppressed immune system in children whose mothers were exposed to PFAS while pregnant. Granum et al. (2013) found that increased concentrations of PFOA, PFNA, PFHxS and PFOS in maternal blood were associated with decreased antibody levels to the rubella vaccine, increased concentrations of PFOA and PFNA were associated with an increased number of common colds, and increased levels of PFOA and PFHxS were associated with increased episodes of gastroenteritis.

In light of the persistence of PFOA and PFOS, as well as their detection in both humans and wildlife, in May 2000, the 3M Company announced that they would be phasing out production of C8 fluorinated chemicals by 2002. Subsequent to this announcement, the company also decided to stop manufacturing C6 and C10 homologues of POSF (3M 2000b).

#### **1.1.6 Guidelines and Regulations related to PFAS**

As a result of the ubiquity, persistence and health related effects associated with PFOS, in 2009, PFOS and its precursors were added to Annex B of the Stockholm Convention Persistent Organic Pollutants list, meaning that measures must be taken to restrict the production and use of PFOS, its salts and derivatives (Ahrens 2011). Due to similar issues related to PFOA, a stewardship agreement was established between the United States Environmental Protection Agency (US EPA) and several leading manufacturers of PFAS worldwide to reduce emissions of PFOA and related precursors, such as FTs that can degrade to PFOA. The goal was to reduce

emissions of PFOA and related chemicals by 95% by 2010, and work toward total elimination by 2015 (US EPA 2017).

In Canada, the Government of Canada has released Federal Environmental Quality Guidelines (FEQG) for PFOS. FEQGs are quantitative or qualitative recommendations that support federal environmental quality monitoring and are provided to protect the ambient environment. If the concentration of a chemical is below the recommended FEQGs, this indicates that there is a low likelihood that the chemical will result in adverse effects on aquatic life that are exposed to the chemical through water or sediment. If the chemical is deemed to bioaccumulate, FEQGs are also given for birds or mammals (not including humans) that might consume aquatic life affected by the chemical (ECCC 2017). FEQGs for PFOS have been reproduced in Table 1-3. The Government of Canada also provides soil and groundwater FEQGs which consider ecological receptors and are established to protect important ecological functions. Soil FEQGs for PFOS are provided for agriculture lands (0.01 mg/kg), residential and parklands (0.01 mg/kg), as well as commercials and industrial lands (0.14 mg/kg for course soil and 0.21 mg/kg of fine soil), while groundwater guidelines are provided for course soil and fine soil (0.068 mg/L for each). (ECCC 2017).

**Table 1-3: Federal Environmental Quality Guidelines (FEQGs) for PFOS prescribed by Environment and Climate Change Canada.**

<b>Water (µg/L)</b>	<b>Fish Tissue (mg/kg)</b>	<b>Wildlife Diet – Mammalian (µg/kg)</b>	<b>Wildlife Diet – Avian (µg/kg)</b>	<b>Bird (µg/g)</b>	<b>Egg</b>
6.8	8.3	4.6	8.2	1.9	

Health Canada has provided drinking water screening values (DWSV) for a number of PFAS (Table 1-4). The purpose of DWSV are to provide guidance in terms of safe levels of the chemical in water intended for human consumption when there are no existing formal guidelines available (HC 2016a). In 2016, Health Canada circulated documents prepared by the Federal-Provincial-Territorial Committee on Drinking Water which assessed the available information on PFOS and PFOA with the intent to develop drinking water guidelines for PFOS and PFOA. The proposed maximum acceptable concentration of PFOS and PFOA in drinking water is 0.6 µg/L and 0.2 µg/L respectively (HC 2016b; HC 2016c).

**Table 1-4: Drinking Water Screening Values (DWSVs) for select PFAS as provided by Health Canada**

<b>PFAS Name</b>	<b>Drinking Water Screening Value (µg/L)</b>
Perfluorooctanoic acid	0.2
Perfluorooctane sulfonate	0.6
Perfluorobutanoate	30
Perfluorobutane sulfonate	15
Perfluorohexanesulfonate	0.6
Perfluoropentanoate	0.2
Perfluorohexanoate	0.2
Perfluoroheptanoate	0.2
Perfluorononanoate	0.2

In 2016, the US EPA established a combined health advisory for PFOS and PFOA of 70 parts per trillion (ppt) in drinking water. Since 2012, PFOS and PFOA are also among the list of contaminants that must be monitored under the third Unregulated Contaminant Monitoring Rule (UCMR 3). The US EPA intends to use data provided by UCMR 3, along with ongoing health assessments in order to determine if national primary drinking water regulations for PFOS and PFOA are required under the Safe Drinking Water Act (US EPA 2016c).

### **1.1.7 Replacements for long chain PFAS**

As a result of the phase out of long chain PFAS and the guidelines and regulations that have been put in place, companies that produce PFAS have had to find alternatives to the long chain PFASs, PFCAs and PFAS that are precursors to these chemicals. Examples of some replacement PFASs, along with their uses are described here.

Perfluoroalkyl and polyfluoroalkyl ether carboxylic acids or carboxylates (PFECAs) are similar to PFCAs but they have one or more ether groups inserted into the fluorinated carbon chain, and therefore some PFECAs can belong to a family of PFAS called perfluoropolyethers (Buck et al. 2011). PFECAs are being utilized as a replacement for APFO and are used in their ammonium salt form as fluoropolymer processing aids (Wang et al. 2013). Examples of PFECAs currently being used in industry are presented in Table 1-5.

F-53 and F-53B are per- and polyfluoroalkyl ether potassium sulfonates that were developed in China as mist suppressants for the hard chrome plating industry in the 1970s, although their use in the industry was not as prevalent as FC-80 and FC-248, both of which are derivatives of PFOS. With growing pressure on the Chinese metal plating industry to move away from the use of PFOS containing chemicals, it is believed that F-53 and F-53B are the most likely alternatives (Wang et al. 2013). Other alternatives to PFOS used in hard chrome plating include derivatives of 6:2 FTS. DuPont used 6:2 FTS-K in their products Forafac®1176 and Capstone®FS-17, while Atotech used 6:2 FTS-H in their product Fumetrol®21 (Yang et al. 2014). C4 fluorinated chemistry has also been adopted in the metal plating industry; N,N,N,-triethylethanamimium 1,1,2,2,3,3,4,4,4-nonafluorobutane-1-sulfonate, also known as tetraethylammonium perfluorobutanesulfonate has been registered under the European Chemicals Agency (ECHA) for use in metal (chromium) plating with a production volume of 0 to 10 tonnes per year (ECHA 2017). A list of PFOS alternatives used in hard chrome plating is provided in Table 1-6.

Table 1-5: PFECAs currently used in industry as replacement chemicals for PFOA/APFO

Chemical Name (CAS Number)	Commercial/ Common Name	Chemical Formula	Uses	Reference
Ammonium 4,8-dioxa-3H-perfluorononanoate (CAS No. 958445-44-8)	ADONA	$\text{CF}_3\text{OCF}_2\text{CF}_2\text{CF}_2\text{-OCHF}_2\text{COO}^- \text{NH}_4^+$	An emulsifier used in the manufacture of fluoropolymers	(Gordon 2011) (Wang et al. 2013)
Ammonium 2,3,3,3-tetrafluoro-2-(heptafluoropropoxy)-propanoate salt (CAS No. 62037-80-3)	GenX	$\text{CF}_3\text{CF}_2\text{CF}_2\text{OCF}(\text{CF}_3)\text{COOH NH}_3$	A processing aid used to manufacture fluoropolymers	(Gannon et al. 2016)
perfluoro[(2-ethoxyethoxy)acetic acid] ammonium salt (CAS No. 908020-52-0)	EEA	$\text{CF}_3\text{CF}_2\text{OCF}_2\text{CF}_2\text{OCF}_2\text{COO}^- \text{NH}_4^+$	An emulsifier used in the manufacture of fluoropolymers	(Efsa Panel on food contact materials and processing 2011) (Gomis et al. 2015)
perfluoro acetic acid, $\alpha$ -substituted with the copolymer of perfluoro-1,2-propylene glycol and perfluoro-1,1-ethylene glycol, terminated with chlorohexafluoropropoxy groups (CAS No. 329238-24-6)	Unknown	$\text{C}_3\text{F}_6\text{ClO-}[\text{CF}_2\text{-CF}(\text{CF}_3)\text{-O}]_n\text{-}[\text{CF}(\text{CF}_3)\text{-O}]_m\text{-CF}_2\text{COOH}$ , where n ranges from 1 to 4 and m from 0 to 2	An emulsifier and a dispersing agent for processing fluorinated polymers	(Efsa Panel on food contact materials and processing 2010)
poly[oxy [trifluoro(trifluoromethyl)-1,2-ethanediyl]], a-(heptafluoromethylethyl)-o-[1,2,2,2-tetrafluoro-1-[[2-hydroxyethyl)amino] carbonyl]ethoxy]- (CAS No. 75888—49-2)	HFPO-Amidol	$\text{CF}_3\text{CF}_2\text{CF}_2\text{O}(\text{CF}(\text{CF}_3)\text{-CF}_2\text{O})_n\text{CF}(\text{CF}_3)\text{C}(\text{O})\text{NHCH}_2\text{CH}_2\text{OH}$ Where n ranges from 2 to 16, with an average of 6	Monomer for polymeric synthesis, film additive, surfactant (all were cited as proposed uses)	(Moilanen et al. 2015)

**Table 1-6: PFOS alternative used as mist suppressants in the hard chrome plating industry**

<b>Chemical Name (CAS Number)</b>	<b>Commercial/ Common Name</b>	<b>Chemical Formula</b>	<b>Reference</b>
2-[(1,1,2,2,3,3,4,4,5,5,6,6,6-tridecafluorohexyl)oxy]-1,1,2,2-tetrafluoroethane sulfonic acid potassium salt (CAS No. 754925-54-7)	F-53	C <sub>8</sub> F <sub>17</sub> O <sub>4</sub> SK	(Wang et al. 2013)
2-[(6-Chloro-1,1,2,2,3,3,4,4,5,5,6,6,6-dodecafluorohexyl)oxy]-1,1,2,2-tetrafluoroethanesulfonic acid potassium salt (CAS No. 73606-19-6)	F-53B	C <sub>8</sub> ClF <sub>16</sub> O <sub>4</sub> SK	(Wang et al. 2013)
Potassium 3,3,4,4,5,5,6,6,7,7,8,8,8-tridecafluorooctanesulfonate (CAS No. 59587-38-1)	Forafac® 1176 Capstone® FS-17 / 6:2 FTS-K	C <sub>8</sub> H <sub>4</sub> F <sub>13</sub> KO <sub>3</sub> S	(Yang et al. 2014)
3,3,4,4,5,5,6,6,7,7,8,8,8-tridecafluorooctanesulfonic acid (CAS No. 27619-97-2)	Fumetrol® 21 / 6:2 FTS-H	C <sub>8</sub> H <sub>5</sub> F <sub>13</sub> O <sub>3</sub> S	(Yang et al. 2014)
N,N,N,-triethylethanamimium 1,1,2,2,3,3,4,4,4-nonafluorobutane-1-sulfonate (CAS No. 25628-08-4)	tetraethylammonium perfluorobutanesulfonate	C <sub>12</sub> H <sub>2</sub> OF <sub>9</sub> NO <sub>3</sub> S	(Wang et al. 2013) (ECHA 2017)

Perfluoroalkylsulfonamido compounds are the key ingredients used by the 3M Company to protect carpets, fabrics and paper products from stains. After their phase-out of perfluorooctane-based sulfonamido compounds, they began using a perfluorobutane-based product, N-methyl perfluorobutane sulfonamidoethanol (NMeFBSE) (D'eon et al. 2006). PFBS-related substances are also being used as surfactants for inks, paints, waxes, etc. Identified substances used in this type of application include fluoroacrylate copolymers, NMeFBSE, N-methyl perfluorobutane sulfonamide (NMeFBSA), N-methyl perfluorobutane sulfonamidoethyl acrylate (NMeFBSAC), and 1-propanesulfonic acid, 3-[hexyl[(nonafluoro-butyl)-sulfonyl]amino]-2-hydroxy-, monoammonium salt (Lassen et al. 2017). Typical concentrations of PFBS-related substances used in this capacity range between 0.01 and 0.3% (Lassen et al. 2017). Other PFBS derivatives currently being used include potassium salts of PFBS as a flame retardant for polycarbonate resins, and imide salt of PFBS as a surfactant, acid catalyst and raw material (Wang et al. 2013). Some types and uses of PFBS related chemicals are shown in Table 1.7.

Prior to 2002, the 3M Company manufactured AFFF which predominantly contained PFOS, although formulations prior to 1976 were also reported as containing PFOA (Prevedouros et al.

2006; Place and Field 2012; Backe et al. 2013). AFFF formulas made by other manufactures contained various types of FTs with C4 – C12 fluorinated chain lengths (Place and Field 2012). AFFF containing PFOS is no longer manufactured in North America as a result of 3M's phase-out of POSF-based chemicals (3M 2000b). Analysis of AFFF samples used by the US military and manufactured in 2012 and 2013 indicated that some manufacturers had begun to either significantly reduce or completely eliminate fluorinated surfactants from their AFFF formulations with C8 – C12 fluorinated chains as required under the US EPA Stewardship Agreement. These formulations now contain almost exclusively 6:2 fluorotelomers (Ouellette et al. 2013).

**Table 1-7: Types and uses of PFBS related chemicals that have replaced their longer chain homologues**

<b>Chemical Name (CAS Number)</b>	<b>Commercial/ Common Name</b>	<b>Chemical Formula</b>	<b>Uses</b>	<b>Reference</b>
C <sub>4</sub> F <sub>9</sub> SO <sub>2</sub> – side-chain fluorinated polymers (CAS No. 949581-65-1, CAS No. 940891-99-6, CAS No. 923298-12-8)	Scotchgard PM-3622, PM-490, PM-930	C <sub>4</sub> F <sub>9</sub> SO <sub>2</sub> -	Surface treatment for textiles, leather or carpet	(Wang et al. 2013)
N,N,N,-triethylethanamimium 1,1,2,2,3,3,4,4,4-nonafluorobutane-1-sulfonate (CAS No. 25628-08-4)	tetraethylammonium perfluorobutanesulfonate	C <sub>12</sub> H <sub>20</sub> F <sub>9</sub> NO <sub>3</sub> S	Metal plating	(ECHA 2017)
1,1,2,2,3,3,4,4,4-nonafluoro-N-(2-hydroxyethyl)-N-methylbutane-1-sulphonamide (CAS No. 34454-97-2)	N-Methyl perfluorobutane sulfonamidoethanol (NMeFBSE)	C <sub>7</sub> H <sub>8</sub> F <sub>9</sub> NO <sub>3</sub> S	An intermediate for the manufacture of other substances, and/or a monomer for the manufacture of thermoplastics	(ECHA 2017; Lassen et al. 2017)
2-[methyl[(nonafluorobutyl)sulphonyl]amino]ethyl acrylate (CAS No. 67584-55-8)	N-Methyl perfluorobutanesulfonamidoethyl acrylate (NMeFBSAC)	C <sub>10</sub> H <sub>10</sub> F <sub>9</sub> NO <sub>4</sub> S	Used in polymerization of C <sub>4</sub> -acrylate and as a laboratory agent	(ECHA 2017; Lassen et al. 2017)
tetrabutyl-phosphonium nonafluoro-butane-1-sulfonate (CAS No. 220689-12-3)	Tetrabutyl-phosphonium perfluorobutanesulfonate	C <sub>20</sub> H <sub>36</sub> F <sub>9</sub> O <sub>3</sub> PS	An additive for the manufacture of plastic products	(ECHA 2017; Lassen et al. 2017)
sodium 1,1,2,2,3,3,4,4,4-nonafluoro-1-butanedisulfinate (CAS No. 102061-82-5)	F-11323 / Sodium perfluorobutanedisulfinate	C <sub>4</sub> F <sub>9</sub> NaO <sub>2</sub> S	Unknown/ Confidential	(ECHA 2017; Lassen et al. 2017)
triphenyl(phenylmethyl)phosphonium 1,1,2,2,3,3,4,4,4-nonafluoro-N-methyl-1-butanedisulfonamide (1:1) (CAS No. 332350-93-3)	E-16368 / Triphenyl(phenylmethyl)phosphonium N-methyl-perfluorobutanedisulfonamide	C <sub>30</sub> H <sub>25</sub> F <sub>9</sub> NO <sub>2</sub> PS	Unknown / Confidential	(ECHA 2017; Lassen et al. 2017)

## 1.2 PFAS in the Environment

### 1.2.1 Literature Review

A literature review was conducted between September 2016 and April 2017 using two independent search engines: Engineering Village and Web of Science. Search words used included AFFF, PFAS, per-and-polyfluoroalkyl substances, perfluoroalkyl substance, polyfluoroalkyl substance, perfluorinated compound, and polyfluorinated compound. After duplicates were deleted, a total of 3381 articles were found with publication years ranging from 1996 to 2017. The number of peer reviewed PFAS related articles published per year are shown in Figure 1-2.

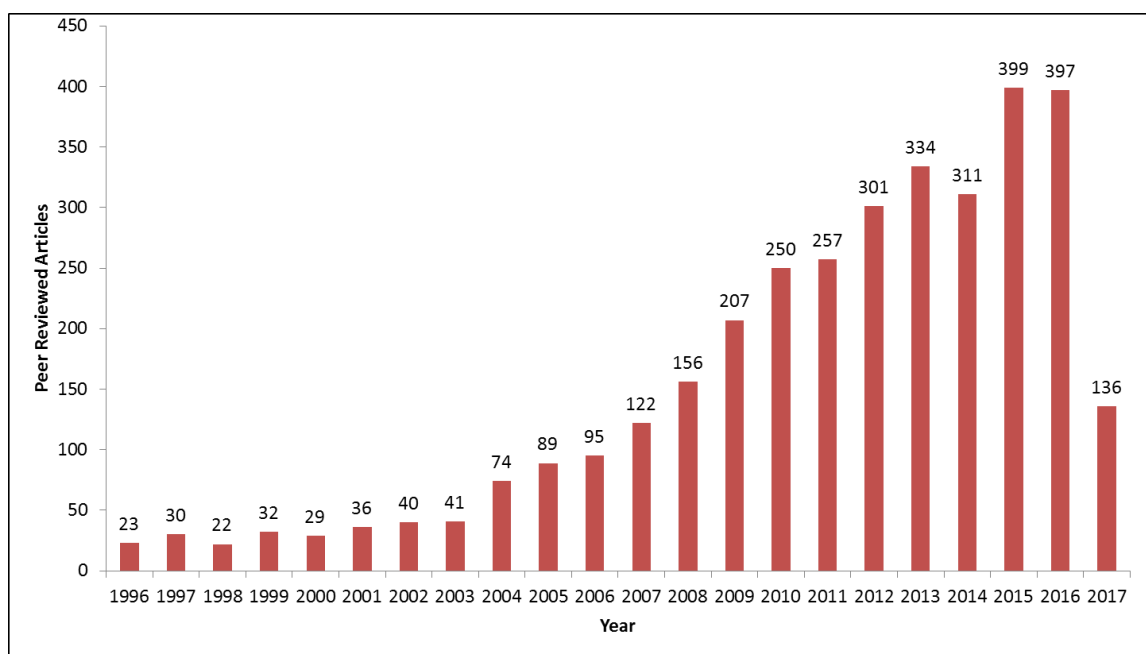


**Figure 1-2: Number of peer reviewed PFAS articles published by year. The number of peer reviewed journal articles published by year as determined using the search engines Engineering Village and Web of Science, and the key words AFFF, PFAS, per-and polyfluoroalkyl substances, perfluoroalkyl substance, polyfluoroalkyl substance, perfluorinated compound, and polyfluorinated compound**

In conducting the literature review, one of the goals was to determine if there was a research trend regarding the types of PFAS being studied related to the introduction of regulations for PFOS and the steps taken to eliminate PFOA as described above. In other words, was research driving the regulations, or were the regulations driving the research? To determine this, each article was categorized according to the types of PFAS being studied. PFCAs and PFSAs were grouped by chain length (short C2 – C5, long C6 – C12, or C13 and greater), and precursors were characterized as either fluorotelomers or sulfonamides. If the PFAS being studied did not fit into any of the previously described categories, they were put into a grouping called “other”. As seen in Figure 1-3, the trends in the types of PFAS being studied over the last five years appears to be consistent, with the study of long chain PFCAs and PFSAs continuing to dominate research. Short chain PFCAs and PFSAs are regularly the second highest category of PFAS being studied.



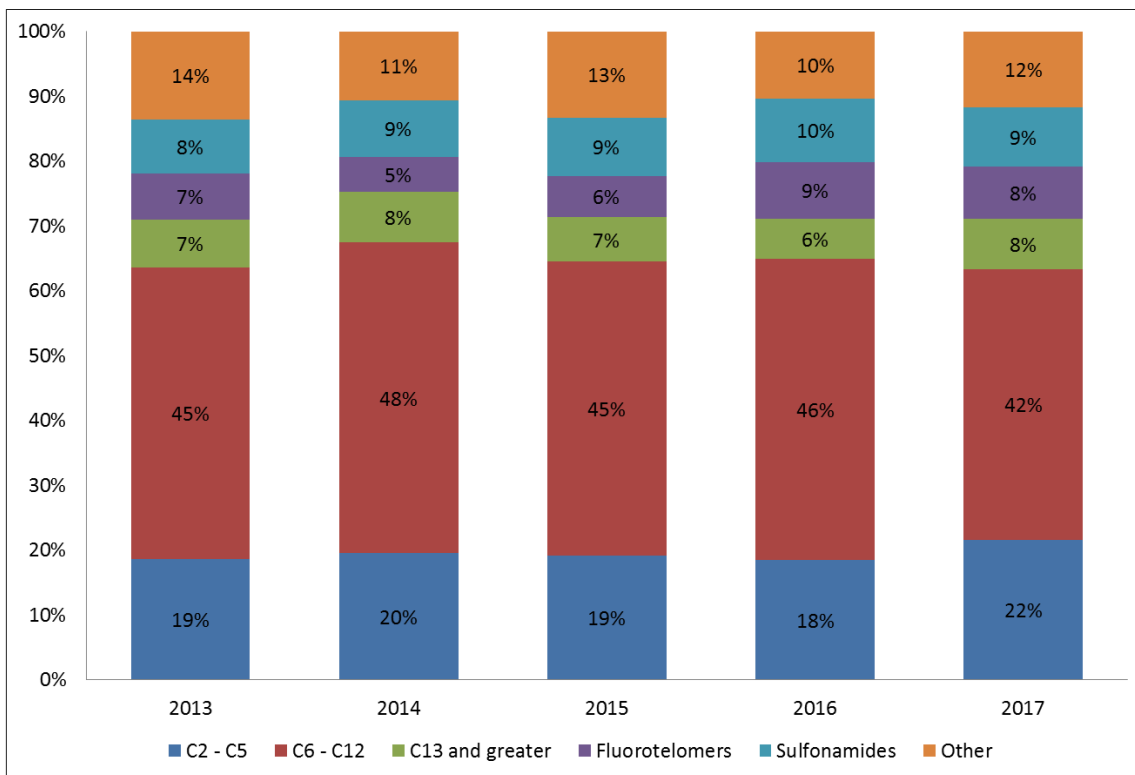


**Figure 1-3: Types of PFAS studied by year. The types of PFAS researched by year are shown for short chain (C2 – C5) PFCAs and PFSAs (blue), long chain (C6 – C12) PFCAs and PFSAs (red), C13 and greater PFCAs and PFSAs (green), fluorotelomers (purple), sulfonamides (light blue) and others (orange), which include all other types of PFAS that do not fit the other categories provided.**

Another goal in performing the literature review was to understand the main focus of PFAS related peer reviewed articles, particularly with respect to PFAS fate in the environment. As such, the main focus of each article was categorized into environmental identification/quantification, fate/transport, remediation, other, and review papers, as shown in Figure 1-4. For studies categorized in “other”, topics included development of analytical methods, synthesis, determination of chemical and/or physical properties, toxicity studies and pharmacokinetic studies. The majority of studies were grouped in this category, with toxicity studies and development of analytical methods dominating this focus group. Environmental identification and quantification has consistently been the second most popular focus area for PFAS related studies over the last five years.

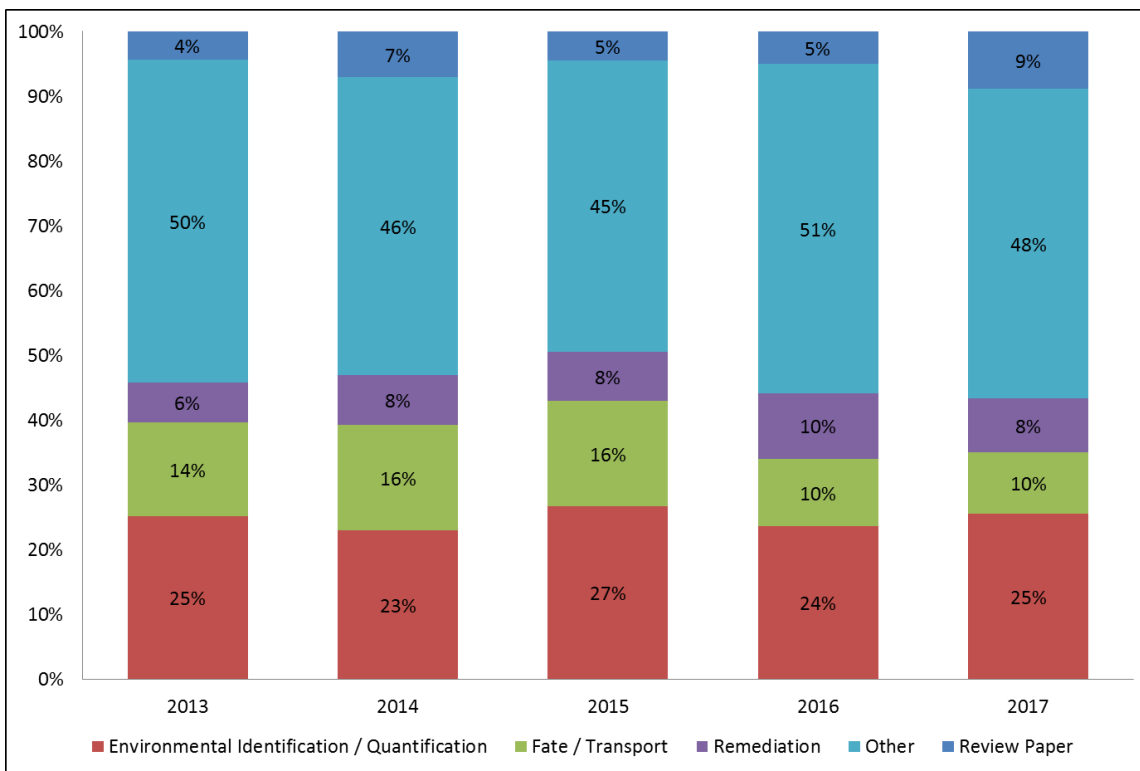


**Figure 1-4: Focus of PFAS research by year. PFAS articles were grouped and quantified according to their focus being either PFAS Environmental Identification/Quantification (red), PFAS Fate/Transport (green), Remediation of PFAS (purple), Other, which includes development of analytical methods, synthesis, determination of chemical and/or physical properties, toxicity studies and pharmacokinetic studies (light blue), and PFAS Review Papers (blue).**

The state of the art with respect to environmental identification, quantification, fate, transport and potential remediation options was investigated based on the information gathered from the literature review described above, and is summarized in sections 1.2.2 through 1.2.4.

### 1.2.2 Sources and Environmental Quantification

PFAS can enter the environment through releases during the manufacturing process, through the industrial or commercial use of products containing PFAS, or through disposal of products containing PFAS. Prevedouros et al. (2006) estimated that between 1951 and 2004, that somewhere between 4400 and 8000 tonnes of PFOA/APFO and PFNA/APFN were produced globally, and that between 470 and 900 tonnes were released into the environment directly as a result of PFOA/APFO and PFNA/APFN manufacturing. Between 3200 and 6900 tonnes of PFCAs were estimated to have entered the environment as a direct result of industrial and consumer uses between 1951 and 2000, and a further 30 to 350 tonnes of PFCAs entering the environment was estimated to be a result of indirect sources from 1960 to 2004 (Prevedouros et al. 2006). More recent work by Wang et al. (2014) estimates that between 2610 and 21,400 tonnes of C4 – C14 PFCAs entered the global environment between 1951 and 2015. They further predict that anywhere from 20 – 6400 tonnes will be released into the environment globally from 2016 – 2030. Although production of PFOS and PFOA were phased out in Europe

and North America, in China, PFOS production plateaued in 2011 at 220 – 240 tonnes/year, and PFOA production plateaued in 2013 at 150 tonnes/year (Liu et al. 2017). It is estimated that over 58 tonnes of PFOS and 28 tonnes of PFOA is released into the environment annually in China as a result of industrial emissions, with the majority entering the environment through wastewater, and a small fraction entering through exhaust gas emissions (Liu et al. 2017). These numbers represent approximately 86% of PFOS and 87% of PFOA released into the environment in central and eastern China. While industrial wastewater was cited as the dominant pollution pathway of PFOS into surface water in China (93.4%), AFFF was listed as the second most likely contributor to PFOS contamination of surface water (5.6%). In terms of PFOS soil contamination, AFFF was estimated to be responsible for more than 53%, followed by the use of pesticides containing PFOS (35.4%). For PFOA, surface water contamination was estimated to be predominantly a result of industrial wastewater (88.3%) followed by domestic wastewater (5.8%), and PFOA soil contamination was believed to have been predominantly caused by atmospheric deposition to land of volatile PFAS (51.4%) followed by landfill leachate (23.6%), pesticide application (19%), AFFF infiltration (5.5%) and bio solid application (0.4%) (Liu et al. 2017).

### **1.2.3 Fate and Transport**

To understand the fate and transport of PFAS in the environment, knowledge of the physicochemical properties and partitioning behaviour of PFAS must first be attained, which has been challenging to determine and highly debated (Kannan 2011). For example, the acid dissociation constant values determined for PFOA have ranged between 0 and 3.8 (Kannan 2011). These values are used to determine whether or not a chemical is expected to dissociate into their anions in media such as water, soil and sediment. Strong acids are expected to dissociate into their anion forms and are therefore highly water soluble. Both PFOS and PFOA have high water solubility in their anionic forms and are therefore transported via water in the environment, although they have also been shown to adsorb to solids (Kannan 2011). Both PFOS and PFOA are solids at room temperature (US EPA 2016a; US EPA 2016b) and are essentially non-volatile with vapour pressures of  $3.31 \times 10^{-4}$  Pa and 2.27 Pa respectively at 20°C (HC 2016b; HC 2016c). The vapour pressure of PFOA will increase as temperatures near its melting point of 54.3 °C (US EPA 2016b).

Due to PFOS's and PFOA's affinity for adsorbing to organic matter, AFFF impacted sites such as former firefighter training grounds remain contaminated with PFAS long after the sites have ceased to be used, as both PFOS and PFOA desorb relatively slowly over time (Arias E et al. 2015). Although shorter chain PFCAs and PFSAs are generally considered to desorb and transport more quickly than longer chain PFCAs and PFSAs, studies have shown that co-contaminants such as non-fluorinated surfactants can actually increase the sorption of shorter chain PFAS. It is believed that this might be the result of mixed hemimicelle formation by the shorter chain PFAS with the non-fluorinated surfactants (Guelfo and Higgins 2013). Figure 1-5, adapted from Weber et al. (2013), shows the difference between mixed hemimicelle adsorption and random adsorption.

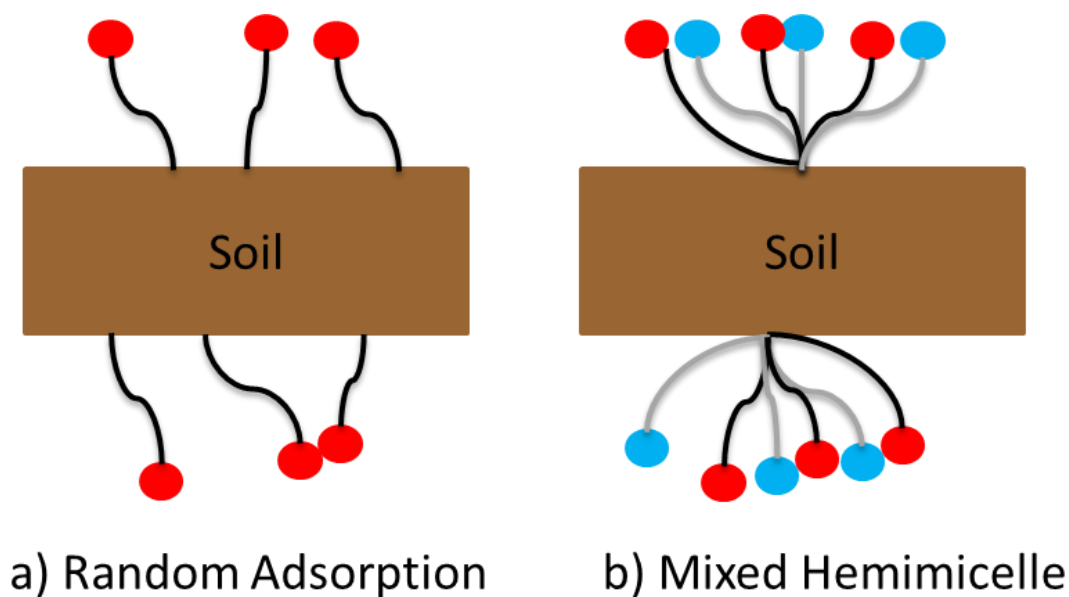


**Figure 1-5: Random adsorption compared to mixed hemimicelle formation.** In random adsorption (a), molecules of PFAS (black tail and red head group) will individually adsorb to soil wherever a free adsorption site exists, whereas in mixed hemimicelle formation (b), molecules of PFAS will adsorb to soil combined with molecules of non-fluorinated surfactants (grey tail and blue head group).

PFAS have been detected in the world's oceans in pg/L concentrations in both surface waters and deep waters. Sources of PFAS in the ocean are believed to be from inflows of PFAS contaminated rivers, as well as partitioning of volatile PFAS from the atmosphere (Ahrens et al. 2009; Lai et al. 2016). Once in the oceans, the vertical and horizontal distributions of PFAS indicate that they travel with global ocean currents and are transported into deeper waters due to down welling events (Yamashita et al. 2008; Ahrens et al. 2009; Brumovsky et al. 2016). It has been hypothesized that PFAS enter remote Arctic and Antarctic environments through ocean transport, and some believe that ocean waters could be the final sink for PFAS in the environment (Ahrens et al. 2009).

Another theory regarding how PFAS are transported to remote Arctic and Antarctic regions is that they are transported through the atmosphere as volatile precursors. Evidence of volatile precursors such as fluorotelomer alcohols, perfluoroalkyl sulfonamides and perfluoroalkyl sulfonamidoethanols have been found in the atmosphere over Northern Greenland (Bossi et al. 2016). Cai et al. (2012) detected PFOS concentrations around 18 pg/L in snow and lake water samples in Antarctica and concluded that the most likely source was volatile precursors that traveled through the atmosphere and eventually transformed to PFOS in the area of detection.

#### **1.2.4 Environmental Recovery, Remediation and Destruction of PFAS**

While the results of the literature review revealed several studies regarding environmental quantification, fate and transport of PFAS, relatively few were investigating potential methods to remediate PFAS from the environment. Studies that did focus on remediation techniques were looking into the decomposition of PFAS from water via sonochemical or electrochemical

treatment, or removal of PFAS from water through adsorption of PFAS to media such as activated carbon.

Sonochemical decomposition breaks chemical bonds using sound frequencies in a sonochemical reactor. While some of the C-F bonds were broken, the results indicated that the C-F tails were still largely intact (Vecitis et al. 2010; Rodriguez-Freire et al. 2016).

Electrochemical decomposition breaks the chemical bonds through the application of current. Using a commercially available Titanium/Rutheniumoxide anode in a divided electrochemical cell, the decomposition of both PFOS and PFOA was investigated at current densities ranging from 0 - 2 mA/cm<sup>2</sup>. This method was relatively successful, with up to 98% recovery of free fluoride for PFOS and 58% recovery for PFOA (Schaefer et al. 2015).

Removal of PFAS from water using granular activated carbon (GAC) has also been studied (Ochoa-Herrera and Sierra-Alvarez 2008). Activated carbon is produced from carbonaceous material such as coal, coconuts, nutshells or lignite. The source material is physically modified in a furnace where the atmosphere and temperature are controlled. The resulting product has a large surface area per unit volume and a network of pores ranging from less than 100 Angstrom to greater than 1000 Angstrom, where adsorption of chemicals can take place (Sherbondy and Mickler 2017). The results of the study by Ochoa-Herrera and Sierra-Alvarez (2008) indicated that PFAS adsorbed best to activated carbon when the influent concentrations of PFAS were highest (up to 80 mg/L). When using Calgon F400 brand of GAC, with an influent concentration of 80 mg/L, adsorption rates of PFOS, PFOA and PFBS were determined to be approximately 225 mg/g of GAC, 60 mg/g of GAC and 50 mg/g of GAC respectively (Ochoa-Herrera and Sierra-Alvarez 2008). Several other studies cited relatively successful use of activated carbon for remediation of PFAS from water, including full scale setups for treating drinking water (Yu et al. 2009; Hansen et al. 2010; Appleman et al. 2013; Appleman et al. 2014; Kempisty 2014). Appleman et al. (2014) reported GAC used for the removal of PFAS in full scale water treatment setups achieved removal rates ranging from 33 % for PFBS to >98% for PFOS. In general, longer chain PFAS adsorb to GAC better than shorter chain PFAS.

### **1.3 Knowledge Gaps**

The literature review yielded many articles that investigated the environmental quantification, fate and transport of PFAS from AFFF used by military installations at land based facilities. However, there was no mention regarding naval use of AFFF, nor the impact that naval use has on the environment. In particular, the answers to the following questions remain unknown:

- a. To what extent does naval use of AFFF contribute to the PFAS burden in the environment;
- b. What is the impact of the Navy's use of AFFF on the surrounding environment; and
- c. If the Navy's use of AFFF does impact the environment, what options exist to either reduce or eliminate PFAS release to the environment due to naval use?

## 1.4 Objectives of Thesis

As a result of the knowledge gaps identified above, the research objectives of this thesis are to:

- a. Identify where PFAS exists in the RCN, what types of PFAS are used in the RCN and in what quantities the PFAS are present;
- b. Understand the quantities of PFAS entering the environment, and the fate and transport of PFAS as a result of washing used AFFF overboard at sea; and
- c. Investigate methods to reduce or eliminate the PFAS released to the environment, and determine the feasibility of implementing one of these methods.

## 1.5 Thesis Organization

This thesis is organized into the following five chapters:

**Chapter 1** is an introduction to PFAS, including relevant background information, and the state of research with respect to PFAS in the environment as determined from an extensive literature review.

**Chapter 2** describes types and estimated quantities of PFAS in items used within the Royal Canadian Navy, focusing in particular on PFAS in AFFF used onboard warships, and the impact of releasing used AFFF into the surrounding environment.

**Chapter 3** presents the results of a hydrodynamic flow model that was employed to determine the fate and transport of PFAS from used AFFF if it is released into the ocean in the area of Halifax Harbour which is home to the RCN's fleet of ships within Canadian Fleet Atlantic Headquarters. This chapter is the basis for a manuscript that will be submitted to Water Research.

**Chapter 4** discusses various methods to reduce or eliminate PFAS entering the environment and investigates the implementation and practicality of employing GAC to remove PFAS from used AFFF onboard a warship using a numerical model.

**Chapter 5** summarizes the thesis, namely the results of Chapter 2 and the modelling studies presented in Chapters 3 and 4, and recommends future work in these areas.

## **Chapter 2 Per- and Polyfluoroalkyl Substances in the Royal Canadian Navy**

### **2.1 Structure and Functions of the RCN**

Canada's Navy was established in 1910 (Douglas 2017). The original fleet consisted of two battle cruisers, Niobe and Rainbow. The former was stationed in Halifax Harbour, and the latter in Esquimalt Harbour (Sarty 2017). Over the years, the size and structure of the Royal Canadian Navy (RCN) has varied, with peak numbers reaching over 90,000 personnel and 385 ships in June 1944 (Douglas 2017). Today, the RCN is comprised of Naval Staff Headquarters and three main formations: Maritime Forces Pacific (MARPAF) headquartered in Esquimalt, British Columbia and employing approximately 4,000 military personnel; Maritime Forces Atlantic (MARLANT) headquartered in Halifax, Nova Scotia and employing around 5,000 military personnel; and the Naval Reserve headquartered in Quebec City, with about 24 Naval Reserve Units located across Canada, each with up to 200 reserve members (RCN 2013).

The RCN is directed by the Commander of the RCN who is responsible for the strategic development and generation of a combat capable and multi-purpose navy. MARPAF and MARLANT are responsible for guarding their respective maritime approaches, and for fulfilling commitments both at home and abroad in order to maintain peace and security (RCN 2013).

In order to carry out its mandate, the RCN has a fleet of naval vessels that are distributed between MARPAF and MARLANT. The current fleet of ships consists of 12 Halifax Class Multi-Role Patrol Frigates each with a crew of 225 personnel, four Victoria Class Long-Range Patrol Submarines with a complement of 48 personnel each, 12 Kingston Class Maritime Coastal Defence Vessels with a crew of 37 to 41 personnel on each vessel, and eight ORCA Class Patrol Craft Training Vessels which carry a complement of 25 personnel each (RCN 2017).

### **2.2 Types and Quantities of PFAS in Items used by the RCN**

Per- and polyfluoroalkyl substances (PFAS) can be found in items used by personnel in the RCN. For example, PFAS is a key ingredient used in wind and water resistant clothing, such as those containing Gore-Tex technology. Personnel in the navy are issued a Navy Gore-Tex Parka, as well as Naval Wind Raingear, and Sea Boots, all of which are likely to contain PFAS (DHH 2017).

Lang et al. (2016) demonstrated that discarded clothing had the potential to release PFAS into the environment through landfill leachate. Using anaerobic model landfill reactors filled with clothing under biologically active and abiotic conditions, PFAS was measured in the aqueous phase leachate at concentrations up to 21.7 nmol/L, with the most predominant PFASs being C8 – C16 perfluoroalkyl carboxylic acids (PFCAs) (9.93 nmol/L) followed by C4 – C7 PFCAs (8.33 nmol/L) (Lang et al. 2016). Schlummer et al. (2013) measured the concentration of fluorotelomer alcohols (FTOHs), a known precursor to PFCAs, in the air of shops selling outdoor clothing at concentrations of up to 390 ng/m<sup>3</sup> with 8:2 FTOH being detected in the largest quantity (approximately 290 ng/m<sup>3</sup>). If 100% of the 8:2 FTOH were to transform to perfluorooctane carboxylic acid (PFOA), Schlummer et al. (2013) estimated that indoor air related intake of PFOA would exceed maximum daily allowable intake of PFOA determined by the Netherlands (0.2 ng/kg body weight/day) by a factor of 117 and would exceed the PFOA

intake for the Swedish population (between 0.35 and 0.69 ng/kg body weight / day) by a factor of 35.

In addition to RCN issued clothing and footwear that contain PFAS, the RCN also uses aqueous film forming foam (AFFF) in ships and submarines to combat Class B (hydrocarbon fuel) fires. The Halifax Class Frigates have fitted AFFF systems to protect compartments containing machinery, as well as the flight deck and hangar. The fitted systems hold 3600 L of 6% AFFF contained in two separate tanks (DND 2005). In a 6% AFFF, the AFFF is mixed with either freshwater or seawater in 6% solution, meaning 6 parts AFFF and 94 parts water. AFFF is also available in 1% and 3% formulas. The frigates also carry 14 cans (19 L each) of 6% AFFF and 158 cans (19 L each) of 3% AFFF for use at hose stations throughout the ship (Gallant 2017). The Kingston Class Maritime Coastal Defence Vessels have a 378 L tank of 6% AFFF for their fitted bilge system, which protects the engine rooms, and 12 cans (19 L each) of 3% AFFF for use in areas containing petroleum, oil and lubricants (McNaughton 2017). The Victoria Class Submarines have nine 20L drums of 6% AFFF, three SFU 90 extinguishers which contain 90 L of pre-mixed 6% AFFF and water, and eleven 9.5 L AFFF extinguishers onboard (Babcock 2015). Currently, AFFF used by the RCN is manufactured by Ansul and meets the US military specification MIL-F-24385F (DNPS 6-2 2016).

Each coast also has a Naval Fleet School Damage Control Division where sailors go to participate in damage control training, which includes firefighting. The Division Commanders at both Naval Fleet School (Atlantic) and Naval Fleet School (Pacific) both indicated that a fluorine free training foam with the brand name Calsoft is used at their respective Damage Control Training Facilities (DCTFs). The last time that an AFFF containing PFAS was used at the DCTF on the east coast was in 2001 during the set-to-work and trial period of the DCTF (Kujath 2017). There were no records of the last time that AFFF containing PFAS was used on the west coast, although it is reasonable to expect that AFFF containing PFAS might have been used up until 2003 when the DCTF on the west coast was commissioned.

According to a database report obtained from the Canadian Forces Fire Marshal (CFFM), there were 62 fires that were reported by Her Majesty's Canadian ships between 2007 and 2017. Only one ship indicated that the fitted AFFF system was used to extinguish the fire, although the quantity of AFFF used was not provided. There were eight fires that indicated hoses were used to extinguish the fire, but there was no indication of whether or not AFFF was used from the hose station (CFFM 2017). A separate report from an engine room fire onboard one of the Halifax Class frigates, which occurred in the early 2000s, indicated that approximately 2000 L of 6% AFFF from the fitted AFFF system was used, along with 27 cans of 3% AFFF in order to extinguish the fire. During this particular incident, AFFF was released overboard, although the exact quantities are unknown (Gallant 2017).

### **2.3 PFAS in AFFF**

Aqueous film-forming foam (AFFF) was developed at the US Naval Research Laboratory (NRL) in the early 1960s (DeYoung 1993). By 1968, the NRL had joined up with the 3M Company to develop a 6% seawater formulation. Testing was carried out in Jacksonville Florida in 1969 in accordance with military specification, MIL-F-24385 (Farley and Scheffey 2016). Place and Field (2012) report that according to the Department of Defense Qualified Products Listing, which



dated back to 1976, AFFF products manufactured by Ansul and National Foam were also certified to MIL-F-24385, in addition to the 3M product “Light Water”. By the mid 90’s Angus Fire and Chemguard were also manufacturing AFFF formulations that met the US Military Specification, followed by Buckeye and Fire Services Plus, Inc. around 2003 and 2010 respectively.

The purpose of PFAS in AFFF is to help the foam to spread evenly over the hydrocarbon fire in order to smother the fire. As the foam, mixed with water, exits the firehose it actually appears to unfold itself as it spreads over the fire. This unfolding occurs due to the chemical properties of the PFAS. As depicted in Figure 2-1, the hydrophobic tails will orient away from the water and towards the hydrocarbon fuel, while the hydrophilic heads orient into the water. Because the heads have a slight charge, they repel each other, which causes the foam to unfold and spread over the fire (Dlugogorski et al. 2002). The PFAS lowers the surface tension enough to allow the foam and water mixture to remain on top of the fuel surface. This foam and water mixture is believed to inhibit evaporation of the fuel and block percolation of the fuel through the foam, thus extinguishing the fire (Williams et al. 2011).

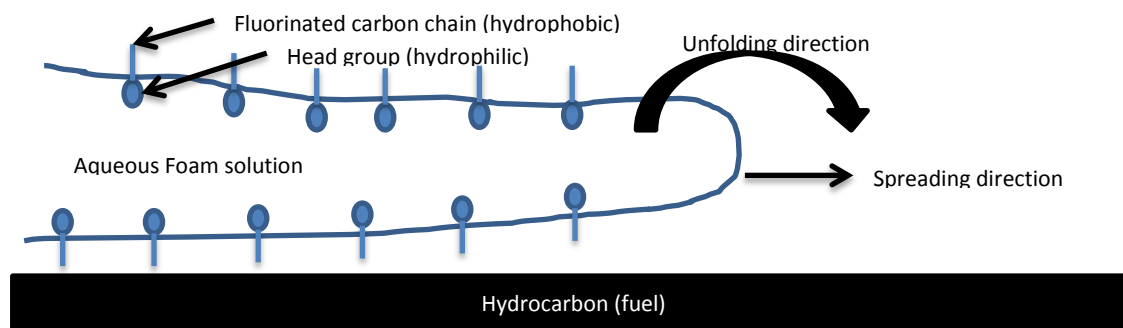


**Figure 2-1: The purpose of PFAS in AFFF. PFAS in AFFF orients itself so that the hydrophobic tails are away from the water and the hydrophilic heads orient into the water where their slight charge causes them to repel each other, which causes the foam to unfold and spread over the fire. Adapted from Dlugogorski *et al.* (2002).**

The chemical composition of the fluorinated surfactants used in AFFF is proprietary. As a result, studies have been undertaken to identify the types of PFAS present in different formulations of AFFF through analysis of the AFFF itself. Table 2-1 contains a compilation of types, and in some instances quantities, of PFAS detected in certain brands of AFFF using different analytical methods of detection and quantification. Place and Field (2012) analyzed 74 samples of AFFF with manufacturing dates ranging from 1984 to 2011 using a combination of fast atom bombardment mass spectrometry (FAB-MS) and high resolution quadrupole-time-of-flight mass spectrometry (QTOF-MS). All AFFF formulas analyzed were qualified for use by the US Military and thus met the stringent specifications of MIL-F-24385. The 3M manufactured foams, which were made using ECF and were manufactured up to 2002, contained C6 – C8 perfluoroalkyl sulfonic acids (PFSAs), and C4 – C6 perfluoroalkyl sulfonamide compounds (Place and Field 2012). Backe et al. (2013) identified C4 – C8 PFCAs in 3M AFFFs manufactured between 1989 and 2001 using large volume injection (LVI, 900 µL) high performance liquid chromatography tandem mass spectrometry (HPLC-MS/MS). Further work by Barzen-Hanson and Field (2015)

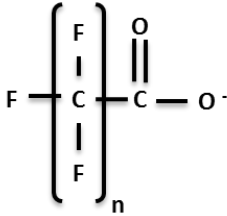
analyzing five samples of 3M AFFF formulations manufactured between 1989 and 2001 using liquid chromatography quadrupole-time-of-flight mass spectrometry (LC-QTOF-MS) also identified the presence of C2 and C3 PFASs. D'Agostino and Mabury (2014) analyzed commercially available 3M brand AFFF formulas using various analytical methods including Fourier transform ion cyclotron resonance mass spectrometry (FTICR-MS), LC-MS/MS and QTOF-MS. They detected a number of novel PFAS including C3 – C8 perfluoroalkyl sulfonamide amino carboxylates, C3 – C6 perfluoroalkyl sulfonamide ammonio dicarboxylic acids, C3 – C8 perfluoroalkyl sulfonamido amines, and C6 – C9 perfluoroalkyl sulfonamido amine oxides (D'Agostino and Mabury 2014). Most recently, Barzen-Hanson et al. (2017) employed a combination of previously used analytical techniques combined with non-target analysis of fluorinated surfactants using Kendrick mass defect (KMD) plots in order to identify 16 novel classes of PFAS in 3M AFFFs manufactured between 1988 and 2001, the majority of which contained variations of perfluoroalkane sulfonamides and one of which was a variation of perfluoroalkane sulfonamidoethanol (not shown in Table 2-1). In addition, five variations of PFASs were also detected in the 3M AFFF samples analyzed (also not shown in Table 2-1) (Barzen-Hanson et al. 2017).

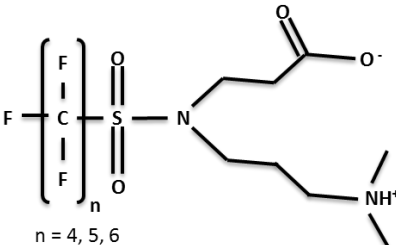
The other AFFF products analyzed by Place and Field (2012) were manufactured using telomerization, and contained various types of fluorotelomers with fluorinated chains ranging from C4 – C12. Backe et al. (2013) also analysed AFFF products manufactured using telomerization and were able to detect C4 – C8 fluorotelomer sulfonates (FTS) in addition to many of the FTs identified by Place and Field (2012). They were also able to quantify the different types of PFAS in the AFFF formulas that were analyzed. A summary of their results is included in Table 2-1. Recent analysis of fluorotelomer based AFFF formulations by Barzen-Hanson et al. (2017) revealed the presence of four more novel classes of PFAS (not shown in Table 2-1). The AFFFs analyzed by Place and Field (2012), Backe et al. (2013), Barzen-Hanson and Field (2015) and Barzen-Hanson et al. (2017) all met the requirements of MIL-F-24385, while D'Agostino and Mabury (2014) analyzed commercial AFFF products that would not necessarily have been tested to military specifications. However, one of the Angus AFFF formulas analyzed was identified by the Nato Stock Number (NSN) N-4210-21-900-4823, which is the NSN used by the RCN when ordering 19L cans of 3% AFFF (Gallant 2017). Novel PFAS detected in this sample of AFFF included perfluoroalkyl sulfonamide amino carboxylates, perfluoroalkyl sulfonamido amines and perfluoroalkyl sulfonamido amine oxides, all of which were also detected in one of the samples of 3M foam that was analyzed (D'Agostino and Mabury 2014).

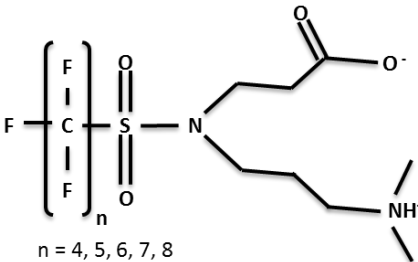
As a result of the phase out of long chain PFAS, it is reasonable to expect that formulations of AFFF available today may be different than those that were analyzed in the studies cited above. In fact, when an analysis was performed comparing formulations of AFFF manufactured in 2012 and 2013 to older versions of the same AFFF, the amount of C8 component in AFFF manufactured by Ansul had been reduced by nearly a factor of 10 (Ouellette et al. 2013). Previous analysis of Chemguard formulas of AFFF indicated that the manufacturer significantly reduced or eliminated the amount of C8 – C12 products sometime between 2007 and 2008 (Ouellette et al. 2013).

Table 2-1: A compilation of the types and quantities of PFAS detected in different formulas of AFFF using various methods of detection and analysis.

MANUFACTURER	DATE OF MANUFACTURE	METHOD OF DETECTION	GENERIC NAME	PROPOSED CHEMICAL STRUCTURE	CONCENTRATION (mg/L)	REFERENCE
3M	1988 - 2001	FAB-MS QTOF-MS	Perfluoroalkyl sulfonates	$  \begin{array}{c}  \left[ \begin{array}{c} \text{F} \\   \\ \text{C} \\   \\ \text{F} \end{array} \right]_n \\    \\  \text{F} - \text{C} - \text{S} \begin{array}{c} \text{O} \\    \\ \text{O} \end{array} - \text{O}^-  \end{array}  $ <p>n = 6,7,8</p>	N/A	Place and Field (2012)
3M	1989 - 2001	LVI (900 μL) HPLC-MS/MS	Perfluoroalkyl sulfonates	$  \begin{array}{c}  \left[ \begin{array}{c} \text{F} \\   \\ \text{C} \\   \\ \text{F} \end{array} \right]_n \\    \\  \text{F} - \text{C} - \text{S} \begin{array}{c} \text{O} \\    \\ \text{O} \end{array} - \text{O}^-  \end{array}  $ <p>n = 4, 5, 6,7,8, 9, 10</p>	PFBS 160 – 380 PFPeS 80 – 210 PFHxS 760 – 1700 PFHpS 93 – 410 PFOS 6700 – 15,000 PFNS 9 – 160 PFDS 11 – 102	Backe et al. (2013)
3M	1989 - 2001	QTOF-MS LC-MS/MS	Perfluoroalkyl Sulfonates	$  \begin{array}{c}  \left[ \begin{array}{c} \text{F} \\   \\ \text{C} \\   \\ \text{F} \end{array} \right]_n \\    \\  \text{F} - \text{C} - \text{S} \begin{array}{c} \text{O} \\    \\ \text{O} \end{array} - \text{O}^-  \end{array}  $ <p>n = 2, 3</p>	PFETs 7.0 – 13 PFPrS 120 – 270	Barzen-Hanson and Field (2015)

3M	1989 - 2001	LVI (900 $\mu$ L) HPLC- MS/MS	Perfluoroalkyl Carboxylates	 <p>n = 4, 5, 6, 7, 8</p>	PFBA 24 – 38 PFPeA 36 – 52 PFHxA 99 – 170 PFHpA 22 – 54 PFOA 83 – 170	Backe et al. (2013)
----	-------------	-------------------------------------	--------------------------------	---	---	------------------------

3M	1993 - 2001	FAB-MS QTOF-MS	Perfluoroalkyl sulfonamide amino carboxylic acid	 <p>n = 4, 5, 6</p>	N/A	Place and Field (2012)
----	-------------	-------------------	---	---	-----	---------------------------

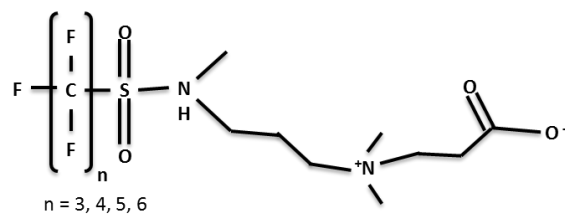
3M	1989 - 2001	LVI (900 $\mu$ L) HPLC- MS/MS	Perfluoroalkyl sulfonamide amino carboxylates	 <p>n = 4, 5, 6, 7, 8</p>	PFBSaAmA ND – 150 PFPeSaAmA 4 – 200 PFHxSaAmA ND – 960 PFHpSaAmA ND – 44 PFOSaAmA ND – 72	Backe et al. (2013)
----	-------------	-------------------------------------	--	--	---	------------------------

3M (FC-203FC  
Light Water)

Unknown, but  
MSDS was  
dated 1999

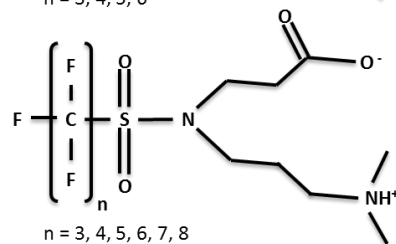
FTICR-MS  
QTOF-MS  
LC-MS/MS

Perfluoroalkyl  
sulfonamide  
amino  
carboxylates



N/A

D'Agostino  
and Mabury  
(2014)

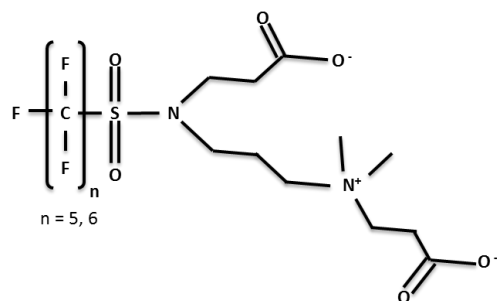


3M

1988 - 2001

FAB-MS  
QTOF-MS

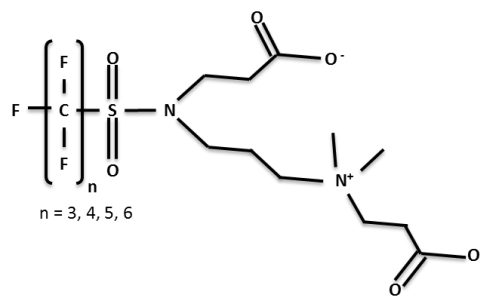
Perfluoroalkyl  
sulfonamide  
ammonio  
dicarboxylic  
acid



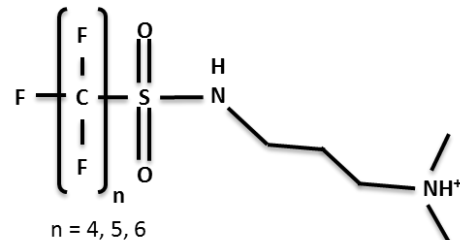
N/A

Place and  
Field (2012)

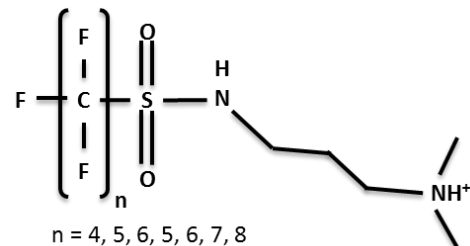
3M (FC-203FC Light Water) Unknown, but MSDS was dated 1999 FTICR-MS QTOF-MS LC-MS/MS Perfluoroalkyl sulfonamide ammonio dicarboxylic acid N/A D'Agostino and Mabury (2014)

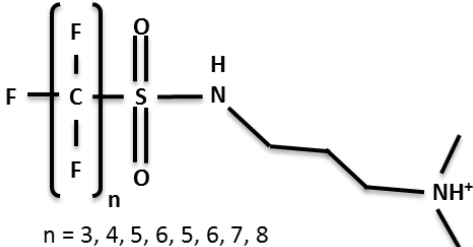


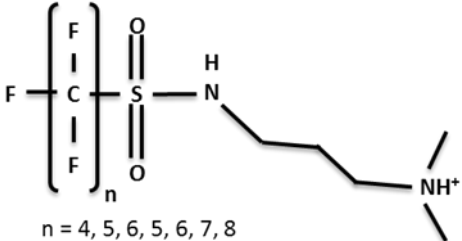
3M 1988 - 2001 FAB-MS QTOF-MS Perfluoroalkyl sulfonamide amine N/A Place and Field (2012)

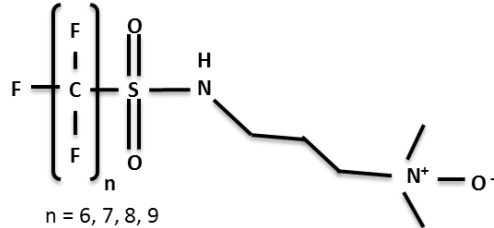


3M 1989 - 2001 LVI (900 μL) HPLC-MS/MS Perfluoroalkyl sulfonamido amines PFBSaAm 9 – 180 PFPeSaAm 8 – 180 PFHxSaAm 189 – 850 PFHpSaAm ND – 30 PFOSaAm 9.9 – 67 Backe et al. (2013)



3M (FC-203FC Light Water)	Unknown, but MSDS dated 1999	but was	FTICR-MS QTOF-MS LC-MS/MS	Perfluoroalkyl sulfonamido amines	 <p>n = 3, 4, 5, 6, 5, 6, 7, 8</p>	N/A	D'Agostino and Mabury (2014)
---------------------------	------------------------------	---------	---------------------------------	-----------------------------------	--	-----	------------------------------

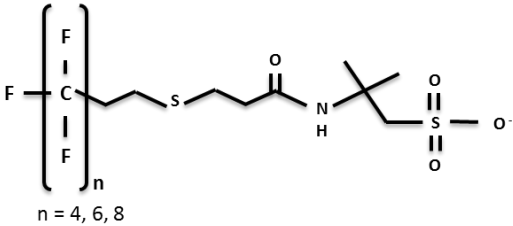
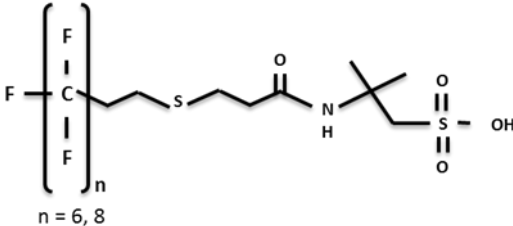
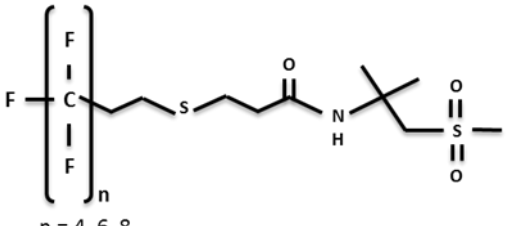
3M (ATC-603 Light Water)	Unknown, but MSDS dated 2005	but was	FTICR-MS QTOF-MS LC-MS/MS	Perfluoroalkyl sulfonamido amines	 <p>n = 4, 5, 6, 5, 6, 7, 8</p>	N/A	D'Agostino and Mabury (2014)
--------------------------	------------------------------	---------	---------------------------------	-----------------------------------	---	-----	------------------------------

3M (ATC-603 Light Water)	Unknown, but MSDS dated 2005	but was	FTICR-MS QTOF-MS LC-MS/MS	Perfluoroalkyl sulfonamido amine oxide	 <p>n = 6, 7, 8, 9</p>	N/A	D'Agostino and Mabury (2014)
--------------------------	------------------------------	---------	---------------------------------	--	---	-----	------------------------------

3M (FC-203FC Light Water)	Unknown, but was MSDS dated 1999	FTICR-MS QTOF-MS LC-MS/MS	N/A	<p style="text-align: center;">n = 4, 5, 6, 7, 8</p>	N/A	D'Agostino and Mabury (2014)
National Foam	2003 - 2008	FAB-MS QTOF-MS	n:2 fluorotelomer sulfonamide amine	<p style="text-align: center;">n = 6, 8</p>	N/A	Place and Field (2012)
National Foam	2003	LVI (900 μL) HPLC- MS/MS	n:2 fluorotelomer sulfonamido amines	<p style="text-align: center;">n = 6, 8</p>	6:2 FtSaAm 2100 8:2 FtSaAm 450	Backe et al. (2013)



National Foam	2003 - 2008	FAB-MS QTOF-MS	n:2 fluorotelomer sulfonamide betaine	<p>n = 4, 6, 8, 10</p>	N/A	Place and Field (2012)
National Foam	2003	LVI (900 $\mu$ L) HPLC- MS/MS	n:2 fluorotelomer sulfonamido betaines	<p>n = 4, 6, 8, 10, 12</p>	6:2 FtSaB 4600 8:2 FtSaB 540 10:2 FtSaB 450 12:2 FtSaB 210	Backe et al. (2013)
National Foam	2003	LVI (900 $\mu$ L) HPLC- MS/MS	n:2 fluorotelomer sulfonates	<p>n = 4, 6, 8</p>	4:2 FtS ND 6:2 FtS 42 8:2 FtS 19 L	Backe et al. (2013)
Ansul	1984 - 2010	FAB-MS QTOF-MS	n:2 fluorotelomer thioether amido sulfonic acid	<p>n = 6, 8</p>	N/A	Place and Field (2012)

Ansul	2005	LVI (900 $\mu$ L) HPLC- MS/MS	n:2 fluorotelomer thioamido sulfonates	 <p>n = 4, 6, 8</p>	4:2 FtTAoS 26 6:2 FtTAoS 6100 8:2 FtTAoS 1100	Backe et al. (2013)
Angus	1994 - 2012	FAB-MS QTOF-MS	n:2 fluorotelomer thioether amido sulfonic acid	 <p>n = 6, 8</p>	N/A	Place and Field (2012)
Angus	2002	LVI (900 $\mu$ L) HPLC- MS/MS	n:2 fluorotelomer thioamido sulfonates	 <p>n = 4, 6, 8</p>	4:2 FtTAoS 25 6:2 FtTAoS 4900 8:2 FtTAoS 170	Backe et al. (2013)

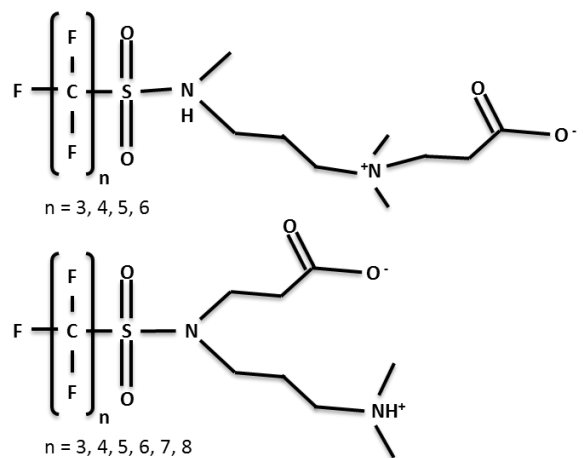
Angus	1994 - 2012	FAB-MS QTOF-MS	n:2 fluorotelomer thio hydroxy ammonium	<p>n = 6, 8</p>	N/A	Place and Field (2012)
Angus	2002	LVI (900 $\mu$ L) HPLC- MS/MS	n:2 fluorotelomer thio hydroxy ammonium	<p>n = 6</p>	6:2 FtTHN 2200	Backe et al. (2013)
Angus (N-4210-21-900-4823)	N/A (sample was obtained in 2005)	FTICR-MS QTOF-MS LC-MS/MS	N/A	<p>n = 3, 4, 5, 6, 7, 8</p>	N/A	D'Agostino and Mabury (2014)

Angus (N-4210-21-900-4823)

N/A (sample was obtained in 2005)

FTICR-MS  
QTOF-MS  
LC-MS/MS

Perfluoroalkyl  
sulfonamide  
amino  
carboxylates



N/A

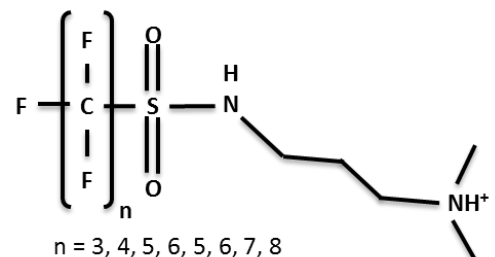
D'Agostino  
and Mabury  
(2014)

Angus (N-4210-21-900-4823)

N/A (sample was obtained in 2005)

FTICR-MS  
QTOF-MS  
LC-MS/MS

Perfluoroalkyl  
sulfonamido  
amines



N/A

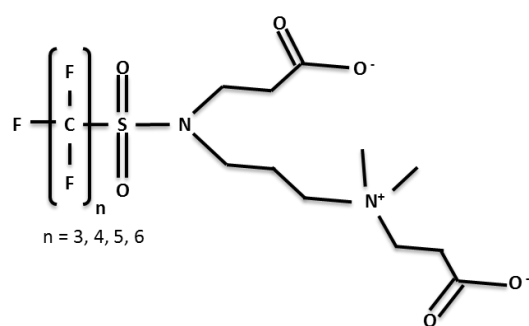
D'Agostino  
and Mabury  
(2014)

Angus (N-4210-21-900-4823)

N/A (sample was obtained in 2005)

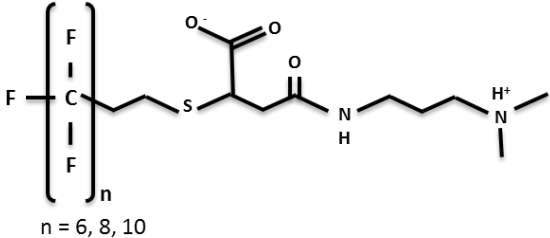
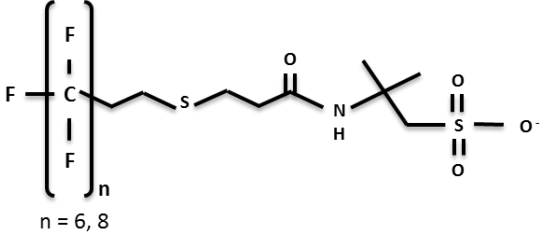
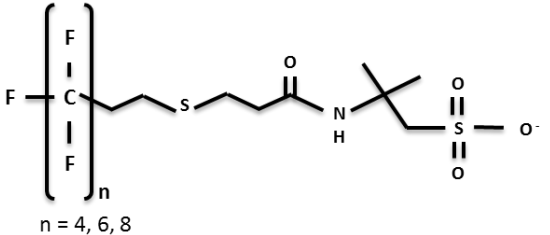
FTICR-MS  
QTOF-MS  
LC-MS/MS

Perfluoroalkyl  
sulfonamido  
amine oxide

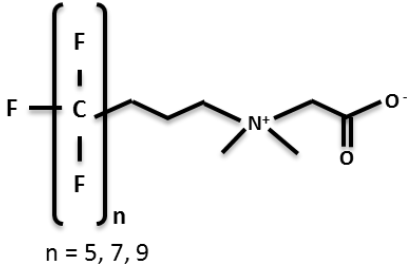
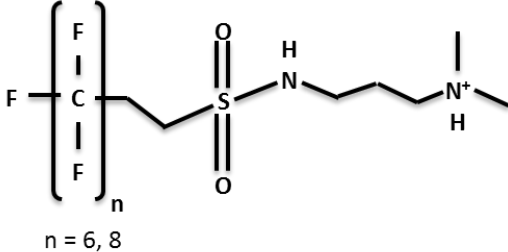
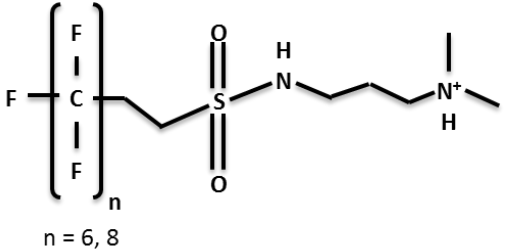


N/A

D'Agostino  
and Mabury  
(2014)

Chemguard	2006 - 2007	FAB-MS QTOF-MS	n:2 fluorotelomer thioether amido amino carboxylic acid	 <p>n = 6, 8, 10</p>	N/A	Place and Field (2012)
Chemguard	2008 - 2010	FAB-MS QTOF-MS	6:2 fluorotelomer thioether amido sulfonate	 <p>n = 6, 8</p>	N/A	Place and Field (2012)
Chemguard	2010	LVI (900 μL) HPLC- MS/MS	n:2 fluorotelomer thioamido sulfonates	 <p>n = 4, 6, 8</p>	4:2 FtTAoS ND 6:2 FtTAoS 11,000 8:2 FtTAoS 24	Backe et al. (2013)

Buckeye	2004 - 2012	FAB-MS QTOF-MS	n:1:2 fluorotelomer betaine	<p>n = 5, 7, 9</p>	N/A	Place and Field (2012)
Buckeye	2009	LVI (900 $\mu$ L) HPLC- MS/MS	n:1:2 fluorotelomer betaine	<p>n = 5, 7, 9</p>	5:1:2 FtB 2000 7:1:2 FtB 4700 9:1:2 FtB 1900	Backe et al. (2013)
Buckeye	2004 - 2012	FAB-MS QTOF-MS	n:3 fluorotelomer betaine	<p>n = 5, 7, 9</p>	N/A	Place and Field (2012)

Buckeye	2009	LVI (900 $\mu$ L) HPLC- MS/MS	n:3 fluorotelomer betaine	 <p style="text-align: center;">n = 5, 7, 9</p>	5:3 FtB 530 7:3 FtB 610 9:3 FtB 430	Backe et al. (2013)
Fire Services Plus	2011 - 2012	FAB-MS QTOF-MS	n:2 fluorotelomer sulfonamide amine	 <p style="text-align: center;">n = 6, 8</p>	N/A	Place and Field (2012)
Fire Services Plus	N/A	LVI (900 $\mu$ L) HPLC- MS/MS	n:2 fluorotelomer sulfonamido amine	 <p style="text-align: center;">n = 6, 8</p>	6:2 FtSaAm 3400 8:2 FtSaAm 720	Backe et al. (2013)

Fire Services Plus	2011 - 2012	FAB-MS QTOF-MS	n:2 fluorotelomer sulfonamide betaine	<p>n = 4, 6, 8, 10</p>	N/A	Place and Field (2012)
Fire Service Plus	N/A	LVI (900 $\mu$ L) HPLC- MS/MS	n:2 fluorotelomer sulfonamido betaine	<p>n = 4, 6, 8, 10, 12</p>	6:2 FtSaB 4800 8:2 FtSaB 1800 6:2 FtSaB 830 4:2 FtSaB 430	Backe et al. (2013)

ND is Not Detected, N/A is Not Applicable.



## 2.4 PFAS in the Environment as a Result of AFFF Usage

Perfluorinated carboxylates containing 6 – 8 perfluorinated carbons were first detected by Moody and Field (1999) in groundwater samples collected from two former US Military firefighter training sites that had been contaminated with AFFF. The concentration of the perfluorinated carboxylates detected ranged from 125 to 7090 µg/L. At the time, the types of PFAS being used in AFFF were unknown, so the authors were unable to determine if the PFAS detected in the groundwater was the same as that used in AFFF, or if it was a result of reactions taking place in the environment (Moody and Field 1999). As time progressed, and analytical methods improved, scientists were able to determine the types of PFAS present in both AFFF and in groundwater. In addition to analyzing PFAS in AFFF, groundwater samples taken from US Military firefighter training areas were also analyzed and the amount of PFAS present quantified by Backe et al. (2013) and Barzen-Hanson and Field (2015) (Table 2-2). The concentrations of individual types of PFAS ranged from below the limit of detection (LOD) to 880,000 ng/L for PFHxS (Barzen-Hanson and Field 2015). PFOS and PFOA were found in quantities ranging from 88 – 550,000 ng/L and 8.6 – 220,000 ng/L respectively (Backe et al. 2013; Barzen-Hanson and Field 2015). Currently, the US EPA has published a combined health advisory for PFOS and PFOA of 70 parts per trillion (ppt) in drinking water, which is equivalent to 0.07 ng/L (US EPA 2016c). This means that as a direct result of AFFF usage, PFOS and PFOA are being detected in groundwater in amounts that are more than several million times greater than what the US EPA consider safe for drinking water use.

Fluorotelomer thioamido sulfonates (FtTAoS) and fluorotelomer sulfonates (FtS) were also detected in groundwater samples from US Military sites (Backe et al. 2013). As previously discussed, three brands of AFFF were found to contain FtTAoS (Ansul, Chemguard and Angus) and two brands contained FtS (National Foam and Fire Services Plus). Backe et al. (2013) observed that the ratios of 4:2, 6:2 and 8:2 FtTAoS homologues in groundwater were different at each site, and also did not correlate with the ratios found in the samples of AFFF. They hypothesized that this could be a result of the PFAS partitioning to the aquifer solids, or as a result of the quantities of FtTAoS in earlier versions of AFFF formulations differing from those that were analyzed in their study (Backe et al. 2013). None of the AFFFs that were available for use during the time periods in which the military sites were in operation contained FtS. It was therefore hypothesized that the presence of FtS in the groundwater samples was a result of the degradation of FtTAoS in groundwater (Backe et al. 2013). Later work by Harding-Marjanovic et al. (2015) showed that 4:2, 6:2 and 8:2 homologues of FtTAoS could be biotransformed in microcosms over a period of 40 days to produce 4:2, 6:2 and 8:2 FtS, as well as 6:2 fluorotelomer unsaturated carboxylic acid (FtUCA), 5:3 fluorotelomer carboxylic acid (FtCA) and C4 – C8 PFCAs. The transformation products and proposed transformation pathway for 6:2 FtTAoS, the most abundant PFAS in Ansul brand AFFF, are shown in Figure 2-2a.

**Table 2-2: Concentrations of PFAS detected in groundwater at various US Military bases.**

Location	Years of Operation	Types of PFAS Detected	Quantities of PFAS Detected (ng/L)	Reference
Tyndall Air Force Base, USA	1980 – 1992	6:2 FtTAoS	<LOD – 8.8	Backe et al. (2013)
		PFBSaAm	<LOD – 720	
		PFPeSaAm	2.8 – 190	
		PFHxSaAm	5.7 – 260	
		PFBSaAmA	<LOD – 660	
		PFPeSaAmA	<LOD – 610	
		PFHxSaAmA	<LOD – 590	
Naval Air Station Fallon, USA	1950s - 1988	PFBSaAm	<LOD – 550	Backe et al. (2013)
		PFPeSaAm	<LOD – 61	
		PFHxSaAm	<LOD – 260	
		PFBSaAmA	<LOD – 9.7	
		PFPeSaAmA	<LOD – 5.8	
		PFHxSaAmA	<LOD – 38	
Wurtsmith Air Force Base, USA	1952 – 1993	PFBSaAm	26	Backe et al. (2013)
		PFPeSaAm	79	
		PFHxSaAm	36	
		PFPeSaAmA	<2.7	
		PFHxSaAmA	<2.7	
US Military Base (referred to as Site A)	1942 – 1990	4:2 FtTAoS	<LOD – 490	Backe et al. (2013)
		6:2 FtTAoS	<LOD – 6000	
		4:2 FtS	370 – 11,000	
		6:2 FtS	8900 – 220,000	
		8:2 FtS	58 – 370	
		PFBSaAm	<LOD – 54	
		PFPeSaAm	<LOD – 8.7	
		PFHxSaAm	<LOD – 45	
		PFBS	7100 – 150,000	
		PFHxS	36,000 – 360,000	
		PFHpS	1100 – 11,000	
		PFOS	15,000 – 78,000	
		PFDS	<LOD – 7	
		PFBA	3400 – 57,000	
		PFPeA	12,000 – 120,000	
		PFHxA	19,00 – 350,000	
		PFHpA	3300 – 45,000	
		PFOA	12,000 – 220,000	
		PFNA	40 – 390	
		PFDA	<LOD – 17	
PFUdA	<LOD - <3.1			

US Military Base (referred to as Site B)	1950 – 1993	6:2 FtTAoS	<LOD – 68	Backe et al. (2013)
		4:2 FtS	<LOD – 160	
		6:2 FtS	<LOD – 37,000	
		8:2 FtS	<LOD – 2300	
		PFBSaAmA	<LOD – 4.1	
		PFHxSaAmA	<LOD – 8.1	
		PFBS	12 – 24,000	
		PFHxS	81 – 170,000	
		PFHpS	<LOD – 4100	
		PFOS	88 – 65,000	
		PFDS	<LOD – 33	
		PFBA	8.5 – 13,000	
		PFPeA	4.9 – 35,000	
		PFHxA	<4.7 – 99,000	
		PFHpA	<6.0 – 7200	
		PFOA	8.6 – 57,000	
		PFNA	<LOD – 680	
		PFDA	<3.1 – 19	
		PFUdA	<LOD – 5.2	
		PFDoA	<LOD – <3.4	
Eleven Different US Military Sites (exact locations not specified)	Not provided	PFEtS	<LOD – 7500	Barzen-Hanson and Field (2015)
		PFPrS	19 – 63,000	
		PFBS	85 – 210,000	
		PFPeS	49 – 220,000	
		PFHxS	740 – 880,000	
		PFHpS	18 – 23,000	
		PFOS	130 – 550,000	
		PFNS	<LOD – 3000	
		PFDS	<LOD – 30	

---

Mejia-Avendano et al. (2016) also studied the biotransformation potential of PFAS used in AFFF, in particular, investigating the biotransformation potential of quaternary ammonium polyfluoroalkyl surfactants. These types of surfactants are documented in patents as being used in AFFF formulations (Mejia-Avendano et al. 2016). Perfluorooctaneamido quaternary ammonium salt (PFOAAmS) and perfluorooctane sulfonamide quaternary ammonium salt (PFOSAms) were aerobically biotransformed over a period of 180 days in soil microcosms. As shown in Figure 2-2b and c, PFOAAmS yielded 30 mol % PFOA after 180 days, while PFOSAms yielded 0.3% PFOS. Other transformation products detected in addition to PFOS, but in lesser concentrations, included PFOSAm, EtFOSA, FOSAA, and FOSA. The significantly slower biotransformation of PFOSAms was believed to be a result of PFOSAms' stronger sorption to the soil due to its longer perfluoroalkyl chain and bulkier sulfonyl group when compared to PFOAAmS (Mejia-Avendano et al. 2016).

As previously mentioned, the RCN employed AFFF at their damage control school for firefighter training until 2001 (Kujath 2017). A typical set up at a firefighting training area would generally include a concrete pad on which some type of hydrocarbon fuel is ignited and subsequently extinguished using either water, AFFF or potentially some other firefighting agent. Training exercises might occur weekly, or even several times per week (Baduel et al. 2015). One such set-up, located in Australia, was studied to determine the distribution and fate of the PFAS present. The surface of the training pad contained concentrations of PFAS ranging from 10 – 200 µg/g, with PFAS being detected as deep as 12 cm into the concrete pad. Kinetic desorption experiments conducted estimated that 50% of the PFOS present would desorb in 25 years, with the estimated time to desorb 90% of the PFOS being 82 years. By comparison, 50% of 6:2 FTS was expected to desorb in 0.7 years, with 90% of it expected to desorb in 2 years (Baduel et al. 2015). Based on the results of this study, it is possible that although AFFF has not been used at the DC school on the east coast since 2001, that PFAS are still present in the area, assuming that no initiatives have been made to remediate PFAS from the site.

Another method of assessing the persistence of the PFAS present in AFFF is to oxidize the PFCA and PFSA precursors in the AFFF or AFFF impacted media by using hydroxyl radicals. When Houtz et al. (2013) oxidized archived formulas of AFFF, between 5.9 and 10.8 g/L of PFCAs were generated, and 3M AFFF formulations also generated PFSAs. When AFFF contaminated groundwater was oxidized, it was determined that 23% of the PFAS present in the groundwater were precursors. The fractions were higher for the aquifer solids and the soil samples tested, where precursors accounted for 35% and 26% of all PFAS present respectively. In soil samples closer to the surface, that percentage increased to 38% on the most contaminated surficial soils (Houtz et al. 2013).

a)

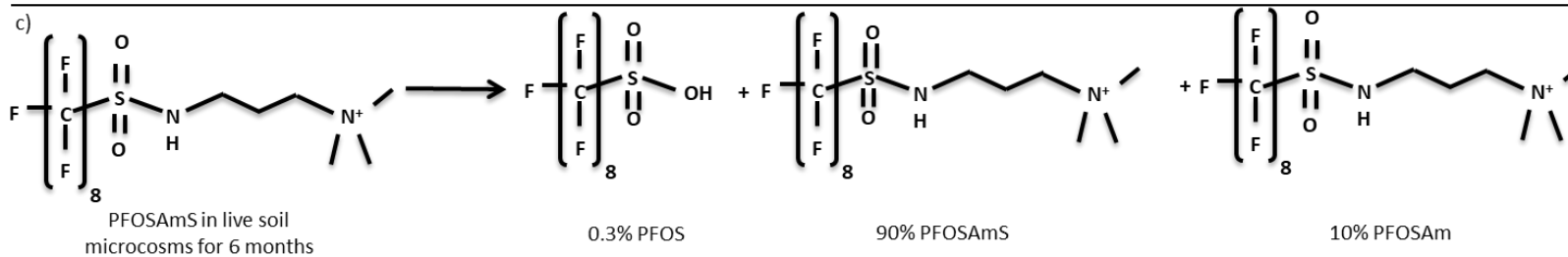
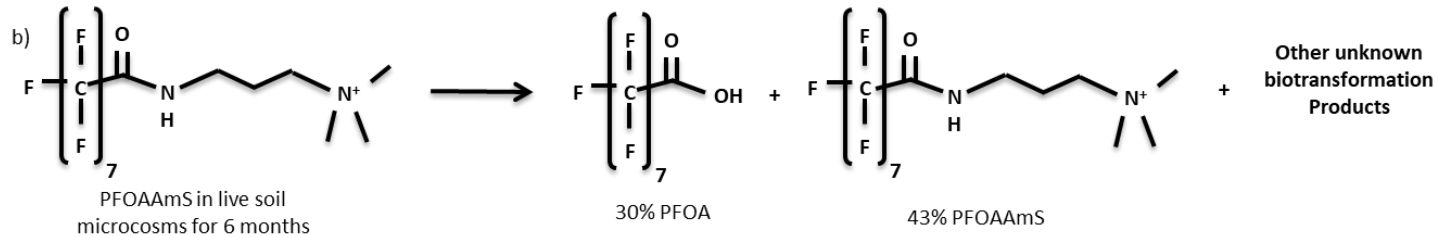
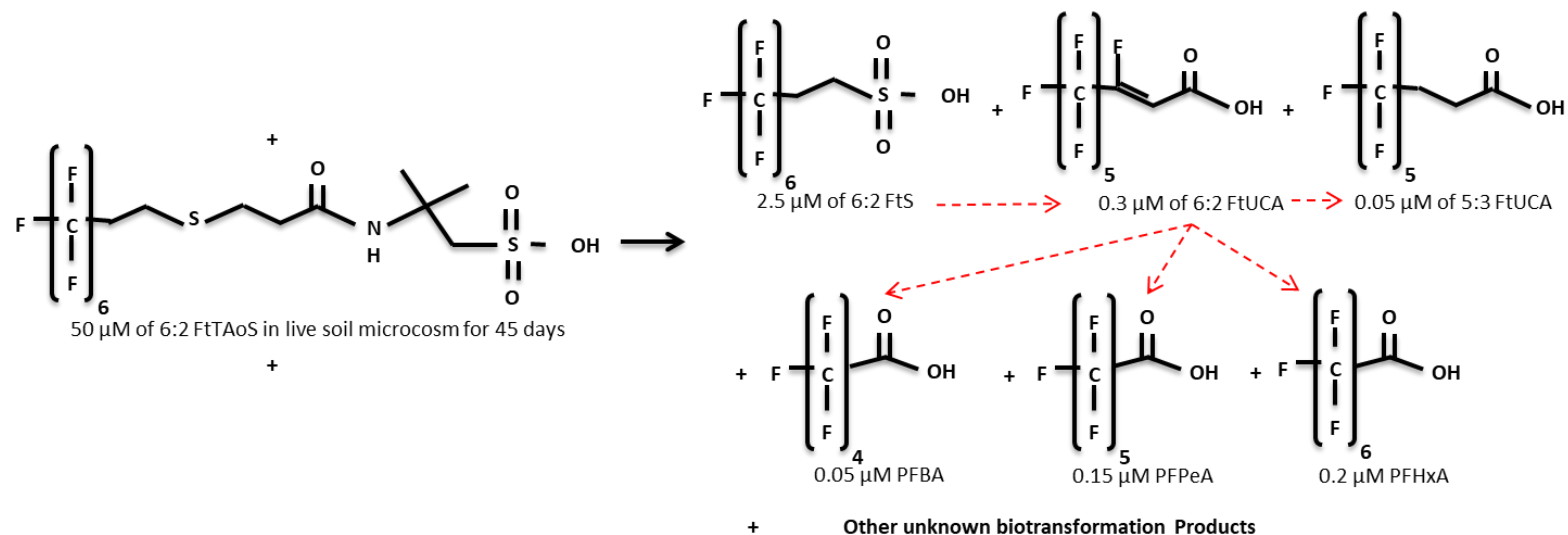


Figure 2-2: Biotransformation products of PFAS from AFFF in soil microcosms. The biotransformation products of 6:2 FtTAoS found in AFFF manufactured by Ansul are shown in a), as adapted from Harding-Marjanovic et al. (2015). The dashed red arrows represent the proposed transformation path. The biotransformation products of PFOAAmS and PFOSAms are shown in b) and c) as adapted by Mejia-Avendano et al. (2016).

The transport of the PFAS from AFFF impacted firefighting training areas can be affected by other components of the AFFF such as solvents and non-fluorinated hydrocarbon surfactants, as well as co-contaminants such as fuel. It is possible that the fuel and solvents may exist as non-aqueous phase liquids (NAPLs). It is believed that NAPLs can affect sorption of PFAS in two ways. They can act either as a sorbent and provide additional sites for sorption of the PFAS, or they can block sorption sites thus interfering with PFAS sorption. The former was observed with C4 – C6 PFCAs in the presence of trichloroethylene (TCE), and the latter was observed with the longer chain PFCAs in the presence of TCE (Guelfo and Higgins 2013). Likewise, hydrocarbon surfactants can facilitate greater sorption of PFCAs through mixed hemimicelles, or they can decrease sorption by competing for available sorption sites. The former was observed with C4 – C7 PFCAs and C4 PFSA in the presence of sodium decyl sulfate (SDS), and the latter was observed with C9 – C10 PFCAs and PFOS in the presence of SDS (Guelfo and Higgins 2013).

In addition to co-contaminants affecting transport of PFAS, PFAS can also affect the remediation of co-contaminants. Trichloroethene is an example of a solvent that might have been used to ignite a fire at a firefighting training area. Trichloroethene can be dechlorinated by *Dehalococcoides mccartyi*, which is a frequently used in the in-situ remediation of contaminated groundwater. When various types of AFFF including those produced by 3M, Ansul and National Foam were added to *D.mccartyi*-containing microbial communities, dechlorination was inhibited by those AFFF formulas containing fluorotelomers, but not by the 3M AFFF (Harding-Marjanovic et al. 2016). Further investigation revealed that 6:2 FtSaB slowed dechlorination at a concentration of 16 mg/L and completely stalled it at 32 mg/L (Harding-Marjanovic et al. 2016).

Once AFFF is released to the environment, the PFAS can impact the surrounding areas for many years. In 2000, an accidental release of 22,000 L of 3M AFFF mixed with 450,000 L of water occurred at the Toronto International Airport. The release contaminated water, sediment and fish in the area. Samples of sediment, water and fish were analyzed in 2003, 2006 and 2009. Nearly a decade after the release of the 3M AFFF, the PFOS concentrations found in the sediment of a nearby pond, which functions to control storm water flow into two creeks, remained elevated. PFOS concentrations in fish in the creeks downstream of the pond also remained elevated, being approximately 2 – 10 times higher than the concentrations of PFOS found in fish upstream of the pond (Awad et al. 2011).

Firefighters can also be affected by the PFAS in AFFF. Rotander et al. (2015) analyzed blood serum from 149 firefighters in Australia and determined that serum PFOS levels were 6 – 10 times higher than those found in the general population (mean of 74 ng/L versus 12 ng/L), and PFHxS levels were 10 – 15 times higher than those of the general population (mean of 33 ng/L versus 3.2 ng/L). The number of years working as a firefighter was positively associated with higher serum concentrations of PFOS and PFHxS (Rotander et al. 2015).

## 2.5 Fluorine Free Foam (FFF) as an Alternative to AFFF

As a result of the persistence and related health concerns of PFAS, it begs the question, why not switch to firefighting foams that are fluorine free? As previously mentioned, with AFFF, the fluorosurfactants allow a thin film to form and spread across the flammable liquid, which in turn blocks the diffusion of the flammable vapours. With the FFF, there is no film formed and consequently, the properties of the foam itself must block the diffusion of the flammable vapours. Schaefer et al. (2008) tested the sealability properties of three different fluorine-free foams against those of an AFFF. Sealability refers to the foams ability to block the diffusion of flammable vapours. The AFFF formulation used by Schaefer et al. (2008) was manufactured by 3M and compliant with the US Military Specification. One of the FFFs used was RF6, which was manufactured by 3M Australia until 2006 and is currently manufactured by Solberg as Rehealing Foam. RF6 was and is still compliant with International Civil Aviation Organization Level B protocol. The other two FFF formulations, referred to as A and B, used in the experiment were purchased in Australia in 2004, but did not contain any approvals or compliance listings. Schaefer et al. (2008) reported that the AFFF suppressed vapours from aviation gasoline for 180 min compared to an average of 67 minutes for RF6, while formulas A and B each provided approximately 10 minutes of protection prior to vapour ignition occurring. When experiments were conducted using n-heptane, the ranking of the films remained consistent, with AFFF outperforming RF6, and both formulations A and B providing little protection. When experiments were performed with seawater, the performance ranking again remained unchanged. Although the RF6 FFF did not perform as well as the AFFF, it still demonstrated satisfactory performance, and depending on the standards required, could be a possible substitute for PFAS containing AFFFs (Schaefer et al. 2008).

In separate tests performed at the NRL's Chesapeake Bay Detachment by Williams et al. (2011) in 2010, two MilSpec (MIL-F-24385F) qualified AFFFs (National Foam 6% concentrate and Buckeye 3% concentrate) and one FFF (Solberg RF6) were tested for fire extinguishment and burnback (re-ignition) performance using four different fuels: gasoline (the current fuel used for MilSpec testing), commercial grade heptane (fuel being considered for MilSpec testing), iso-octane (2,2,4-trimethylpentane) and methylcyclohexane (MCH). Testing procedures used were those indicated in the MilSpec with the exception of the foam application time for the burnback tests, which was reduced from 90 s to 60 s. In order to achieve the MilSpec requirements, the foam must extinguish 28 ft<sup>2</sup> of burning gasoline within 30 s, and burnback (re-ignition) must not occur within the first 360 s following foam application. The surface tension of both heptane and iso-octane is less than gasoline (0.02 and 0.0187 versus 0.0237 N/m respectively), whereas the surface tension for MCH is similar to gasoline (0.0236 N/m). As a result of the lower surface tension for heptane and iso-octane, the Buckeye foam was only marginal on iso-octane (fuel ignited on some attempts), and the National foam was unable to produce a film. The National foam was also considered marginal on heptane, as a flame occurred after a 5 s wait time, but not after a 60 s wait time. As the Solberg foam does not contain fluorosurfactants, no film was formed on any of the fuels. The fire extinguishment times on gasoline, heptane and MCH (all fuels where some degree of film was formed) were better by approximately 15 to 20 s for both National and Buckeye foams than they were for the Solberg foam, however, on iso-octane, the fire out time for the Solberg foam was approximately 3 seconds better than that for both National and Buckeye foams. Consequently, the formation of a film appears to be in important

factor in achieving the desired fire extinguishment performance in AFFFs. Despite this conclusion, the Solberg's foam performance on iso-octane indicates that a foams ability to extinguish fires can be improved through optimization of mechanical properties of the foam such as yield stress. In the burnback performance tests, all foams were able to achieve burnback times being greater than 360 seconds, as prescribed by the MilSpec. Despite iso-octane having the lowest surface tension and hence lower ability for film formation, the longest burnback times were achieved with this fuel. The shortest burnback times were with MCH. The results indicate that film formation does not influence burnback time performance (Williams et al. 2011).

Although the test results cited demonstrate that in the majority of cases, the AFFF outperformed the FFF, the results observed by Williams et al. (2011) provide some evidence that other properties besides film formation contribute to foam performance, and it is possible that these properties may one day be optimized to meet the stringent requirements of MIL-F-24385F. In Australia, the government has, in some cases, authorized the use of FFF. According to an Australian Government Department of Defence document that was published in June 2007, 3M RF6 was one of two brands of foam that were permitted for procurement, the other being Ansulite. According to their quick reference guide, RF6 was permitted for use in emergency situations involving air crashes, vehicle fires and/or building fires, whereas the only brand of foam permitted for use by the Navy was Ansulite (Australian Government 2007). Although RF6 does not contain any fluorinated compounds, it was deemed more toxic than Ansulite and more persistent than Ansulite according to the Australian Government (2007).

## **2.6 Summary and Conclusions.**

An investigation was conducted to determine the types and estimated quantities of PFAS in items within the RCN. It was found that the greatest quantities of PFAS exist in the AFFF used onboard RCN vessels. Combined, the RCN fleet of ships and submarines carries just over 90,000 L of undiluted AFFF. Historical reports indicate that AFFF has previously been used to extinguish fires on RCN vessels, and personal accounts indicate that used AFFF was released into the environment in some cases. At present, the RCN uses AFFF manufactured by Ansul that meets the U.S Military Specification MIL-F-24385F, and contains 6:2 FtTAoS, which can biotransform into 6:2 FTS, 6:2 FtUCA, 5:3 FtUCA, PFBA, PFPeA and PFHxA. AFFF usage at land based installations has resulted in PFOS and PFOA being detected in groundwater in quantities that are several million times higher than the US EPA's combined health advisory limit for PFOS and PFOA of 70 ppt. Studies conducted at former fire fighter training areas and former sites of AFFF releases indicate PFAS from AFFF can impact the surrounding environment and wildlife in the area for many years, and even decades. The results of the investigation presented in this chapter suggest that AFFF used by the RCN at sea could potentially result in the addition of PFAS into the environment, which could potentially impact the affected areas for an extended time period. As the number of vessels in the RCN is quite small compared to other nations, such as the United States or Russia, who each possess hundreds of commissioned warships, the results of this investigation suggest that globally, naval use of AFFF at sea could potentially contribute substantial quantities of PFAS to the environment.



## Chapter 3 Hydrodynamic Modelling of PFAS Fate and Transport from AFFF in Halifax Harbour

### 3.1 Introduction

Per- and polyfluoroalkyl substances (PFAS) are a key ingredient used in aqueous film forming foam (AFFF) (Buck et al. 2011), which is a fire extinguishing agent primarily used to combat Class B (flammable liquid) fires such as hydrocarbon fuels. The unique properties of PFAS are essential in AFFF to lower the surface tension of the foam, which allows it to form a film over hydrocarbon fuels. This prevents fuel vapours from transporting through the foam barrier and coming into contact with oxygen in the air, and thus extinguishes fuel based fires (Ouellette et al. 2013). The Royal Canadian Navy (RCN), which operates out of Halifax, Nova Scotia and Esquimalt, British Columbia, employs AFFF onboard warships and submarines to extinguish Class A (normal combustibles) and Class B fires. (DNPS 6-2 2016). On the Halifax Class Canadian Patrol Frigates (CPFs), AFFF fitted systems are installed to protect a number of compartments onboard including the Hangar, Flight Deck and Quarterdeck, all of which are located on the upper deck (DNPS 6-2 2016). When the AFFF system is used at sea, the AFFF can wash overboard resulting in the addition of PFAS to the surrounding environment.

PFAS are considered persistent in the environment and are ubiquitous in water, sediments, air, food, wildlife and humans (Ahrens et al. 2010). PFAS has been detected in oceans around the world on the order of 1 – 10,000 pg/L concentration. In the mid-northwest Atlantic Ocean, Benskin et al. (2012) reported PFAS in quantities ranging from 77 – 190 pg/L and up to 5800 pg/L just off the coast of Rhode Island. Yamashita et al. (2008) found that vertical profiles of PFAS in the oceans reflect global ocean circulation and suggested that PFAS could be used as chemical tracers to study open ocean circulation. In coastal areas, the PFAS concentrations are also measured in harbour sediments. Some examples include 0.61 – 3.4 ng/g in sediments in Vancouver Harbour, British Columbia (Benskin et al. 2012), 5.96 ng/g in Baltimore Harbor, Maryland (Higgins et al. 2005), and 0.224 – 19.14 ng/g in Charleston Harbor (White et al. 2015). Since PFAS does not degrade in the environment, transport from the source by coastal circulation naturally reduces the concentrations over time.

Modelling the transport and fate of PFAS in nearshore environments has been studied in other coastal areas. As examples, Li et al. (2017) predicted PFAS transport in the Daling River to the Bohai Sea in China using the one-dimensional Mike-11 model, and Happonen et al. (2016) simulated the transport of PFAS in the River Kokemäenjoki in Finland using the one-dimensional SOBEK model. In these studies, PFAS was treated as a conservative tracer. Miyake et al. (2014) used a three-dimensional chemical fate prediction model (National Institute of Advance Industrial Science and Technology – Risk Assessment Model: AIST-RAM) to estimate PFAS concentrations in the water column and sediment in Tokyo Bay. In this study, the vertical transport of PFAS was estimated by considering the adsorption of PFAS to phytoplankton and detritus in combination with their sinking rate.

The contribution of PFAS to the marine environment and transport of these contaminants as a result of AFFF usage in warships has not been studied and are not well understood. To gain a

better understanding of this issue, a hydrodynamic model is used to predict the transport of a conservative tracer that represents PFAS released into Halifax Harbour, Nova Scotia. Circulation, flushing time and transport of passive tracers has been studied in this region (Shan and Sheng 2012) using a hydrodynamic model, however this study of Halifax Harbour did not include the effects of surface waves. In the present study, the contaminant transport is simulated for three different time periods with different wind and wave conditions, and the transport of PFAS released from several locations inside and outside the Harbour is computed. The results of this study inform whether PFAS, from AFFF, released from warships is of a concern in the Halifax Harbour area.

## **3.2 Observations**

### **3.2.1 Study Area**

Halifax Harbour is located on the east coast of Nova Scotia. The harbour has five distinct regions: the Bedford Basin, the Narrows, the Northwest Arm, the Inner Harbour and the Outer Harbour (Fader 2007) as depicted in Figure 3-1. A small river with a mean annual discharge of approximately  $5 \text{ m}^3/\text{s}$  (Buckley and Winters 1992) flows into the head of the Harbour, making it an estuary. The depth of the Harbour varies from approximately 70 m deep in the deepest part of the Bedford Basin to just over 20 m deep in the Narrows (Fader 2007). The tide in Halifax Harbour is semi-diurnal and has a maximum range of 2.1 m, and the mean circulation in the Harbour is two-layer estuarine type circulation with net transport in the top layer toward the ocean and net transport in the bottom layer into the system (Shan et al. 2011). Off the southeast (SE) coast of Nova Scotia is the Scotian Shelf where a current runs southward with a mean velocity of approximately 0.1 m/s (Hannah et al. 2001). Wave data for Halifax Harbour is available at two locations; the Halifax Harbour Buoy (44258) located in the Approaches to Halifax Harbour at  $44.500^\circ\text{N}$  and  $63.400^\circ\text{W}$  and the SmartAtlantic Buoy (Smart) located just off of Herring Cove at  $44.559^\circ\text{N}$  and  $63.546^\circ\text{W}$ . On a calm day, waves at station 44258 will be approximately 1 m, but can increase substantially during storm events. During Hurricane Juan, one of the most damaging storms in recent history, waves in the Outer Harbour reached a maximum height of 19.9 m and a maximum significant wave height of 9.0 m (Xu and Perrie 2012). Wind speed and direction data are available from both station 44258 and the Smart Buoy. The Smart Buoy also provides current speed and direction data from a current profiler that has 20 vertical bins of 2 m each, with the top bin located at 5 m below the sea surface. Water level data is available from the Bedford Basin (491) tide gauge located at  $44.694^\circ\text{N}$  and  $63.624^\circ\text{W}$ . Data from a 300 kHz Teledyne RDI Workhorse Sentinel Acoustic Doppler Current Profiler (ADCP) deployed by Defence Research and Development Canada in the Bedford Basin at approximately  $44.685^\circ\text{N}$  and  $63.621^\circ\text{W}$  in July 2013 was also available. The ADCP was upward facing with 65 depth cells of 0.5 m each. The range of the first cell was 2.71 m and the range of the last cell was 34.71 m (Crawford 2014). The locations of the instruments described above are shown in Figure 3-1, and a summary of the data available from each of the instruments is listed in Table 3-1.

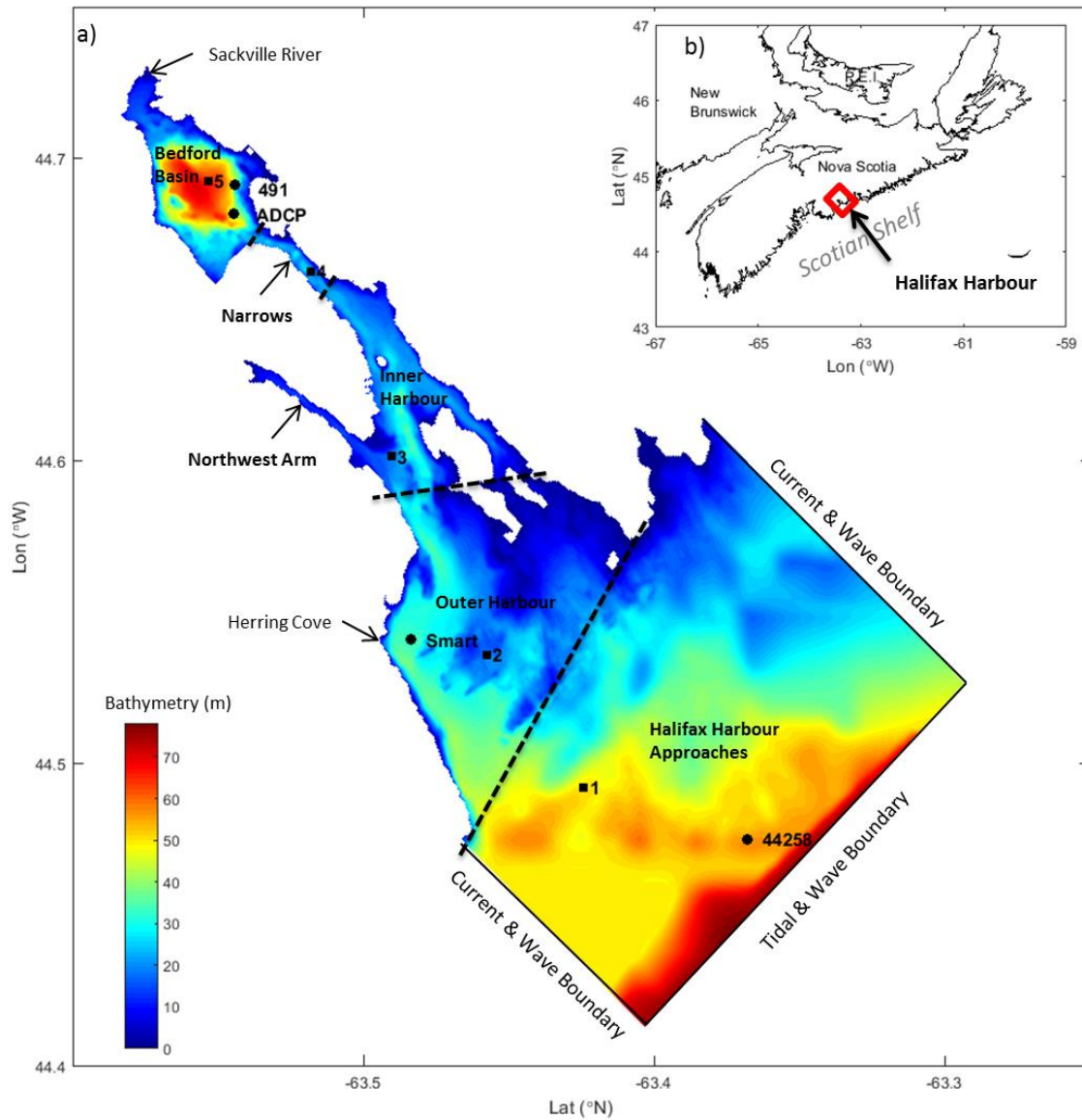


Figure 3-1: Location and Layout of Halifax Harbour. Halifax Harbour is located on the southeast coast of Nova Scotia as shown on the inset (b). The layout, bathymetry, location of instruments whose data was used to either force or validate the model (black circles) and the five PFAS release locations used in the model simulation (black squares) are shown in (a).

**Table 3-1: Hydrographic and meteorological, stations, instruments and data.**

Station/Instrument	Available Data (units)							
	$\eta$ (m)	U(m/s)	$U_{dir}$ ( $^{\circ}$ )	u(m/s)	$u_{dir}$ ( $^{\circ}$ )	$H_s$ (m)	$T_p$ (s)	MWD( $^{\circ}$ )
Bedford 491 Tide Gauge	•							
Herring Cove Smart Buoy		•	•	•	•	•	•	•
Halifax Harbour 44258 Buoy		•	•			•	•	
ADCP				•	•			

Water Level ( $\eta$ ), Wind Speed (U), Wind Direction ( $U_{dir}$ ), Current Speed (u), Current Direction ( $u_{dir}$ ), Significant Wave Height ( $H_s$ ), Peak Wave Period ( $T_p$ ), Mean Wave Direction (MWD)

The Canadian Forces Base Halifax Naval Dockyard is located on the southwest shore of the Narrows. The dockyard is homeport to seven of the RCN’s 12 CPFs. Onboard the CPFs, AFFF systems are installed in compartments that are vulnerable to Class B fires (DNPS 6-2 2016). The CPFs are fitted with two AFFF supply tanks, each containing 1.8 m<sup>3</sup> of 6% AFFF (DND 2005). The design pressure of the AFFF system is 10 bar (DNPS 6-2 2016). The flow rate of AFFF varies from 2.16 to 136.44 m<sup>3</sup>/h depending on the location and size of the AFFF protected compartment (DND 2005). Currently, AFFF used by the RCN is manufactured by Ansul and meets the US military specification MIL-F-24385F (DNPS 6-2 2016).

According to a database report received from the Canadian Forces Fire Marshal, between 2007 and 2017, there were 62 fires that were reported by Her Majesty’s Canadian ships. Of those 62 fires, only one entry indicated that the fitted AFFF system was used to extinguish the fire, but the quantity of AFFF used was not provided (CFFM 2017).

### 3.2.2 Observations in the Three Study Periods

To investigate the effects of wind and waves on the distribution of PFAS from used AFFF washed overboard, three distinct scenarios were chosen; a period with moderate wind and wave influence, a second period with little wind and no wave influence, and finally, a third time period with stronger wind and wave influence. The first scenario, referred to as Scenario A from this point on, occurred over a three day time period from year day (YD) 256 to 258 in 2014 (13 - 15 September). This time period was chosen based on a relatively calm period in which the wind was blowing from the northwest (NW) at an approximate speed of 2 m/s (Figure 3-2b and c), followed by a small storm where the wind direction abruptly changed so that it was blowing from the east, and gradually increased to greater than 10 m/s. During this time period, the waves changed from a significant wave height of 0.5 m to greater than 2 m (Figure 3-2d). This small storm lasted almost 24 hours, and was immediately followed by a period of calm. The current magnitude measured at the Smart Buoy (Figure 3-2e) shows an increase in the bins located within 20 m of the surface that correspond with the change in wind direction. The observed water levels measured at the 491 tide gauge are shown in Figure 3-2a. Hindcasting of Scenario A was used to calibrate the model.

The second scenario, referred to as Scenario B, covered a period of ten days in July 2013, from YD 190 to YD 199. During this time, data from an ADCP deployed in Bedford Basin was also available. This data allowed for validation of the modelled currents in the Bedford Basin. In the first three days of this time period (YD 190 to 192) the winds were light, peaking around 7 m/s (Figure 3-2g) and changed in a clockwise direction (Figure 3-2h). The waves at 44258 remained

constant with a significant wave height of 0.5 – 1.0 m (Figure 3-2i). Current magnitude recorded at the ADCP (Figure 3-2j) appears to be linked closely with the tides at the 491 tide gauge (Figure 3-2f). Data from the Herring Cove Smart Buoy was not available during this time period.

The third scenario, referred to as Scenario C, occurred during YDs 84 through 86 in 2014 (25 – 27 March). This scenario was used to validate the performance of the model during a storm scenario in which significant wave height at the Smart Buoy reached approximately 5 m (Figure 3-2n). During this storm, the wind was changing in a counter clockwise direction (Figure 3-2m) and reached speeds greater than 15 m/s (Figure 3-2l). At the peak of the storm, water levels surged approximately 0.5 m above the previous high tide level (Figure 3-2k). Observed current magnitude at the Smart Buoy also peaked during the height of the storm (Figure 3-2o).

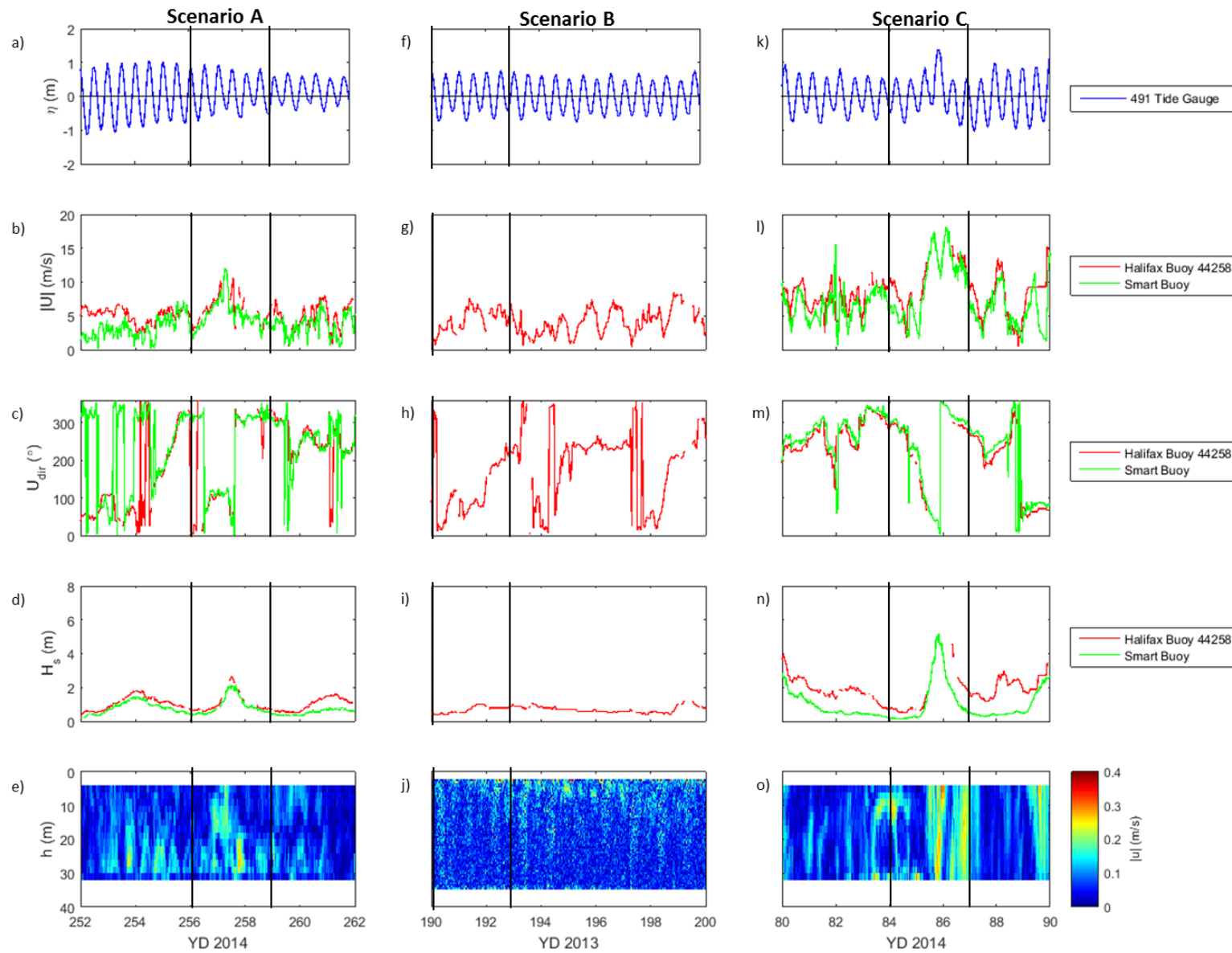


Figure 3-2: Data for Modelling Scenarios. Data from Scenario A (a through e) in September 2014 was used to calibrate the model, while data from Scenario B (f through j) in July 2013 and Scenario C (k through o) in March 2014 were used to validate the model. The year days between the black vertical lines were modelled for each of the three scenarios.

## 3.3 Modelling

### 3.3.1 Model Description

Hydrodynamic modelling of Halifax Harbour was accomplished using the coupled Delft3D-FLOW and Delft3D-WAVE modules. This modelling software has successfully been used to model circulation in tidal environments such as Minas Basin, Nova Scotia (Ashall et al. 2016) , wave-driven circulation in Lunenburg Bay, Nova Scotia (Mulligan et al. 2008), and transport of conservative tracer-like substances (Brown et al. 2014).

Delft3D-FLOW is a hydrodynamic flow model that calculates non-steady flow using both tidal and meteorological forcing in both two (depth averaged) and three dimensions (Elias et al. 2001). The flow module solves the following system of equations using a finite difference method (Lesser et al. 2004):

Horizontal momentum equations

$$\frac{\partial U}{\partial t} + U \frac{\partial U}{\partial x} + V \frac{\partial U}{\partial y} + \frac{w}{h} \frac{\partial U}{\partial \sigma} - fV = -\frac{1}{\rho_0} P_x + F_x + M_x + \frac{1}{h^2} \frac{\partial}{\partial \sigma} \left( v_V \frac{\partial u}{\partial \sigma} \right) \quad [1]$$

$$\frac{\partial V}{\partial t} + U \frac{\partial V}{\partial x} + V \frac{\partial V}{\partial y} + \frac{w}{h} \frac{\partial V}{\partial \sigma} - fU = -\frac{1}{\rho_0} P_y + F_y + M_y + \frac{1}{h^2} \frac{\partial}{\partial \sigma} \left( v_V \frac{\partial v}{\partial \sigma} \right) \quad [2]$$

Continuity equation

$$\frac{\partial \zeta}{\partial t} + \frac{\partial [h\bar{U}]}{\partial x} + \frac{\partial [h\bar{V}]}{\partial y} = S \quad [3]$$

Transport equation

$$\frac{\partial [hC]}{\partial t} + \frac{\partial [hUC]}{\partial x} + \frac{\partial [hVC]}{\partial y} + \frac{\partial [wC]}{\partial \sigma} = h \left[ \frac{\partial}{\partial x} \left( D_H \frac{\partial C}{\partial x} \right) + \frac{\partial}{\partial y} \left( D_H \frac{\partial C}{\partial y} \right) \right] + \frac{1}{h} \frac{\partial}{\partial \sigma} \left[ D_V \frac{\partial C}{\partial \sigma} \right] + hS \quad [4]$$

The meaning of the symbols used in Equations [1] through [4] and their associated units are provided in Table 3-2.

**Table 3-2: Nomenclature and units for the system of equations in Delft3D-FLOW.**

Symbol	Units	Meaning
C	kg/m <sup>3</sup>	Mass concentration
D <sub>Hr</sub> , D <sub>V</sub>	m <sup>2</sup> /s	Horizontal and vertical diffusion coefficient
f	1/s	Coriolis coefficient
F <sub>x</sub> , F <sub>y</sub>	m/s <sup>2</sup>	Horizontal Reynold's stresses
h	m	Water depth
M <sub>x</sub> , M <sub>y</sub>	m/s <sup>2</sup>	External sources and sinks of momentum
P <sub>x</sub> , P <sub>y</sub>	Pa	Horizontal pressure terms
S	m/s	Source and sink terms
t	s	time
u, v, w	m/s	Eulerian velocity components
U, V	m/s	Generalized Lagrangian Mean (GLM) velocity components
Ū, V̄	m/s	Depth-averaged GLM velocity components
x, y, z	m	Cartesian coordinates
ν <sub>Hr</sub> , ν <sub>V</sub>	m <sup>2</sup> /s	Kinematic viscosity
ρ <sub>0</sub>	kg/m <sup>3</sup>	Reference density of water
σ	---	Scaled vertical coordinate; σ=0 at surface, and σ=-1 at bed level
ω	s <sup>-1</sup>	Vertical velocity component in σ coordinate system
ζ	m	Water surface elevation above reference datum

The Delft3D-WAVE module uses the third generation shallow-water wave model Simulating WAVes Nearshore (SWAN) to estimate wave parameters while accounting for refractive propagation, wind growth, bottom dissipation, depth induced wave breaking and current dissipation (Booij et al. 1999; Elias et al. 2001; Lesser et al. 2004). In SWAN, the evolution of the wave spectrum is given by the spectral action balance equation:

$$\frac{\partial}{\partial t} N + \frac{\partial}{\partial x} c_x N + \frac{\partial}{\partial y} c_y N + \frac{\partial}{\partial \sigma} c_\sigma N + \frac{\partial}{\partial \theta} c_\theta N = \frac{S}{\sigma} \quad [5]$$

The terms on the left side of Equation [5], from left to right, represent: (1) the local rate of change of action density, N, in time; (2) the propagation of action in the x direction where  $c_x$  is the propagation velocity in the x direction; (3) the propagation of action in the y direction where  $c_y$  is the propagation velocity in the y direction; (4) the shifting of the relative frequency,  $\sigma$ , as a result of variations in depths and currents in the  $\sigma$  direction where  $c_\sigma$  is the propagation velocity in the  $\sigma$  direction; and (5) depth-induced and current-induced refraction where  $c_\theta$  is propagation velocity in the  $\theta$ -space where  $\theta$  represents the wave direction (Booij et al. 1999). The term S on the right side of Equation [5] is an energy density term that represents the effects of generation, dissipation and non-linear wave-wave interactions (Booij et al. 1999).

### 3.3.2 Model Setup

For the FLOW module, a rectangular grid of Halifax Harbour with 50 m horizontal resolution was constructed with 10 equally spaced vertical layers in topography-following coordinates where each layer has a thickness equal to 10% of the local depth. A tidal boundary was established on the SE side of the grid and current boundaries simulating a 0.1 m/s shelf current were set on the northeast (NE) and SW sides of the grid as depicted in Figure 3-1. The tidal boundary used a reflection parameter alpha of 10,000. The purpose of the reflection parameter is to reduce the spin up time of the model from a cold start (Deltares 2014). Use of the reflection parameter



alpha was able to smooth out the results of the modelled water levels, but at the same time, introduced an offset between the modelled and observed data of approximately 1 hour. This offset was corrected by subtracting 1 hour from the modelled time points prior to plotting the modelled results data.

For the WAVE module, a coarser grid with 100 m resolution was used for the wave computations, and hydrodynamic values were used from the FLOW module. Wave boundaries were established on the NE, southeast (SE) and SW sides of the grid.

Bathymetry for the model, shown in Figure 3-1, was obtained from Canadian Hydrographic Service (CHS) and consisted of 5m multi-beam bathymetric data. Any gaps in the bathymetric data provided by CHS were filled in using the bedrock layer of the ETOPO1, 1 arc-minute, global relief model available from the National Oceanic and Atmospheric Administration. Bathymetry within 500 m of the tidal boundary was altered to maintain a consistent depth along the boundary in order to reduce abnormal current spikes along the boundary itself.

Observed wind and wave data from the Halifax Harbour Buoy 44528 was used for input into the model, along with tide predictions obtained from the WebTide Tidal Prediction Model (v0.7.1) for Halifax Harbour. Any gaps in the wind and wave data were dealt with by repeating the last data entry until the next observed data was available. Data from the Bedford Basin 491 tide gauge was used to validate modelled water level results, and the Herring Cove Smart Buoy was used to validate modelled current and wave results for Scenarios A and C. Since the mean wave direction (MWD) was only available from the Herring Cove Smart Buoy, and not station 44258, and there were no other buoys in the area that provided MWD, the MWD data from the Smart Buoy was used as input into the model. Data from the ADCP was used to validate modelled current for Scenario B. Observation points were entered into the model to correspond with the location of the Bedford Basin 491 tide gauge, the ADCP, the Smart Buoy and the Halifax Harbour 44258 Buoy (Figure 3-1).

Default formulas in both the FLOW and WAVE modules were used, with the exception of the formula for whitecapping, in which case the formula of Van der Westhuysen (2007) was chosen over the default formula of Komen et al. (1984) as it has been shown to provide more accurate results (Mulligan et al. 2008). The sensitivity of the model in depth averaged mode was tested against different values for the horizontal eddy viscosity and the Chezy coefficient for bottom friction. Sensitivity was evaluated by comparing the magnitude of the averaged current,  $|u_{avg}|$ , produced by the model given the different values of horizontal eddy viscosity and Chezy coefficient that were tested.

The horizontal eddy viscosity is associated with horizontal turbulent motions, and the default value in Delft3D-FLOW is  $1 \text{ m}^2/\text{s}$  (Deltares 2014). However, for strongly stratified bodies of water, a smaller horizontal eddy viscosity value is often more suitable (Deltares 2014). The values of horizontal eddy viscosity tested in this model were 0.01, 1, and  $100 \text{ m}^2/\text{s}$ .

The default formula used by Delft3D-Flow to simulate bottom roughness is the Chezy formula, which uses a Chezy coefficient,  $c$ , in order to calculate bed shear stress,  $\tau_b$ , in accordance with Equations [6] and [7] when using the depth averaged mode (Deltares 2014).

$$\tau_b = \frac{\rho_0 g \bar{U} |\bar{U}|}{c^2} \quad [6]$$

$$\tau_b = \frac{\rho_0 g \bar{V} |\bar{V}|}{c^2} \quad [7]$$

The default value used by Delft3D-FLOW for  $c$  is  $65 \text{ m}^{1/2}/\text{s}$  (Deltares 2014). The model was also tested using a  $c$  of  $92 \text{ m}^{1/2}/\text{s}$ . This value of  $c$  corresponds to a decrease in  $\tau_b$  by a factor of 2.

Inflow from the Sackville River into the Bedford Basin was represented in some early model runs by using a discharge of  $5 \text{ m}^3/\text{s}$ . As this parameter did not have any effect on the modelled currents at the ADCP or Smart Buoy locations, it was not included in the model runs discussed in this Chapter.

The model was calibrated by matching the modelled data to observed data for four different parameters including water level, current magnitude, significant wave height and peak wave period for Scenario A. The different forcing mechanisms (tide, wind and waves) were added to each run in succession in order to understand the effects of the forcing mechanism on the model's ability to accurately hind cast the four different parameters being evaluated. Validation of the model was accomplished by comparing water levels and current magnitude for both Scenarios B and C. Comparison of modelled and observed significant wave height and peak wave period was also used to validate the model for the Scenario C. The root-mean-square-error was calculated for the near surface current magnitude using Equation [8], where  $|u_o|$  is the observed current magnitude,  $|u_m|$  is the modelled current magnitude and  $n$  is the number of data points. The different model runs discussed in this study are summarized in Table 3-3.

$$\text{RMSE} = \sqrt{\frac{\sum (|u_o| - |u_m|)^2}{n}} \quad [8]$$

**Table 3-3: Summary of Model Runs. List of the model runs discussed in this paper, the model scenario that they covered and the model forcing mechanisms that were applied.**

Run ID	Model Scenario	Forcing Mechanisms
R01	A	Tide
R02	A	Tide + Wind
R03	A	Tide + Wind + Waves
R04	B	Tide + Wind
R05	C	Tide + Wind + Waves

### 3.3.3 Modelling Scenarios

The release of PFAS from five different locations was simulated in model runs R03, R04 and R05. The five PFAS release locations shown in Figure 3-1 were chosen based on the likelihood of a CPF transiting through or conducting training or other evolutions in that particular area. PFAS release location 1 was placed in the Approaches to Halifax Harbour in order to determine whether or not a PFAS release outside of Halifax Harbour would impact the nearshore environments within the Harbour. PFAS release locations 2 and 3 were placed in the Outer

Harbour and Inner Harbour respectively along the route used to enter and exit Halifax Harbour. Release location 4 corresponds with where the ships are tied up when they are in home port, and release location 5 corresponds with the route taken by the ships when transiting to and from the Canadian Forces Ammunition Depot, which is located on the NE shore of Bedford Basin. It is also possible that ships might conduct trials or other evolutions in the Bedford Basin.

The model required three inputs for the release of PFAS: (1) the input concentration of PFAS; (2) the input flow rate of PFAS; and (3) the start and stop date and time of the PFAS release. The input concentration of PFAS was determined based on information available for Ansulite 6% (AFC-6MS) AFFF concentrate. The safety data sheet lists four chemicals used in the product that are considered hazardous under the US Occupational Safety and Health Administration, one of which is listed as “Trade secret” with a proprietary Chemical Abstracts Service number. The PFAS used in AFFF are often listed in the safety data sheets as proprietary, secret or confidential, so it is reasonable to assume that the chemical referred to as “Trade secret” in the Ansulite safety data sheet is referring to the PFAS present in the product. The mass fraction,  $w_i$ , for this component of the AFFF is listed between 0.07 and 0.13 (Tyco 2015). The density of Ansulite 6% (AFC-6MS) AFFF is  $1030 \text{ kg/m}^3$  at  $25^\circ\text{C}$  (Johnson 2017). Given this information, the concentration of PFAS for input into the model can then be determined by combining and simplifying Equations [9] through [13] to come up with Equation [14]. Nomenclature and units for Equations [9] through [14] are provided in Table 3-4.

$$C_{\text{PFAS}} = \frac{M_{\text{PFAS}}}{V_{\text{T}}} \quad [9]$$

$$V_{\text{T}} = Q \times t \quad [10]$$

$$M_{\text{PFAS}} = w_i \times M_{\text{AFFF}} \quad [11]$$

$$M_{\text{AFFF}} = \rho_{\text{AFFF}} \times V_{\text{AFFF}} \quad [12]$$

$$V_{\text{AFFF}} = 0.06 \times V_{\text{T}} \quad [13]$$

$$C_{\text{PFAS}} = w_i \times \rho_{\text{AFFF}} \times 0.06 \quad [14]$$

A PFAS concentration of  $6 \text{ kg/m}^3$  was input into the model, which represents a median mass fraction of 0.10.

**Table 3-4: Nomenclature and Units for Equations [9] through [14].**

<b>Symbol</b>	<b>Units</b>	<b>Meaning</b>
$C_{\text{PFAS}}$	$\text{kg/m}^3$	Concentration of PFAS
$M_{\text{PFAS}}$	kg	Mass of PFAS
$V_{\text{T}}$	$\text{m}^3$	Volume of AFFF + Seawater
$Q$	$\text{m}^3/\text{s}$	Flow of AFFF + Seawater
$t$	s	Duration of flow of AFFF + Seawater
$w_i$	--	Mass fraction of PFAS in AFFF by weight
$M_{\text{AFFF}}$	Kg	Mass of AFFF
$\rho_{\text{AFFF}}$	$\text{kg/m}^3$	Density of AFFF

Q was estimated as 0.006 m<sup>3</sup>/s based on the rated flow through a standard VARI nozzle at 6.9 bar, such as would be applied if AFFF were deployed through either the port or starboard hangar lobby hydrants, or the port or starboard quarterdeck hydrants. This most likely would not be the exact flowrate, as that would depend on the system pressure at the hydrants, as well as any frictional losses through the firehose. The AFFF systems are designed to operate at 10 bar pressure, but friction losses through the fire hose would result in a lower flow rate than the flow at the hydrant. Due to the uncertainty of the losses due to friction in the fire hoses, a flow rate of 0.006 m<sup>3</sup>/s, based on the rating of the nozzle, is a reasonable estimate for the input flow of PFAS into the ocean.

The release duration of PFAS was set to 10 minutes for model runs R03, R04 and R05. At the chosen flow rate, 0.216 m<sup>3</sup> of AFFF is consumed from the 3.600 m<sup>3</sup> of AFFF contained in the system, which equates to approximately six percent of the AFFF held in the system.

The PFAS released in the model was treated as a conservative tracer. According to the data sheet for Ansulite 6% (AFC-6MS) AFFF, the formulation contains C-6 fluorochemicals that were manufactured using a telomer based process (Johnson 2017). Based on the PFAS in this formulation being a fluorotelomer, it is likely that the PFAS would partition to the atmosphere, or react in the environment. However, since this study is looking at a worst case scenario in terms of the quantity of PFAS in the ocean, and different formulations will include different PFAS, it was deemed appropriate to treat the PFAS as a conservative tracer. In addition, the monthly mean temperature of the water in Halifax Harbour ranges from approximately 2°C in the winter to a high of 14°C in the summer (Shan and Sheng 2012), and the vapour pressure of fluorinated compounds has been shown to increase with increasing temperatures (Dias *et al.* 2005), indicating that partitioning to the atmosphere would be less likely in the cold waters of the Atlantic Ocean.

## 3.4 Results and Discussion

### 3.4.1 Model Calibration

Modelled results from Scenario A, using default values for horizontal eddy viscosity and the Chezy coefficient for bottom friction, compared to observed data for water level, near surface current magnitude, significant wave height and peak wave period are presented in Figure 3-3 a, b, c and d respectively. The model results for current magnitude for all layers of the model for runs R01, R02 and R03 are compared to those observed at the Smart Buoy for bins ranging from 5 to 29 m from the surface in Figure 3-4 a, b, c and d respectively. The observed water levels at the 491 tide gauge were fairly well matched by the model when only tidal forcing was used (R01). The addition of wind and wave forcing (R02 and R03) for this particular scenario did not have any impact on the water levels at the 491 location. For comparison of the near surface currents at the Smart Buoy location, the results from the second layer of the model were compared to the observed data from the 5 m bin. At the Smart buoy location, the second layer of the model is located between 3.2 and 6.4 m from the surface. Although addition of wind forcing in R02 was able to increase the near surface current magnitude slightly compared to the tidal only forcing of R01, the wave forcing added in R03 was key to achieving a very good match

between the modelled and observed data, particularly during the small storm event on YD 257. The RMSE for the near surface current magnitude in run R03 was calculated to be 0.03 m/s. The model was not as good at replicating the current magnitude at greater depths, although it was able to capture the increase in current magnitude at all depths during the small storm event on YD 257. The model was also able to accurately replicate the significant wave height in R03, and was fairly good at modelling the peak wave period, particularly on YD 257.

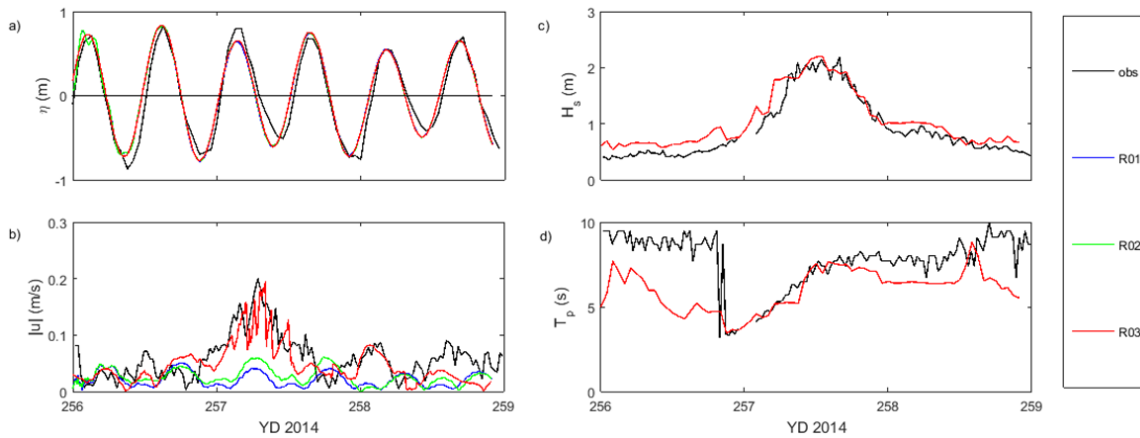


**Figure 3-3: Model Calibration Results.** Comparison of observed data with model results for tide only forcing (R01), tide + wind forcing (R02), and tide + wind + wave forcing (R03) for a) water level, b) near surface current magnitude, c) significant wave height and d) peak wave period.

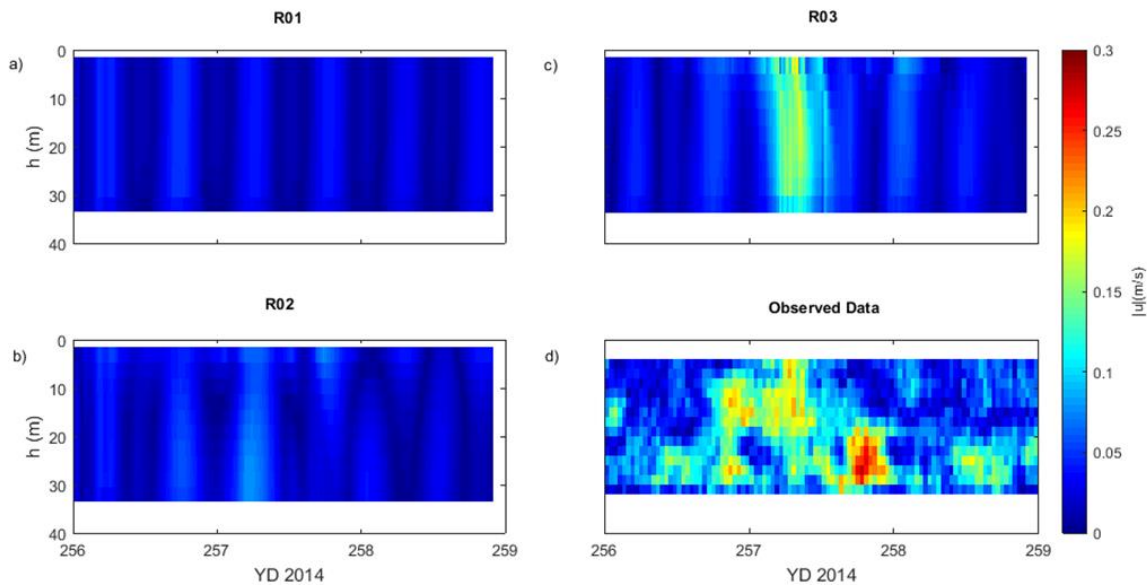


**Figure 3-4: Model Calibration Results for Current Magnitude at all Depths.** Comparison of modelled current magnitude,  $|u|$ , in all depth layers for a) tide only forcing, b) tide + wind forcing and c) tide + wind + wave forcing with d) the observed data.

A sensitivity analysis was conducted in order to understand the effects of changing the horizontal eddy viscosity on the averaged current magnitude, as well as the effects of altering

the Chezy coefficient for bottom friction on the averaged current magnitude. The results presented in Table 3-6 show that changing these parameters had very little effect on the modelled current magnitude. Increasing the Chezy coefficient was able to slightly increase the averaged current magnitude by 0.003 m/s, but this increase was considered so minor that the default value of  $65 \text{ m}^{1/2}/\text{s}$  was used for the remainder of the model runs in order to more easily facilitate cross study comparisons in the future.

**Table 3-5: Sensitivity Analysis Results. A comparison of different values of horizontal eddy viscosity and Chezy coefficient for bottom friction on the modelled average current speed for simulation of YD 256 to 259 in 2014.**

Horizontal Eddy Viscosity ( $\text{m}^2/\text{s}$ )	Chezy Coefficient ( $\text{m}^{1/2}/\text{s}$ )	Modelled $ u_{\text{avg}} $ (m/s)
1 (default)	65 (default)	0.022
0.01	65 (default)	0.019
100	65 (default)	0.012
1 (default)	92	0.025

### 3.4.2 Model Validation

Model validation results for Scenario B, run R04, and for Scenario C, run R05, are shown in Figure 3-5 and 3-6 respectively. The model accurately matched the observed water levels at the 491 tide gauge (Figure 3-5a) for Scenario B. The model also captured the tidal patterns (Figure 3-5c) visible in the observed ADCP current magnitude (Figure 3-5d), although the averaged current magnitude produced by the model in the top 10 m is slightly off in terms of when the current magnitude peaked, as well as the variation between the highs and lows. The modelled lows were around 0.01 m/s, whereas the observed lows were around 0.05 m/s. The RMSE calculated for the near surface current at the ADCP location was 0.06 m/s. While it is possible that the model is just not correctly reproducing the currents, it is equally possible that the differences in the modelled and observed current magnitudes are a result of the observation location in the model not being at the exact location as the deployed ADCP. The grid size used in the model made it virtually impossible to locate the observation locations at the exact grid coordinates as the actual instruments that collected the observed data.

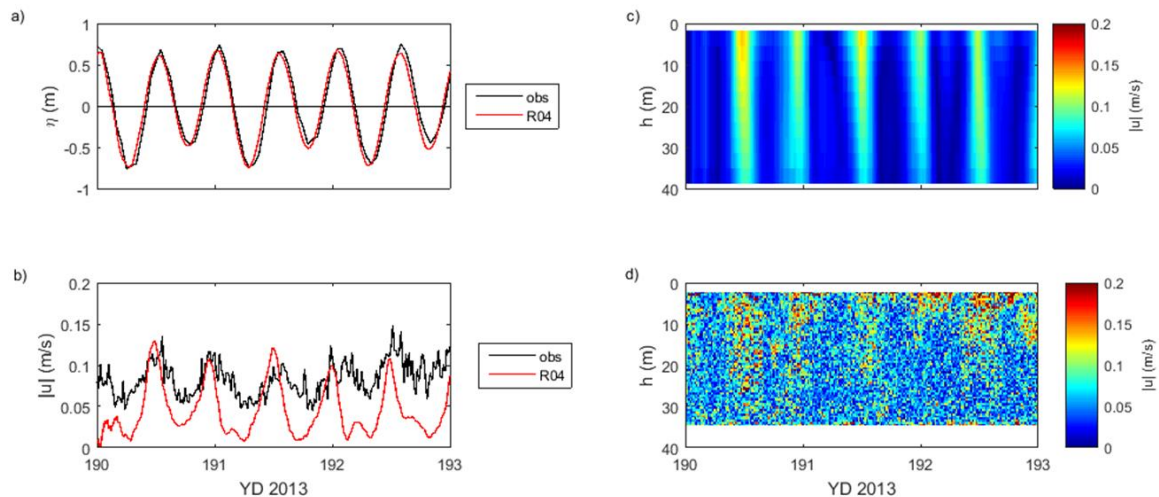


**Figure 3-5: Model Validation Results for Scenario B. Modelled versus observed results for a) water level,  $\eta$ , b) near surface current magnitude,  $|u|$ , as well as c) the depth profile of the modelled current magnitude and d) the depth profile of the observed current magnitude.**

For Scenario C, the model replicated the water levels well leading up to the storm event, but was unable to capture the water level setup during the storm event (Figure 3-6 a). This is likely due to the fact that the tidal inputs were obtained from the WebTide model, and would not have considered any water level changes due to weather patterns. Regardless of the model's inability to match the water level setup, it was still able to replicate the significant wave height (Figure 3-6 b), peak wave period (Figure 3-6c) and near surface current magnitude (Figure 3-6d) with a fair degree of accuracy, particularly during the storm event on YD 85. The RMSE for the near surface current magnitude was 0.09 m/s. The model did not always produce accurate current magnitude at all depths, particularly at the start of the model runs as seen on YD 84 in run R05 (Figure 3-6e and f), but, in general, was able to capture increases and decreases in the current magnitude at various depths at approximately the correct time.

Despite some inaccuracies in the model output for current magnitude, particularly within the first 24 hours of the model run, the hydrodynamic model was able to replicate increases and decreases in current magnitude resulting from tidal, wind and wave events, providing confidence that it could be used to predict the potential approximate distribution of PFAS following a release of AFFF into the modelling domain. In order to have better confidence in the modelled PFAS distribution, PFAS was released from each of the release sites at the start of day 2 for each of the scenarios modelled.

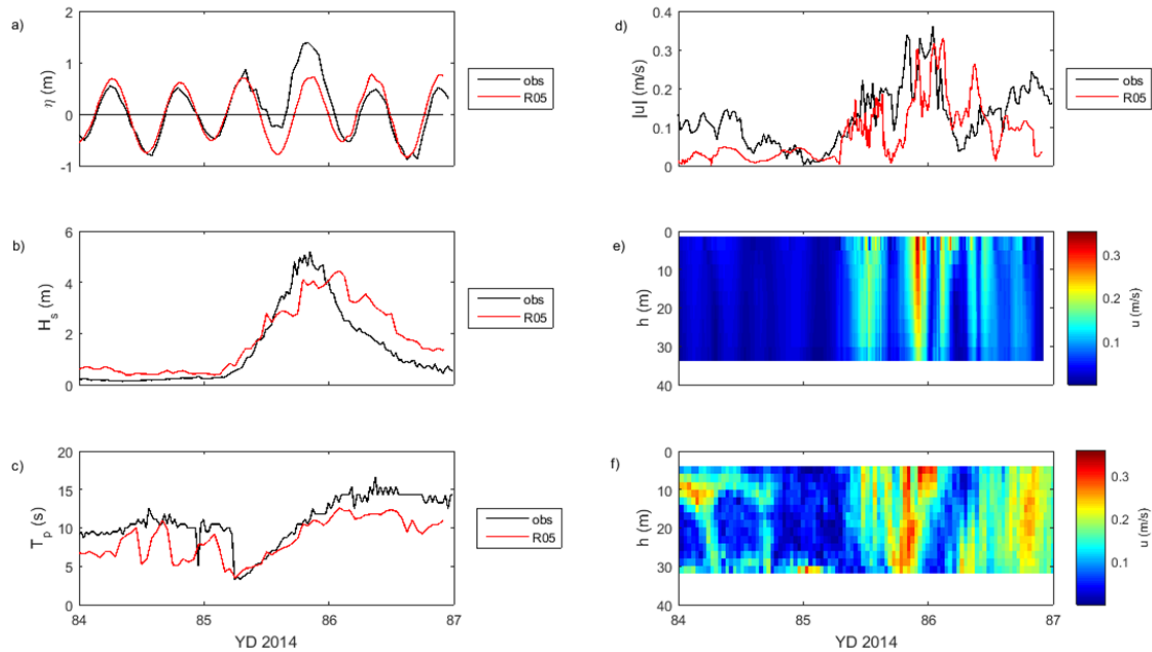


**Figure 3-6: Model Validation Results for Scenario C. Modelled versus observed results for a) water level,  $\eta$ , b) significant wave height,  $H_s$ , c) peak wave period,  $T_p$ , and d) near surface current magnitude,  $|u|$ , as well as the depth profile of e) modelled current magnitude and f) observed current magnitude.**

### 3.4.3 PFAS Release

In Scenario B, the PFAS release time,  $T_R$ , was YD 191 at 00:00 hrs, and for Scenario C, it was YD 85 at 00:00 hrs. The meteorological conditions were similar at  $T_R$  for both scenarios. The wind was light, being approximately 7 m/s and from the east in Scenario B (Figure 3-2g and h) and 5 m/s and from the west in Scenario C (Figure 3-2 l and m). It was the start of the ebb tide in Scenario B (Figure 3-2f) and the tail end of the ebb tide in Scenario C (Figure 3-2k). Following the PFAS release, the weather conditions in Scenario B did not vary considerably, while in Scenario C, a storm developed causing both the current magnitude and significant wave height at the Smart Buoy location to peak near the beginning of YD 86 (Figure 3-5b and c). As a result of the storm, the near surface current magnitude in Scenario C was higher in many areas of the Harbour compared to Scenario B as shown in Figure 3-7. The concentration of PFAS,  $C_{PFAS}$ , in the near surface layer for Scenarios B and C are shown at  $T_R + 1$  hr,  $T_R + 12$  hrs and  $T_R + 47$  hrs for release locations 2, 3, 4 and 5 in Figures 8, 9, 10 and 11 respectively. For each plot the release location is identified with a black circle, the concentration of PFAS is given in pg/L and a magenta contour line is drawn at  $C_{PFAS} = 1$  pg/L.



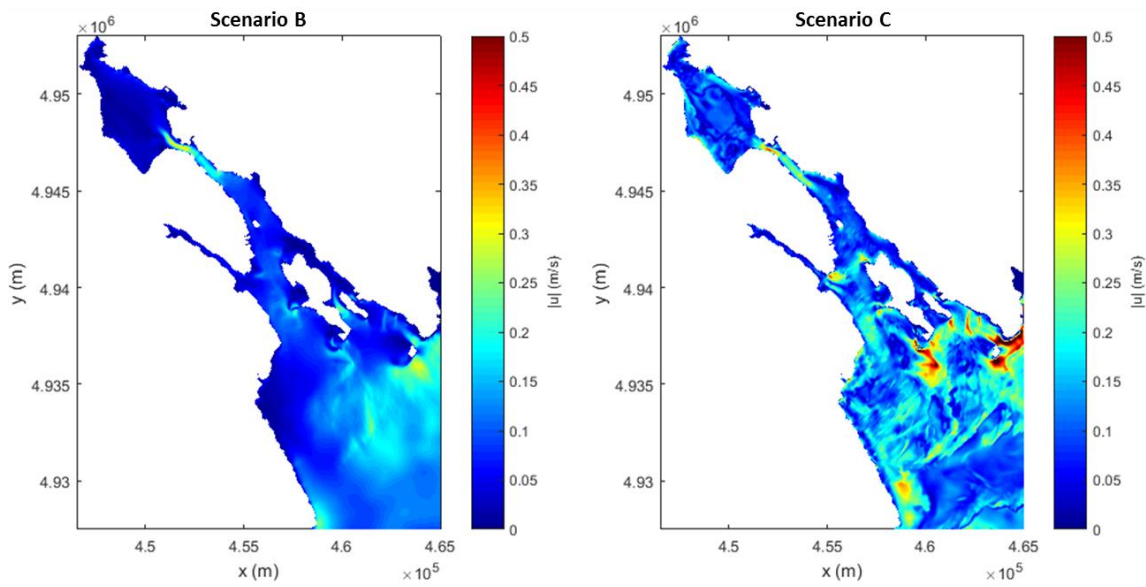


**Figure 3-7: Map of Near Surface Current Magnitude.** The near surface current magnitude is shown for modelling scenarios B (left) and C (right) at 12 hours following the release of PFAS, which corresponds to YD 191 at 12:00 hrs for Scenario B and YD 85 at 12:00 hrs for Scenario C.

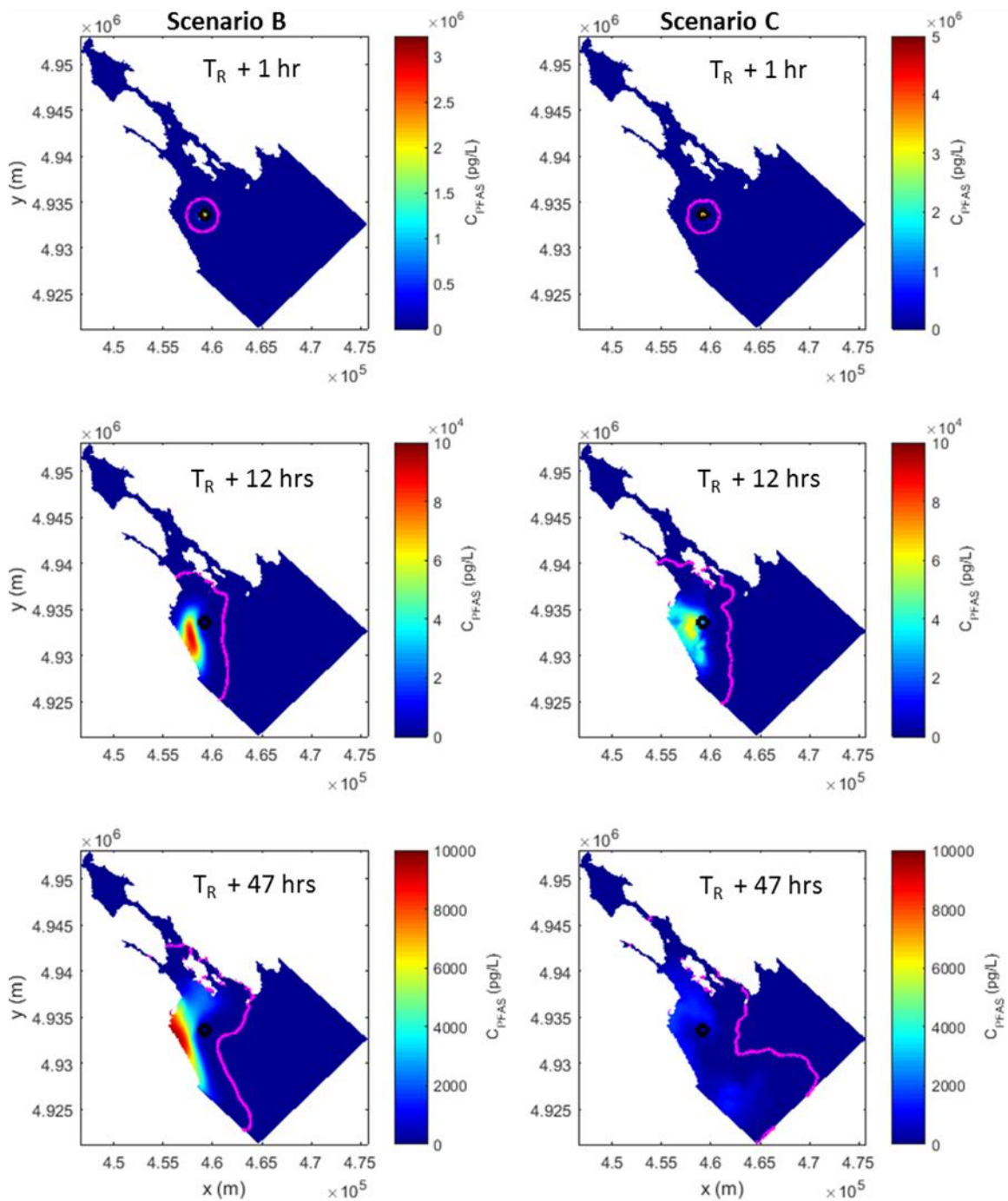


Figure 3-8: PFAS transport in the Near Surface for Release Site 2. Shown is a comparison of PFAS transport from release location 2 at 1 hr, 12 hrs and 47 hrs following the release of PFAS at time,  $T_R$ , for scenarios B and C. The PFAS release location is identified by a black circle, and a magenta contour line has been drawn at 1 pg/L. Note the change in scales between subplots.

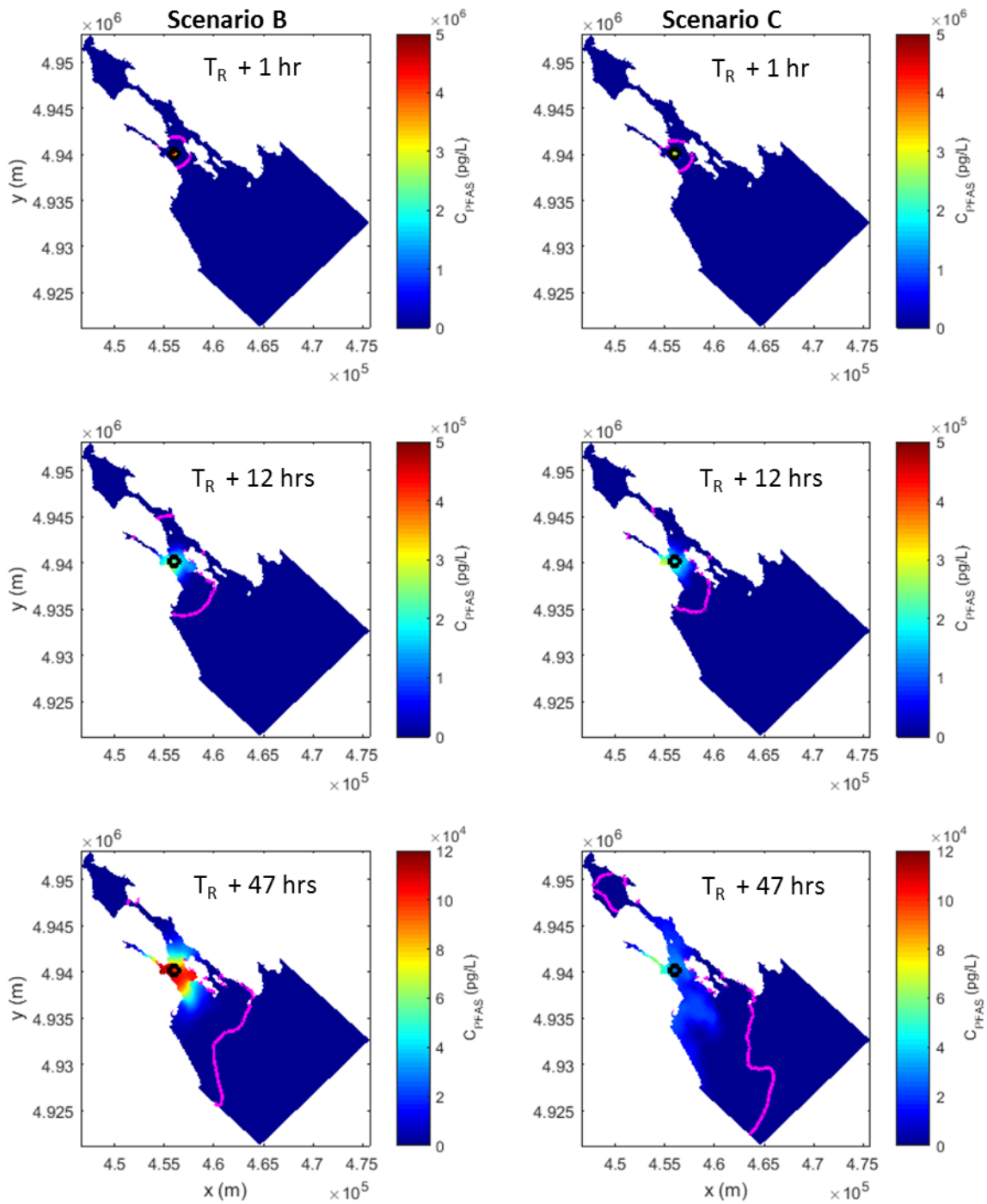


Figure 3-9: PFAS transport in the Near Surface for Release Site 3. Shown is a comparison of PFAS transport from release location 3 at 1 hr, 12 hrs and 47 hrs following the release of PFAS at time,  $T_R$ , for scenarios B and C. The PFAS release location is identified by a black circle, and a magenta contour line has been drawn at 1 pg/L. Note the change in scales between subplots.

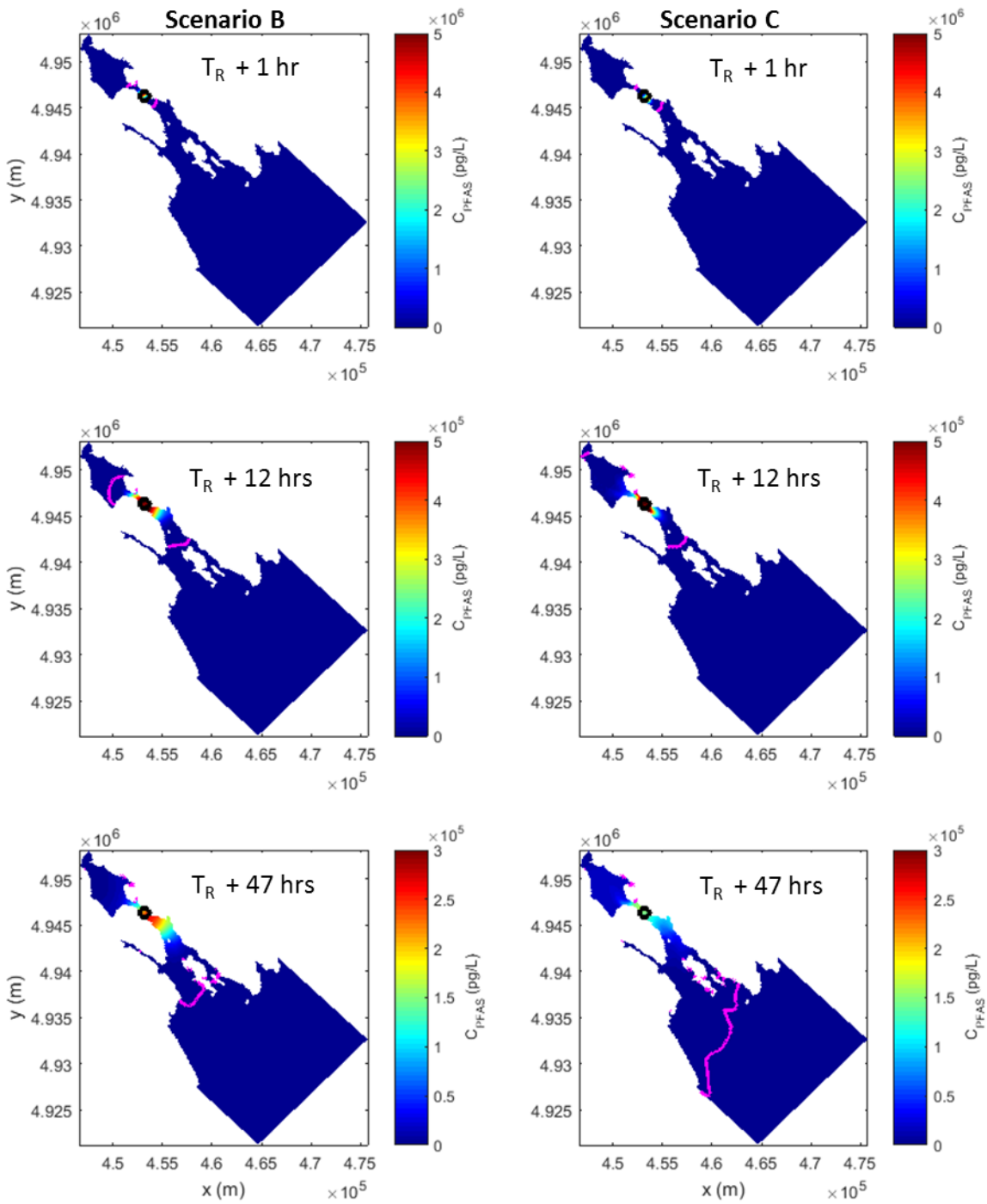


Figure 3-10: PFAS transport in the Near Surface for Release Site 4. Shown is a comparison of PFAS transport from release location 4 at 1 hr, 12 hrs and 47 hrs following the release of PFAS at time,  $T_R$ , for scenarios B and C. The PFAS release location is identified by a black circle, and a magenta contour line has been drawn at 1 pg/L. Note the change in scales between subplots.

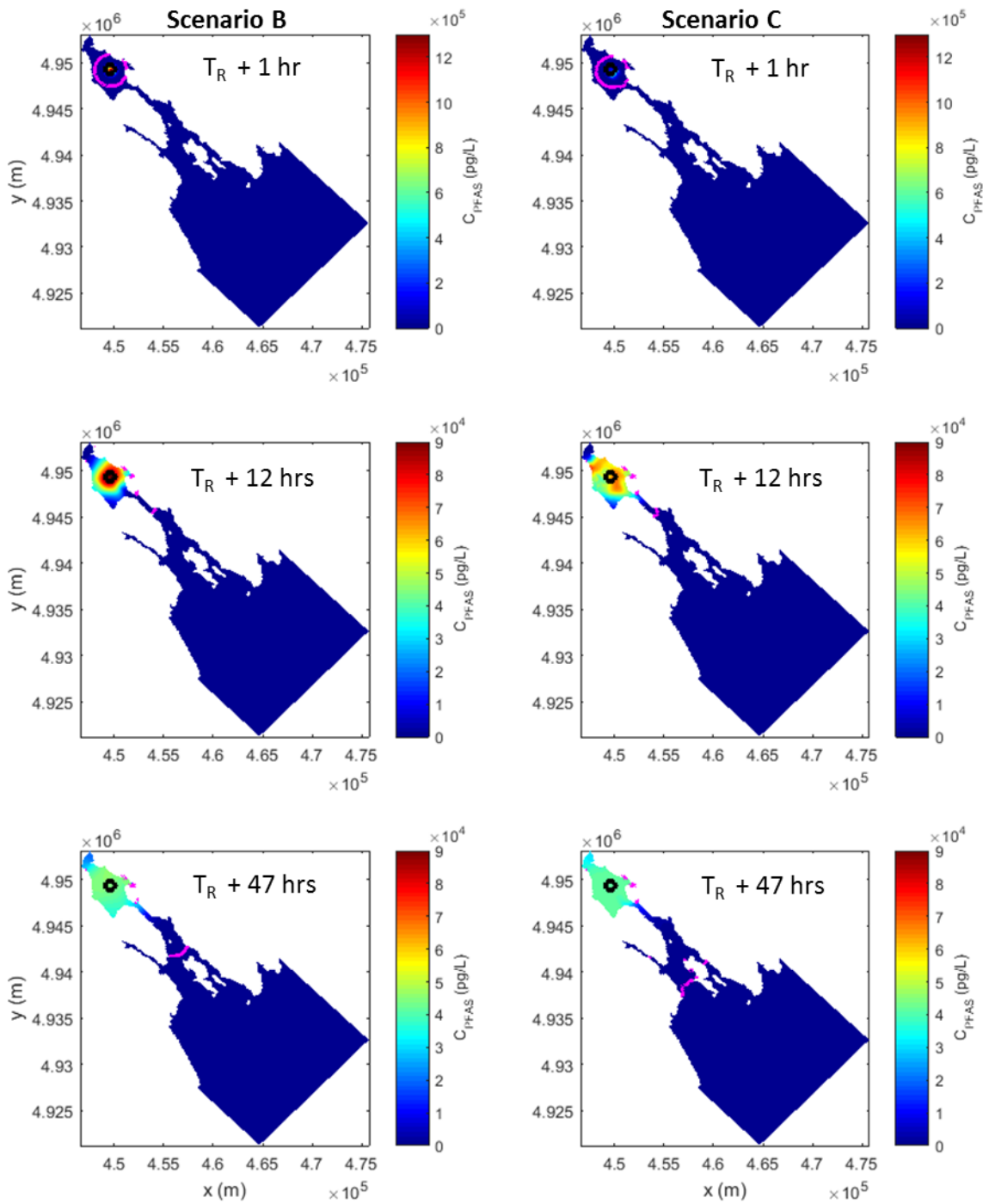
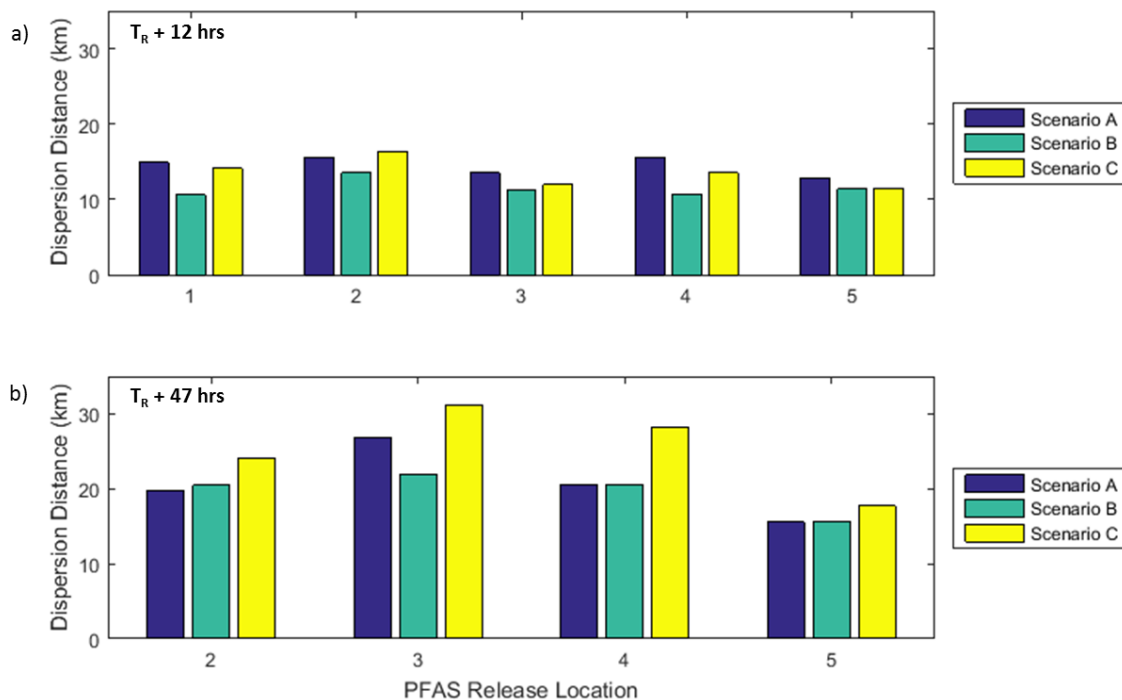


Figure 3-11: PFAS transport in the Near Surface for Release Site 5. Shown is a comparison of PFAS transport from release location 5 at 1 hr, 12 hrs and 47 hrs following the release of PFAS at time,  $T_R$ , for scenarios B and C. The PFAS release location is identified by a black circle, and a magenta contour line has been drawn at 1 pg/L. Note the change in scales between subplots.

### 3.4.3.1 Outer Harbour

At release site 2 in the Outer Harbour at  $T_R + 1$  hr (Figure 3-8), the PFAS had travelled radially outward from the release site in the near surface layer and had a diameter of approximately 4 km when measured to the 1 pg/L contour line. The upper limit of  $C_{PFAS}$  is substantial at  $T_R + 1$  hr ( $3 \times 10^6$  pg/L), being over 1000 times greater than the highest concentration of PFAS determined by Benskin et al. (2012) in Narragansett Bay (5800 pg/L).

At  $T_R + 12$  hrs, the storm in Scenario C is just beginning. The wind has steadily increased from 5 to 15 m/s (Figure 3-2l) and the wind has changed in a counter clockwise direction and is blowing from the east at  $T_R + 12$  hrs (Figure 3-2m). The near surface current produced by the model is higher in the Outer Harbour in Scenario C than in Scenario B (Figure 3-7). As shown in Figure 3-12a, at  $T_R + 12$  hrs, PFAS from release site 2 in Scenario C has travelled slightly further into the Harbour (16.3 km) than in Scenario B (13.5 km), likely due to the increased onshore wind in Scenario C. Consequently, the upper limit for  $C_{PFAS}$  (Figure 3-8) is less for Scenario C (60,000 pg/L) than Scenario B (90,000 pg/L). In each case, PFAS has made contact with the shoreline. In Scenario B, the length of coastline in contact with PFAS is slightly less, but the concentration of PFAS impacting the shore is slightly more (70,000 pg/L) than in scenario C (40,000 pg/L).



**Figure 3-12: Comparison of PFAS Transport.** A comparison of the distance of PFAS transport along a SW-NE transect at a)  $T_R + 12$  hrs and b)  $T_R + 47$  hrs for PFAS released at locations 1 through 5 in modelling Scenarios A, B and C. Release site 1 was not included at  $T_R + 47$  hrs because the results were questionable due to the loss of PFAS through the model boundary.

Between  $T_R + 12$  hrs and  $T_R + 47$  hrs, the wind in Scenario C changed direction counter clockwise from an onshore wind blowing from the east to an offshore wind blowing from the west (Figure 3-2m). The storm in Scenario C peaked during this time period, and the wind reached speeds of

approximately 18 m/s (Figure 3-2l). For Scenario B, wind speeds remained steady around 5 m/s (Figure 3-2g) and wind direction altered clockwise from the east to the southwest (Figure 3-2h). In the Outer Harbour, the modelled significant wave height in Scenario C reached around 4 m at the Smart buoy location (Figure 3-6b), and the near surface current magnitude peaked at about 0.3 m/s (Figure 3-6d). At release site 2 in the Outer Harbour,  $C_{PFAS}$  in Scenario C has an upper limit of approximately 2000 pg/L (Figure 3-8), which could be associated with background levels of PFAS found in a working harbour of a city in North America. For Scenario B at this same location, the upper limit for  $C_{PFAS}$  is around 9000 pg/L (Figure 3-8). The transport of PFAS from the Harbour Approaches to the tip of the Basin is only about 3.6 km longer for Scenario C than Scenario B (Figure 3-11b). The difference in the PFAS concentrations and distances travelled indicate that wind and waves only moderately affected the transport of PFAS from release site 2. This might be because the PFAS was exiting the model domain from the SW current boundary. For Scenario C, PFAS also appeared to be exiting the model through the tidal boundary, in which case, the modelled PFAS concentrations may actually have been higher, as due to the setup of the model, PFAS that exited the model through the tidal boundary could not re-enter the model. After 47 hours, PFAS released from site 2 was detectable at sites 2 (120 pg/L) and 3 (75 pg/L) for Scenario B and sites 1 (30 pg/L), 2 (600 pg/L) and 3 (700 pg/L) for Scenario C, as depicted in Figure 3-13.

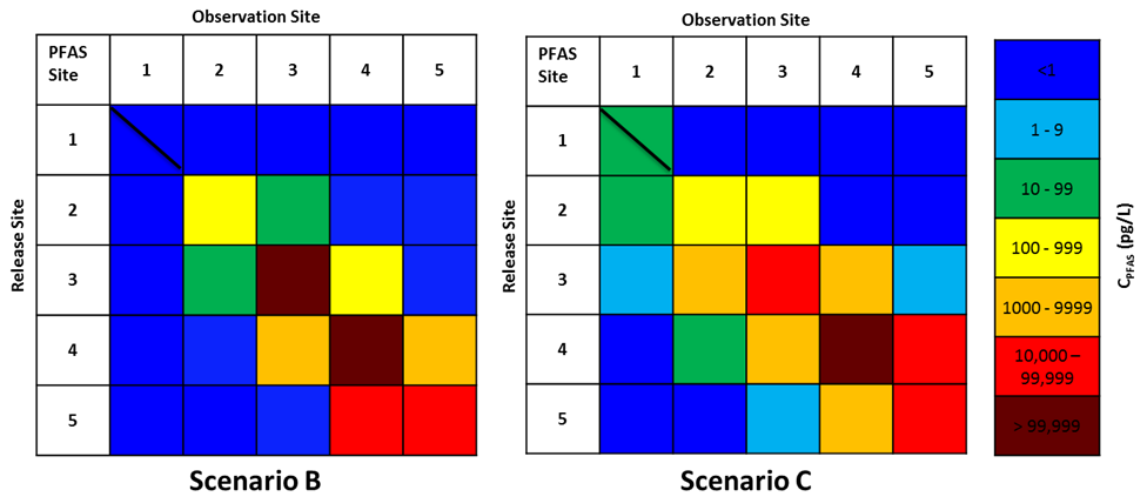
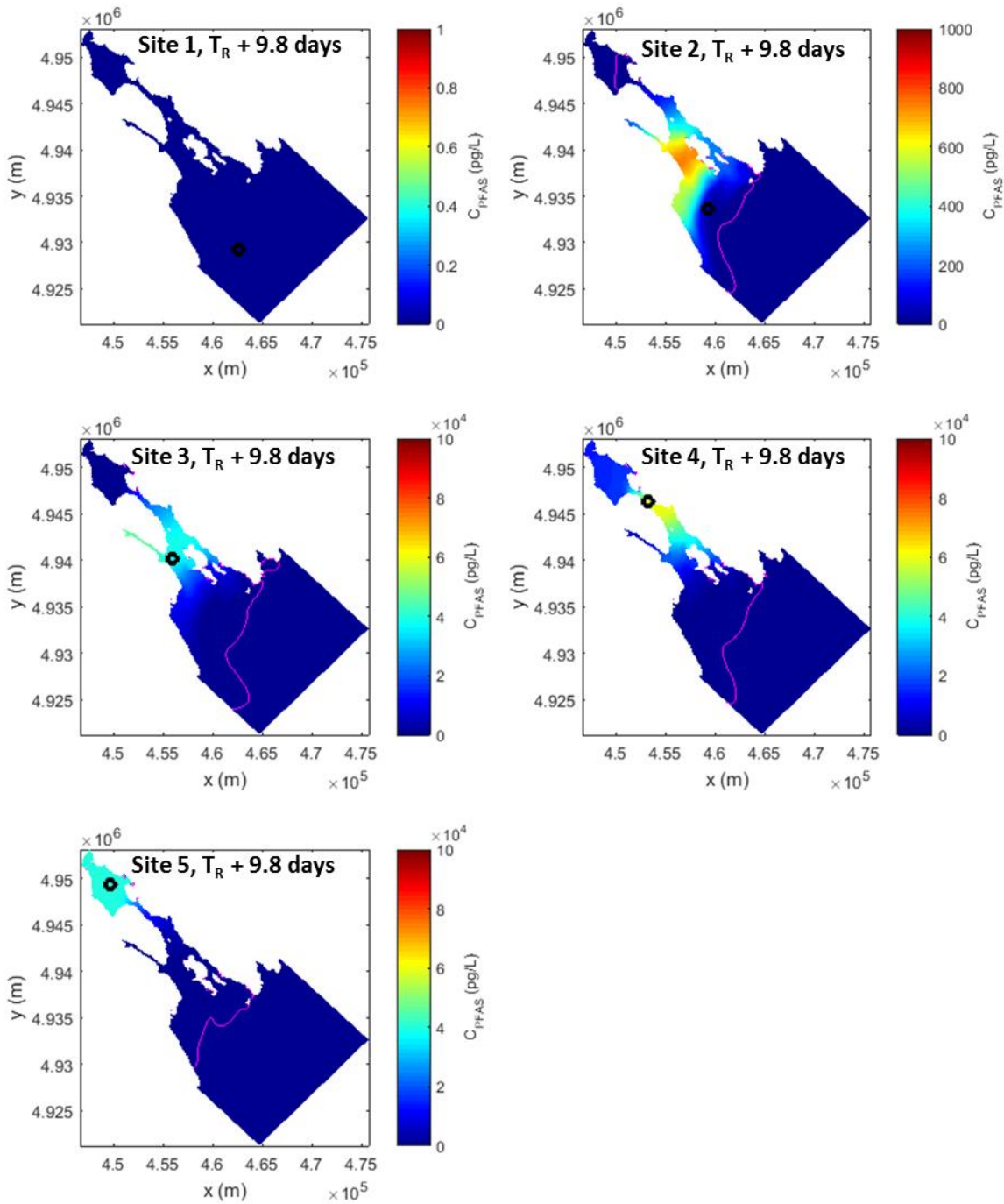


Figure 3-13: PFAS concentrations for Scenario B (left) and Scenario C (right) are provided in pg/L at 47 hours after release. The release location is given vertically on the left of each table, and the observation locations are given horizontally at the top of each table. For example, at  $T_R + 47$  hrs, the concentration of PFAS released at PFAS site 5 in Scenario C was less than 1 pg/L at PFAS sites 1 and 2, between 1 and 9 pg/L at PFAS site 3, between 1000 and 9999 pg/L at PFAS site 4 and between 10,000 and 99,999 pg/L at PFAS site 5. The diagonal line represents concentrations that are likely too low due to the PFAS leaving the model through the boundaries.

Modelling of Scenario C only encompassed 3 days, but Scenario B was modelled for nearly 10 days. At  $T_R + 236$  hrs, or 9.8 days PFAS released from site 2 remained in the Outer Harbour, Inner Harbour, Northwest Arm and the Narrows in concentrations ranging from 100 to 800 pg/L, with the greatest concentration of PFAS being found in the Inner Harbour, as shown in Figure 3-14.



**Figure 3-14: PFAS Transport in the Near Surface after 9.8 Days.** Shown is the PFAS transport from release locations 1 through 5 at 9.8 days following the release of PFAS at time, T<sub>R</sub>, for Scenario B. The PFAS release location is identified by a black circle, and a magenta contour line has been drawn at 1 pg/L. Note the change in scales between subplots.

In Scenario B, where winds were light, it is reasonable to conclude that the main cause of the PFAS transport was due to the tide. Therefore, it is equally reasonable to conclude that the



differences in transportation of PFAS between scenarios B and C were a result of the wind and waves that were present in Scenario C. We know that the combination of wind and waves is an important factor for matching current magnitude in the Outer Harbour, as the current magnitude at the Smart Buoy location could only be matched by the model once the effects of both wind and waves were considered for both Scenarios A and C.

#### **3.4.3.2 Inner Harbour**

The PFAS released at site 3 (Figure 3-9) in the Inner Harbour made contact with the shoreline by  $T_R + 1$  hr in both Scenarios. PFAS transport patterns and concentrations remained similar between the two Scenarios at 12 hours after release. PFAS in Scenario B travelled 11.3 km and PFAS in Scenario C travelled 12.0 km (Figure 3-12a). At 47 hrs after release, the PFAS in Scenario C had travelled much further than the PFAS in Scenario B, and impacted all areas of the Harbour, as well as the Harbour Approaches (Figure 3-9). The PFAS in Scenario C travelled 9.2 km further than the PFAS in Scenario B (Figure 3-12b). The upper limit of  $C_{PFAS}$  in Scenario C (60,000 pg/L) was approximately half that of Scenario B (120,000 pg/L) (Figure 3-9). After 47 hours, PFAS released from site 3 was detectable at sites 2 (75 pg/L), 3 (100,000 pg/L) and 4 (110 pg/L) for Scenario B and sites 1 (8 pg/L), 2 (7000 pg/L), 3 (30,000 pg/L), 4 (6000 pg/L) and 5 (5 pg/L) for Scenario C, as depicted in Figure 3-13. For PFAS released in the Inner Harbour, the greatest concentrations after 9.8 days were found in the Northwest Arm at 45,000 pg/L (Figure 3-14). PFAS was also present in concentrations above 10,000 pg/L in both the Narrows and the Inner Harbour (Figure 3-14).

#### **3.4.3.3 Narrows**

At  $T_R + 1$  hr, the model indicates that both sides of the Narrows are considerably impacted by the PFAS with concentrations up to  $5 \times 10^6$  pg/L reaching the coastline (Figure 3-10). At  $T_R + 12$  hrs, the strong onshore wind in Scenario C has resulted in the PFAS travelling further into the Bedford Basin (13.5 km) than in Scenario B (10.6 km), as shown in Figure 3-12a. Over the next 35 hours, the storm in Scenario C continues to increase the distance that the PFAS travels over that of Scenario B. PFAS transport in Scenario C is 7.7 km longer than that of Scenario B (Figure 3-12b). Despite this increase, the upper limit of  $C_{PFAS}$  remains high for Scenario C at around 150,000 pg/L and for Scenario B at approximately 250,000 pg/L (Figure 3-10). After 47 hours, PFAS released from site 4 was detectable at sites 3 (1200 pg/L), 4 (250,000 pg/L) and 5 (5500 pg/L) for Scenario B and sites 2 (70 pg/L), 3 (4,000 pg/L), 4 (150,000 pg/L) and 5 (20,000 pg/L) for Scenario C, as depicted in Figure 3-13. For PFAS released in the Narrows, after 9.8 days, the upper limit of  $C_{PFAS}$  was greatest in the Inner Harbour at 60,000 pg/L (Figure 3-14). There was also a large quantity of PFAS in the Basin from release location 4, where  $C_{PFAS}$  was around 20,000 pg/L after 9.8 days (Figure 3-14).

#### **3.4.3.4 Bedford Basin**

At 1 hr after release,  $C_{PFAS}$  for release site 5 ( $1.2 \times 10^6$  pg/L) shown in Figure 3-11 is less than  $C_{PFAS}$  for each of the other release sites (Figures 3-8, 3-9 and 3-10). The differences between the upper limits of  $C_{PFAS}$  at each release location are likely due to a combination of the depth of the Harbour and the current magnitude. The Bedford Basin is the deepest part of the Harbour being just over 70 m deep. The PFAS immediately distributed throughout the lower levels, thus explaining why the upper limit of  $C_{PFAS}$  in the Basin was lower than in the other locations. The PFAS transport distances shown in Figure 3-12b only vary by 2.1 km, and there are no

noticeable differences in the upper limit of  $C_{PFAS}$  between Scenarios B and C, indicating that this area of the Harbour is not as affected by storm events. After 47 hours, PFAS released from site 5 was detectable at sites 4 (11,000 pg/L) and 5 (42,000 pg/L) for Scenario B and 3 (5 pg/L), 4 (7000 pg/L) and 5 (42,000 pg/L) for Scenario C, as depicted in Figure 3-13. After 9.8 days, the upper limit of  $C_{PFAS}$  as release site 5 was 40,000 pg/L (Figure 3-14). The majority of the PFAS released in the Basin stayed in the Basin, but some had migrated to the Narrows where concentrations varied from 15,000 to 35,000 pg/L, and to the Inner Harbour where the upper limit of  $C_{PFAS}$  was around 10,000 pg/L (Figure 3-14). The concentration of PFAS after nearly 10 days remained elevated in all areas of the harbour indicating that the time required to flush PFAS from the Harbour is greater than 9.8 days. According to Shan and Sheng (2012) who investigated both flushing time and transport of passive tracers in Halifax Harbour, the e-folding flushing time for the entire Bedford Basin is slightly greater than 90 days.

#### **3.4.3.5 Halifax Harbour Approaches**

PFAS released in the Approaches to Halifax Harbour (release site 1) was likewise affected by the wind, waves and currents. In Scenario A, where the wind direction was originally from the east, and then abruptly changed in a counter clockwise direction to blow from the NW, the PFAS traveled further into Halifax Harbour than in the other two scenarios (Figure 3-12a and b). For Scenario B, where the winds were light, the PFAS from release location 1 had the least amount of transport into the Harbour, and by  $T_R + 47$  hrs, had almost entirely exited the modelling domain through the SW current boundary (Figure 3-13), indicating that the 0.1 m/s shelf current most likely influenced the path of the PFAS in Scenario B. The upper limit of  $C_{PFAS}$  at  $T_R + 12$  hrs for release location 1 was approximately 50 000 pg/L for all three scenarios (Figure 3-13). In both Scenarios A and C, PFAS reached the SW shoreline of the Outer Harbour at an upper limit of around 40 000 pg/L (Figure 3-13). At 47 hrs after the PFAS release, Scenario B showed the lowest concentrations of PFAS with an upper limit of 2 pg/L (Figure 3-13), which is most likely below the background concentration of PFAS in the ocean at that location. The upper limits of  $C_{PFAS}$  in Scenario A and C were 70 pg/L and 1000 pg/L respectively (Figure 3-13). For Scenario C, it appeared that PFAS may have been exiting the modelling domain through the tidal boundary, in which case, it is likely that the concentration of PFAS might have been higher than indicated. After 47 hours, PFAS released from site 1 was not detected above 1 pg/L at any of the other release sites for Scenario B and was only detected at site 1 (3 pg/L) for Scenario C, as depicted in Figure 3-13. After 9.8 days, the PFAS released at site 1 in Scenario B was completely flushed from the area.

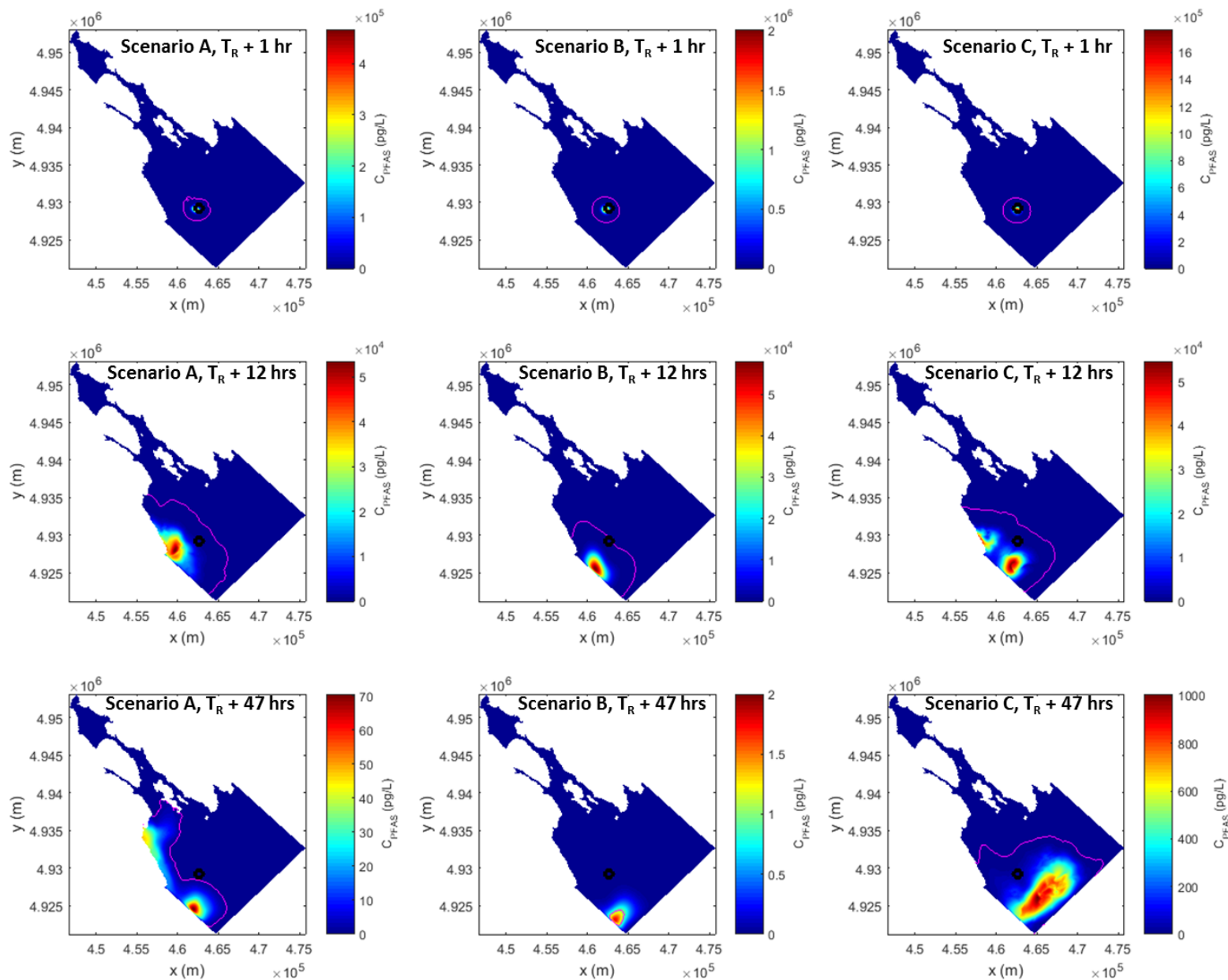


Figure 3-15: PFAS Transport in the Near Surface for Release Site 1. Shown is a comparison of PFAS transport from release location 1 at 1 hr, 12 hrs and 47 hrs following the release of PFAS at time,  $T_R$ , for scenarios A, B and C. The PFAS release location is identified by a black circle, and a magenta contour line has been drawn at 1 pg/L. Note the change in scales between subplots.

### **3.5 Summary and Conclusion**

A hydrodynamic model was used to predict the transport of PFAS from AFFF used by the RCN if released overboard either within Halifax Harbour or outside of the Harbour in the Approaches. The model results indicate that PFAS from AFFF released into the Harbour will result in elevated levels of PFAS reaching upwards of 1000 times the background concentration of PFAS currently found in coastal regions of North America. Even after 10 days, the model predicts that PFAS levels will remain up to 10 times more concentrated than what one might expect to see in a working harbour located in a North American city. Shoreline communities could be impacted by the PFAS in as little as one hour following a release of AFFF into the Harbour, if the release was in a narrower area of the Harbour such as the region where the Naval Dockyard is located. Within 12 hours of a release, PFAS will impact the coastline regardless of where it was released within the Harbour. In general, the further into the Harbour that a release occurs, the more likely that the concentration levels of PFAS will remain elevated for a longer duration. At present, the Canadian government has not published any recreational water guidelines for PFAS, but has provided drinking water screening values for several perfluoroalkyl carboxylic acids, and perfluoroalkyl sulfonic acids, which range from 0.2 up to 30 ug/L (200,000 to  $3 \times 10^7$  pg/L).

The distribution of the PFAS within the Harbour can be affected by tidal currents, meteorological events and waves. The tidal currents have more impact on PFAS that is further into the Harbour such as in the Narrows or the Basin, while wind driven currents and waves can have more impact on PFAS distribution in the Inner and Outer Harbour. Wind and waves will result in the PFAS travelling faster through the near surface layer. An onshore wind can also result in PFAS being pushed further into the Harbour.

Although the results of the study were not able to definitively answer the question as to how far outside the Harbour AFFF could be released into the ocean without impacting the shoreline communities, the model results do indicate that PFAS entering the ocean in the Approaches west of the Halifax Harbour Buoy 44258 could be expected to impact the coastline within the Harbour.

## **Chapter 4 Sizing of a GAC Based PFAS Adsorption Column for a RCN Frigate**

### **4.1 Introduction**

Aqueous film forming foam (AFFF) is a fire extinguishing agent used to combat class B fires. This type of fire extinguishing system is fitted onboard Royal Canadian Navy vessels in compartments that are vulnerable to Class B fires (DNPS 6-2 2016). Per-and polyfluorinated substances (PFAS) are essential ingredients in AFFF as they allow the foam to spread evenly over a fire (Dlugogorski et al. 2002). Additionally, they lower the surface tension of the foam and water mixture allowing it to remain on top of the fuel surface where it acts as a barrier preventing the fuel from evaporating or percolating through the foam, and thus extinguishing the fire (Williams et al. 2011).

PFAS have been detected in the environment due to AFFF usage at airports (Awad et al. 2011), Military Bases in both the US and Australia (Backe et al. 2013; Arias E et al. 2015), and the site of accidents such as the train derailment that occurred in Lac-Mégantic, Québec in 2013 (Munoz et al. 2017). When the AFFF system is used to extinguish a fire onboard a warship, the used AFFF may end up going overboard. Accounts from a major engine room fire onboard a Canadian Patrol Frigate (CPF) in the early 2000s indicate that AFFF was released overboard, although the exact quantities that went into the ocean are unknown (Gallant 2017). Previous modelling work on the potential transport of PFAS in Halifax Harbour due to the release of AFFF overboard, described in Chapter 3, suggests that the concentration of PFAS from even a modest amount of AFFF released into the ocean could potentially result in levels of PFAS in the Harbour that are initially up to 1000 times that which have been detected by Benskin et al. (2012) in coastal areas of the US Eastern seaboard (5800 pg/L).

The removal of PFAS from water is possible. One method which has been successfully used is adsorption of PFAS to activated carbon. Following the train derailment in Lac-Mégantic, Québec, an activated carbon filter was used to remove PFAS from AFFF impacted water with removal rates ranging between 77 and 99.8% (Paquin 2014). In a full-scale water treatment facility in Minnesota, granular activated carbon (GAC) was used to remove PFAS from groundwater. This system was able to remove PFAS with 6 to 8 fluorinated carbons with success rates ranging from 22% to >95% (Appleman et al. 2014). Two possible interactions are thought to be able to occur between PFAS and GAC; electrostatic interaction where a negatively charged functional group is attracted to the positively charged GAC, or hydrophobic interaction where the hydrophobic fluorinated tail sorbs to the GAC (Yu et al. 2009).

Modelling of PFAS adsorption to GAC has been previously undertaken. Laboratory scale experimental results for sorption kinetics of perfluorooctane sulfonate (PFOS) and perfluorooctanoate (PFOA) adsorption to GAC were successfully modelled using a pseudo-second-order equation (Yu et al. 2009). In this study, a numerical model was used to simulate PFAS adsorption to GAC for a full scale operation to determine if a GAC treatment system would be a viable option for removal of PFAS from used AFFF onboard a warship. A numerical model was developed based on the data available from the full scale water treatment facility in Minnesota, which used GAC to remove PFAS from groundwater. The size of GAC system

required for removal of all PFAS from the used AFFF and an assessment of the viability of this option for installation and use on a warship is presented.

## 4.2 Methods

### 4.2.1 Model Setup

The GAC setup employed in Minnesota is shown in Figure 4-1 and consisted of two basins, each with a diameter of 3.66 m and holding 2.71 m of Calgon F600 GAC (Appleman et al. 2014). The setup was run in a lead lag configuration with a flow ranging from 1.4 to 1.5 m<sup>3</sup>/min, providing an empty bed contact time of 13 minutes (Appleman et al. 2014). Calgon F600 is a coal based GAC with a bed density,  $\rho_{bed}$ , of 630 kg/m<sup>3</sup> (Kempisty 2014).

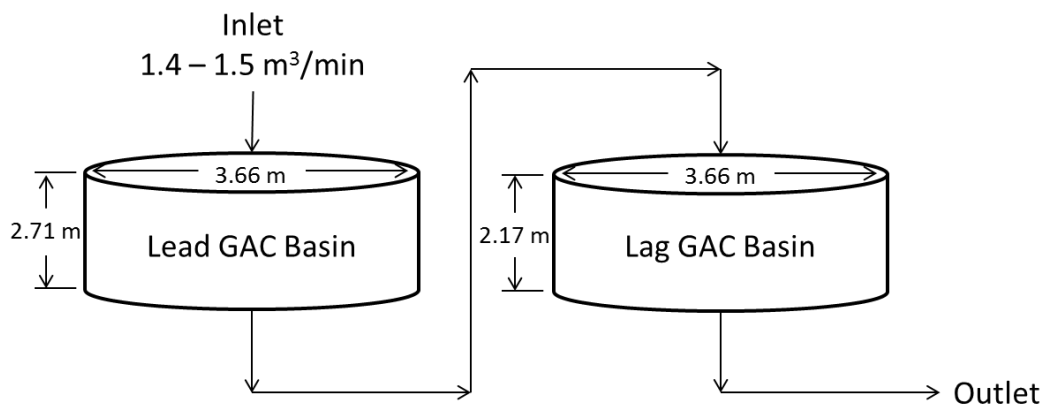


**Figure 4-1: Configuration of the GAC System used in Minnesota. The setup consisted of two basins of GAC, with the dimensions shown, in a lead-lag configures. Influent flowed into the lead basin at 1.4 to 1.5 m<sup>3</sup>/min.**

Data for this set up, taken from Appleman et al. (2014), was available on the lead basin from October 2006 until June 2011 and on the lag basin from April 2007 to August 2008. On 13 August 2008 and 21 September 2009, the flow was redirected so that the lag basin became the lead basin and the GAC in the original lead basin was replaced with virgin GAC, and on 7 October 2010, the GAC in both basins was replaced (Appleman et al. 2014). Seven different PFAS were monitored, including perfluorobutanoic acid (PFBA), perfluoropentanoic acid (PFPeA), perfluorohexanoic acid (PFHxA), PFOA, perfluorobutane sulfonic acid (PFBS), perfluorohexane sulfonic acid (PFHxS) and PFOS. PFBS was never detected above the limit of detection (LOD) of 0.05 µg/L. PFBA was the most detected with an averaged influent concentration of 1.43 µg/L. PFBA readily adsorbed to the GAC in the beginning, however it had almost entirely desorbed over the time period that the GAC was in use. For this reason, data for PFBA was not used for model calibration or validation. The average influent concentration from October 2006 to June 2011 of the other PFAS monitored is shown in Figure 4-2, and ranged from 0.06 µg/L for PFPeA to 0.81 µg/L for PFOS.

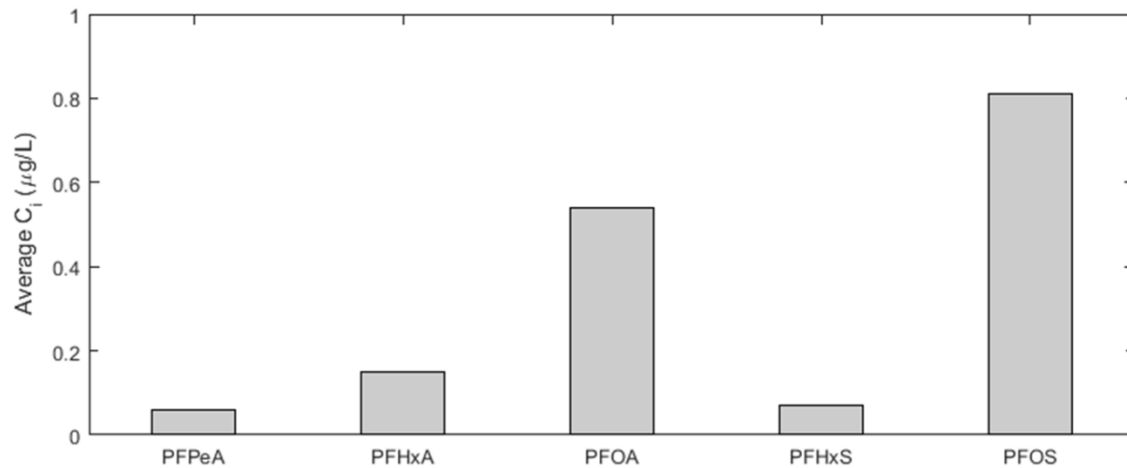


**Figure 4-2: Average influent concentrations of individual PFAS into the lead basin.**

Calibration and validation of the model was based on flow through one basin only. Data from Basin 1, the lead basin from 26 October 2006 to 13 August 2008, was used to calibrate the model. Data from Basin 2 was used to validate the model. Basin 2 was in the lag configuration from 26 October 2006 until 13 August 2008, after which was switched to the lead configuration until 21 September 2009. The effluent concentrations of the different PFAS are shown in Figure 4-3a and b for the calibration and validation data respectively. The quantities of individual PFAS adsorbed to GAC are shown in Figure 4-3c and d for the calibration data and validation data respectively. The use of this data for calibration and validation of the model was not ideal because the concentration of PFAS in AFFF impacted water is much greater than the concentration of PFAS found in groundwater. However, since this was the only data available, the intent was to achieve a preliminary estimate for the quantity of GAC required to remove PFAS from used AFFF, that could be later be refined.

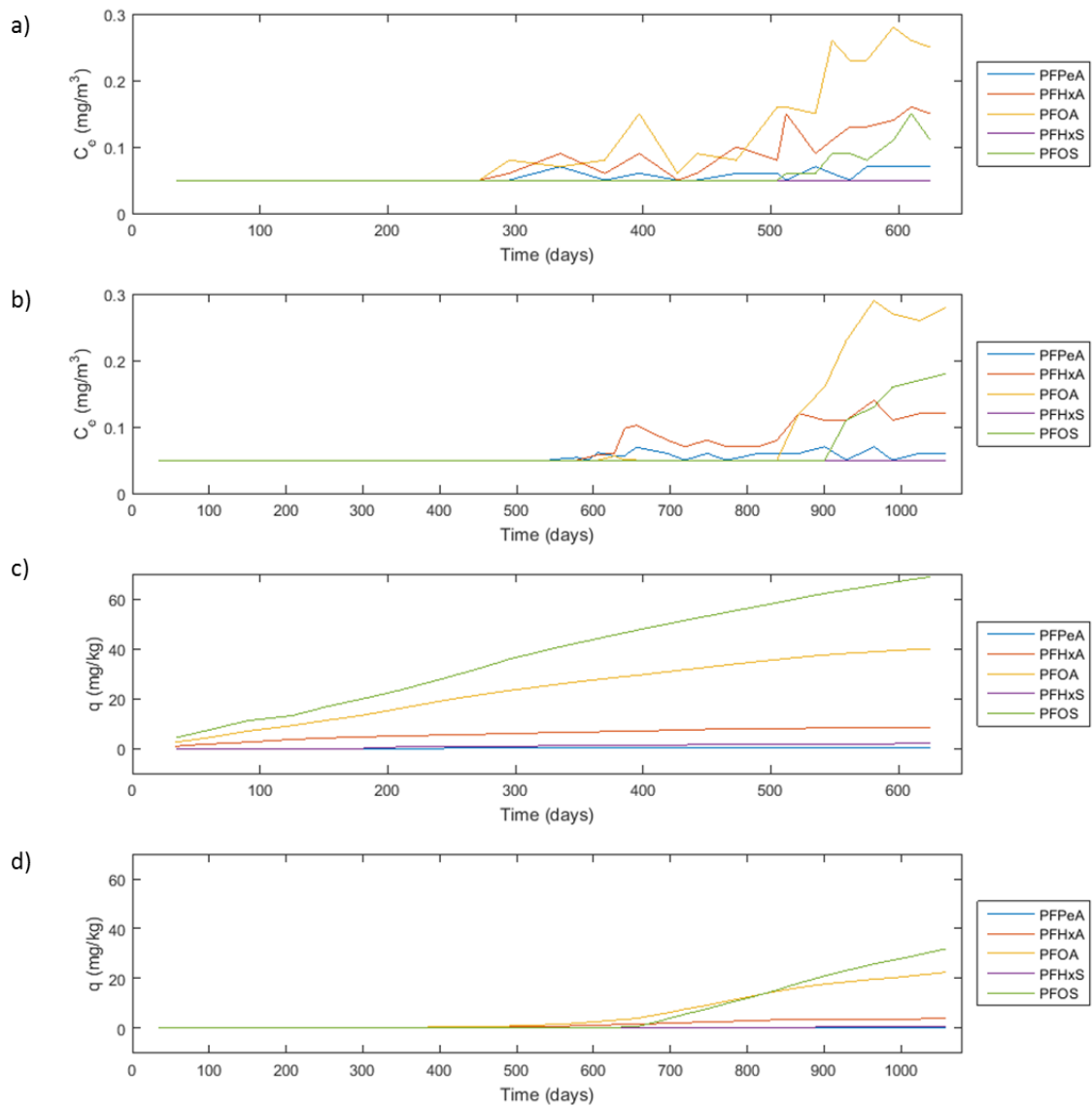


**Figure 4-3: Observed Data Plots.** Effluent concentrations of individual PFAS are shown for the calibration data (a) and validation data (b). The quantities of individual PFAS adsorbed per mass unit of GAC is shown in (c) for the calibration data and (d) for the validation data. Data obtained from Appleman *et al.* (2014).



#### 4.2.2 Governing Equations

The transport mechanisms involved in the flow of influent containing PFAS through the GAC basin includes advection, dispersion and adsorption. As there was only one inlet and one outlet, the transport through the basin was only considered in one dimension. Transport of PFAS through the GAC basin is represented by Equation [1] (Van Genuchten and Alves 1982).

$$\frac{\partial C}{\partial t} = \frac{E}{R} \frac{\partial^2 C}{\partial x^2} - \frac{u}{R} \frac{\partial C}{\partial x} \quad [1]$$

In Equation [1], C is the concentration of PFAS ( $\mu\text{g/L}$ ), t is time (s), E is the dispersion coefficient for PFAS ( $\text{m}^2/\text{s}$ ), R is the retardation factor due to adsorption and is unitless, x is the distance traveled through the basin (m), and u is the average pore velocity (m/s). Equation [1] was solved using Microsoft Excel software by employing a finite difference transient solution using a central difference approximation. For a central difference approximation, Equation [1] becomes Equation [2].

$$\frac{C_x^{t+1} - C_x^t}{\Delta t} = \frac{E}{R} \left( \frac{C_{x+1}^t - 2C_x^t + C_{x-1}^t}{\Delta x^2} \right) - \frac{u}{R} \left( \frac{C_{x+1}^t - C_{x-1}^t}{2\Delta x} \right) \quad [2]$$

In Equation [2],  $\Delta t$  is the time step,  $\Delta x$  is the distance step,  $C_x^t$  represents the concentration of PFAS at a distance x down the column and a time t,  $C_x^{t+1}$  represents the concentration of PFAS at the same distance x down the column, but at time t+1, and  $C_{x+1}^t$  and  $C_{x-1}^t$  represent the concentration of PFAS at time t and x+1 distance step and x-1 distance step respectively.

In order to solve Equation [2], values for the dispersion coefficient, E, and the retardation factor, R, had to be determined. The dispersion coefficient is a combination of mechanical dispersion and molecular diffusion and is represented by Equation [3], where  $\alpha u$  denotes mechanical dispersion of PFAS through the GAC basin and D signifies the molecular diffusion of PFAS.

$$E = \alpha u + D \quad [3]$$

The molecular diffusion of PFOS in water, as determined through numerical modelling, ranges between  $0.3 \times 10^{-9}$  to  $0.6 \times 10^{-9} \text{ m}^2/\text{s}$  (Pereira et al. 2014). These values are much smaller than mechanical dispersion, and were therefore considered negligible. The mechanical dispersion is the product of the dispersivity constant,  $\alpha$  (m), and the pore velocity, u (m/s). The pore velocity can be calculated using Equation [4] given the flow rate, Q ( $\text{m}^3/\text{s}$ ), the cross-sectional area of the basin, A ( $\text{m}^2$ ), and the porosity of the GAC bed,  $\phi$ .

$$u = \frac{Q/A}{\phi} \quad [4]$$

The porosity for the GAC bed is given by Equation 5 where  $\rho_{\text{bed}}$  is the bed density of GAC and  $\rho_{\text{carbon}}$  is the density of carbon, both in  $\text{kg}/\text{m}^3$ .

$$\phi = 1 - \frac{\rho_{\text{bed}}}{\rho_{\text{carbon}}} \quad [5]$$

A value for the dispersivity constant,  $\alpha$ , could not be found in the literature. Instead, an approximate value was calculated using Equation [6] where  $x$  represents the distance traveled. Equation [6] is a formula used to determine the dispersivity of a monoaromatic hydrocarbon such as benzene or toluene in groundwater where the distance traveled was less than 100 m (Lovanh et al. 2000). The intent with using this formula was to achieve a dispersion coefficient that was “in the ball park” and could later be refined during model calibration.

$$\alpha = 0.0175x^{1.46} \quad [6]$$

The retardation factor,  $R$ , was calculated using Equation [7] where  $K_d$  is the distribution coefficient which represent the chemical partitioning between the influent and the GAC and has units of  $m^3/kg$ .

$$R = 1 + \frac{\rho_{bed}K_d}{\phi} \quad [7]$$

Equation [7] is generally applied in groundwater (porous media) applications (Van Genuchten and Alves 1982), but was considered appropriate for flow through a porous media such as GAC. The values of  $K_d$  for PFHxA, PFOA and PFOS were determined from the slope of the line by plotting the effluent concentration of PFAS,  $C_e$ , versus the amount of PFAS adsorbed per mass of GAC,  $q$  (Figure 4-4). Only values above the LOD of 0.05  $\mu g/L$  were plotted. As a result of the low influent concentration of PFPeA and PFHxS,  $K_d$  could not be determined for these PFAS.

The amount of PFAS adsorbed per unit mass of GAC,  $q$ , was determined using Equation [8] where  $C_i$  is the influent concentration ( $\mu g/L$ ),  $C_e$  is the effluent concentration ( $\mu g/L$ ),  $V$  is the volume of influent ( $m^3$ ) and  $M_{GAC}$  is the mass of the GAC (kg). Where either the observed influent or effluent concentrations were below the LOD, a value of 0.05  $\mu g/L$  was used in the calculation of  $q$ .

$$q = \frac{(C_i - C_e) \times V}{M_{GAC}} \quad [8]$$

The retardation factor used for input into the model, 47,000, was an average of the three retardation factors calculated based on the value of  $K_d$  for PFHxA, PFOA and PFOS shown in Table 4-1.

**Table 4-1: Distribution Coefficients and Retardation Factors.**

<b>PFAS</b>	<b>Distribution Coefficient, <math>K_d</math> (<math>m^3/kg</math>)</b>	<b>Retardation Factor, <math>R</math> (unitless)</b>
PFHXA	13.976	12,230
PFOA	55.176	48,280
PFOS	92.467	80,910

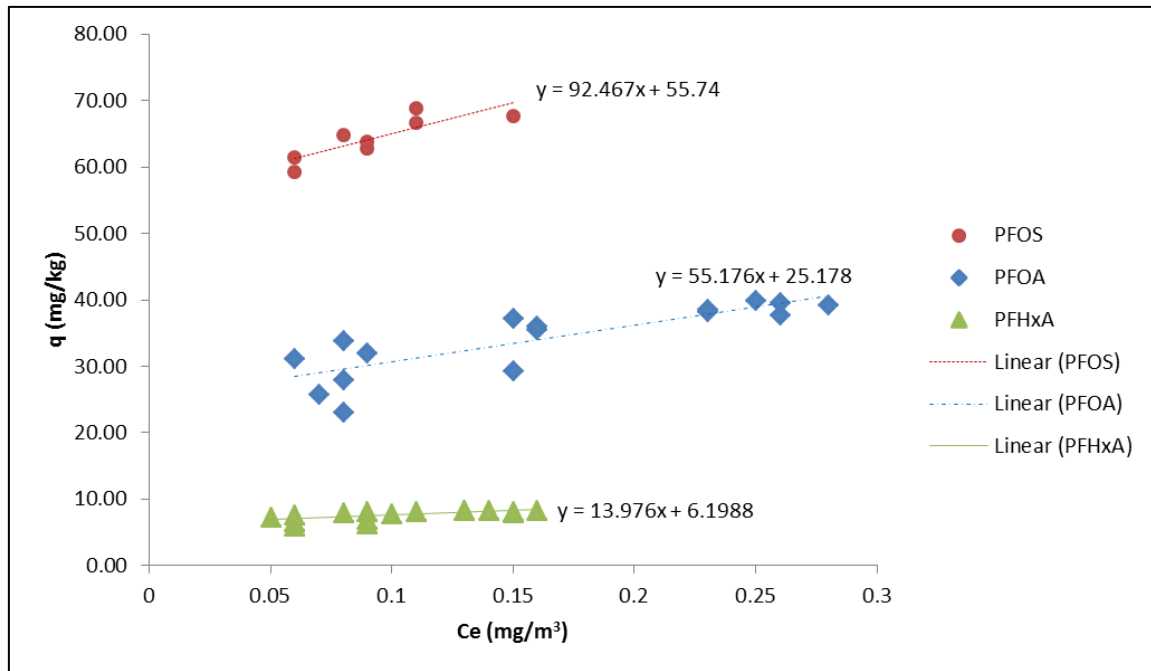


Figure 4-4: Plot used to determine  $K_d$ . The effluent concentration of PFAS was plotted against the amount of PFAS adsorbed per kg of GAC for PFHxA, PFOA and PFOS. The partition coefficient  $K_d$  was estimated by the slope of the linear trend line.

Model input parameters based on the data from Basin 1 of the Minnesota GAC setup are given in Table 4-2.

Table 4-2: Model Input Parameters Prior to Calibration

Parameter	Value	Units
Distance Step, $\Delta x$	0.09	m
Time Step, $\Delta t$	1	day
Velocity, $u$	0.00238	m/s
Dispersion coefficient, $E$	0.0002	$m^2/s$
Average influent concentration, $C_i$	1.88	$\mu g/L$
Retardation factor, $R$	47 000	--

### 4.2.3 Model Calibration, Sensitivity Analysis and Validation

Two different methods of calculating error were used; the root-mean-square-error (RMSE) shown in Equation [9], and the Nash-Sutcliffe efficiency (NSE) shown in Equation [10].

$$RMSE = \sqrt{\frac{\sum(C_o - C_M)^2}{n}} \quad [9]$$

$$NSE = 1 - \frac{\sum(C_o - C_M)^2}{\sum(C_o - \bar{C}_o)^2} \quad [10]$$

In both Equations [9] and [10],  $C_o$  is the observed concentration ( $\mu\text{g/L}$ ) and  $C_M$  is the modelled concentration ( $\mu\text{g/L}$ ). In Equation [10],  $\overline{C_o}$  is the averaged observed concentration ( $\mu\text{g/L}$ ), and in Equation [9],  $n$  is the number of data points. For the RMSE, a smaller number indicates better agreement between the modeled and measured data. For the NSE, a value of 1 indicates a perfect match between the modeled and measured data, and a value between 0 and 1 is generally considered acceptable. A value of 0 or less indicates that the averaged observed values over the simulation period are a better way of predicting the expected value than the model simulated value (Moriasi et al. 2007). The observed data was subjected to a LOD. Different methods can be applied to deal with a LOD including replacing the LOD with zeroes, reducing the LOD by half, or keeping the LOD as is. For this study, the LOD was left as is, but only data above the LOD were used to calculate RMSE and NSE.

Sensitivity of the model to changes in the dispersion coefficient,  $E$ , and the retardation factor,  $R$ , was tested by altering one or the other and noting the effect on the RMSE and NSE for the effluent concentrations. Calibration of the model was conducted through optimization of RMSE and NSE for the effluent concentrations only by altering both  $E$  and  $R$ . Validation of the model was accomplished using the data from Basin 2 in conjunction with the calibrated values of  $E$  and  $R$ . Basin 2 was in lag configuration for the first 656 days and lead configuration for another 403 days. The average influent concentration of PFAS was much less when Basin 2 was in lag configuration ( $0.38 \mu\text{g/L}$ ) than in lead configuration ( $1.54 \mu\text{g/L}$ ). Therefore, an average influent concentration of  $0.38 \mu\text{g/L}$  was used for the first 656 days, and an average influent concentration of  $1.54 \mu\text{g/L}$  was used for the remaining 404 days.

#### 4.2.4 Application of the Model to a Warship

Onboard the Halifax Class CPFs, the fitted AFFF system contains  $3.6 \text{ m}^3$  of 6% AFFF divided equally between two tanks (DND 2005; DNPS 6-2 2016). The AFFF used by the RCN is manufactured by Ansul and meets the US military specification MIL-F-24385F (DNPS 6-2 2016). The safety data sheet lists four chemicals used in the product, one of which is listed as “Trade secret”. The PFAS used in AFFF are often listed in the safety data sheets as proprietary, secret or confidential, so it is reasonable to assume that the chemical referred to as “Trade secret” in the Ansulite safety data sheet is referring to the PFAS present in the product. The mass fraction ( $w_i$ ) for this component of the AFFF is listed between 0.07 and 0.13 (Tyco 2015). The density ( $\rho_{\text{AFFF}}$ ) of Ansulite 6% (AFC-6MS) AFFF is  $1030 \text{ kg/m}^3$  at  $25^\circ\text{C}$  (Johnson 2017). The concentration of PFAS ( $C_{\text{PFAS}}$ ) in AFFF was determined to be  $8 \text{ kg/m}^3$  using Equation [11] and a mass fraction of 0.13 for PFAS.

$$C_{\text{PFAS}} = (w_i) \times \rho_{\text{AFFF}} \times 0.06 \quad [11]$$

Previous work by Backe et al. (2013) determined that a sample of AFFF manufactured by Ansul in 2005 contained  $7 \text{ kg/m}^3$  of 4:2, 6:2 and 8:2 fluorotelomer thioamido sulfonates (FtTAoS), with the majority of the PFAS containing 6 fluorinated carbons. This concentration equates to a mass fraction of 0.11 of PFAS in the AFFF.

A 6% AFFF combines with either fresh or seawater in a 6% solution (6 parts AFFF and 94 parts water). Therefore, to remove PFAS from  $3.6 \text{ m}^3$  of AFFF, the total volume of used AFFF + seawater that must pass through the GAC column is  $60 \text{ m}^3$ . The corresponding average influent

concentration of PFAS for AFFF + seawater used in the model to size the GAC column was  $0.48 \text{ kg/m}^3$  or  $480,000 \text{ }\mu\text{g/L}$ .

### 4.3 Results and Discussion

#### 4.3.1 Model Calibration and Sensitivity Analysis

The results of the model prior to any calibration are shown in Figure 4-5. Only data to the right of the vertical dashed line in Figure 4-5a were used to calculate the RMSE and NSE for the concentration of PFAS in the effluent. The RMSE for the modelled effluent concentration prior to any calibration was  $0.19 \text{ }\mu\text{g/L}$  and the NSE was  $-0.90$ , indicating that it was not a good predictor of  $C_e$ .

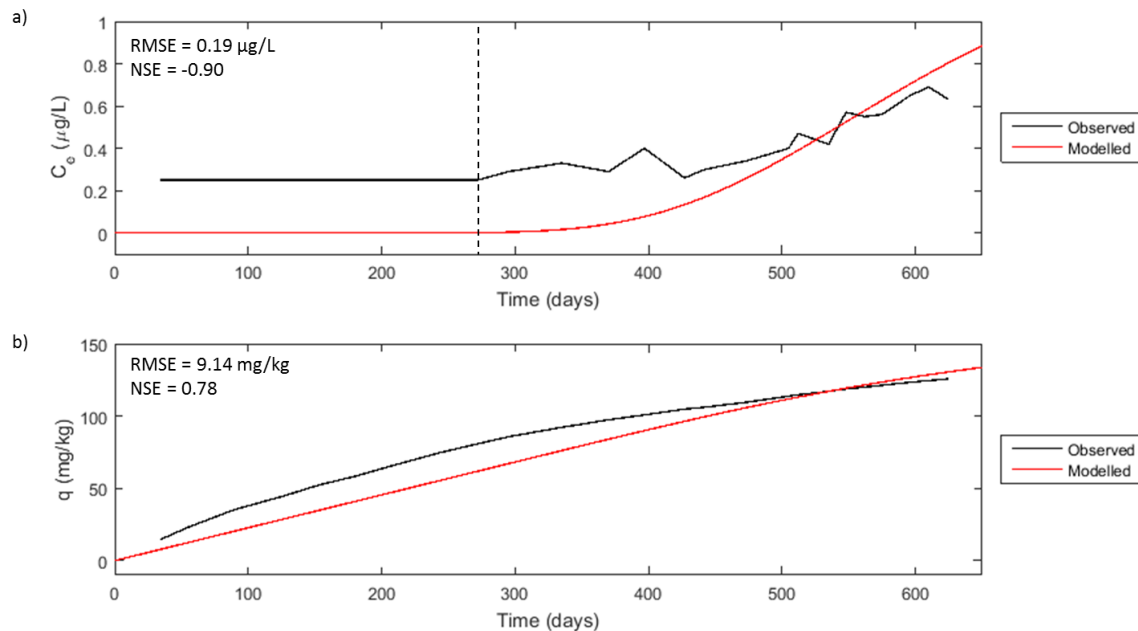


**Figure 4-5: Model Results Prior to Calibration.** The observed (black) and pre-calibrated modelled (red) effluent concentration,  $C_e$ , of PFAS is compared in (a) and the quantity of PFAS adsorbed per kg of GAC is compared in (b).

The results of the sensitivity analysis shown are in Table 4-3. Both E and R were decreased by multiplying by a factor of 0.5, and both were increased by multiplying by a factor of 1.5. When E was reduced, both the RMSE and NSE worsened slightly ( $0.32 \text{ }\mu\text{g/L}$  and  $-4.23$ ), but when E was increased, both RMSE and NSE improved slightly ( $0.14 \text{ }\mu\text{g/L}$  and  $0.01$ ). Changes to the retardation factor, R, had a much greater effect on the RMSE and the NSE, indicating that the model was more sensitive to changes made to this parameter. Decreasing R increased RMSE to  $0.79 \text{ }\mu\text{g/L}$  and decreased NSE to  $-31.23$ . Increasing R also increased RMSE, but only to  $0.41 \text{ }\mu\text{g/L}$  and NSE was decreased to  $-7.63$ . RMSE and the NSE were optimized at values of  $0.13 \text{ }\mu\text{g/L}$  and  $0.11$  when R remained at  $47,000$  and E was increased by a factor of two to  $0.0004 \text{ m}^2/\text{s}$  as shown in the calibrated model results in Figure 4-6a. The difference between the calculated and calibrated values of E may be related to differences in the chemical properties of hydrocarbons versus fluorinated carbons, but could also be a result of the properties of the GAC compared to the properties of typical aquifer solids. Bromly *et al.* (2007) found that the dispersion coefficient

and the dispersivity were affected by changes in the pore velocity, bulk density, clay content and silt content of aquifer solids such as different types of soil and sand. The largest deviations between the observed and modelled data occur early on. This is not unexpected, as the PFAS broke through in the effluent at different times as shown in Figure 4-3a. As long as there were PFAS that had not broken through, the observed data were affected by the LOD. PFHxA and PFOA were the first PFAS to breakthrough, both being detected on day 295. PFPeA was detected on day 473 and PFOS, the most abundant PFAS in the influent, was not detected until day 512. PFHxS did not breakthrough.

**Table 4-3: Results of Sensitivity Analysis. The values for E and R that are bold were used in the calibrated model.**

Changes	E (m <sup>2</sup> /s)	R	RMSE (µg/L)	NSE
---	0.0002	47,000	0.19	-0.90
E x 0.5	0.0001	47,000	0.32	-4.23
E x 1.5	0.0003	47,000	0.14	0.01
<b>E x 2.0</b>	<b>0.0004</b>	<b>47,000</b>	<b>0.13</b>	<b>0.11</b>
R x 0.5	0.0002	23,500	0.79	-31.23
R x 1.5	0.0002	70,500	0.41	-7.63

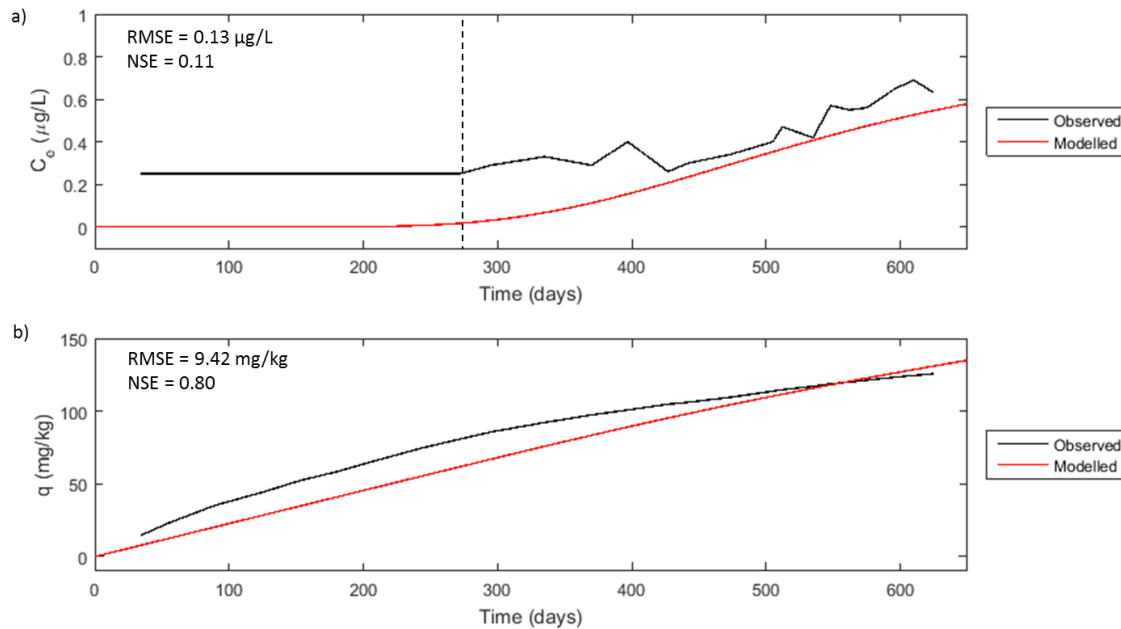


**Figure 4-6: Calibrated Model Results. The observed (black) and calibrated modelled (red) effluent concentration,  $C_e$ , of PFAS is compared in (a) and the quantity of PFAS adsorbed per kg of GAC is compared in (b).**

### 4.3.2 Model Validation

The results using the validation data are presented in Figure 4-7. The RMSE was 0.28 µg/L for the modelled concentration of PFAS in the effluent and 20.60 mg/kg for modelled adsorption of

PFAS to GAC. The NSE of -1.92 for the modelled effluent concentration suggests that the model is not reliably predicting this parameter, but for PFAS adsorption, the NSE of 0.80 suggests that the model is providing acceptable results. In the observed data, both PFPeA and PFHxA were first detected in the effluent on day 606, PFOA was next on day 627, but then was not detected again until day 867. PFOS was detected on day 926 and PFHxS was not detected at all in the effluent. In the modelled data, PFAS broke through on day 1056. One reason why the observed PFAS may have broken through into the effluent much faster than the modelled PFAS is that the adsorption sites on the GAC were being used up by other organic molecules. As a result of the longer duration in which the GAC in Basin 2 was in use, it would have had much more opportunity to become fouled with other organic matter. In a study completed by Yu et al. (2012), organic matter has been found to greatly reduce the adsorption capacities and sorption rates of PFOS and PFOA onto powdered activated carbon.

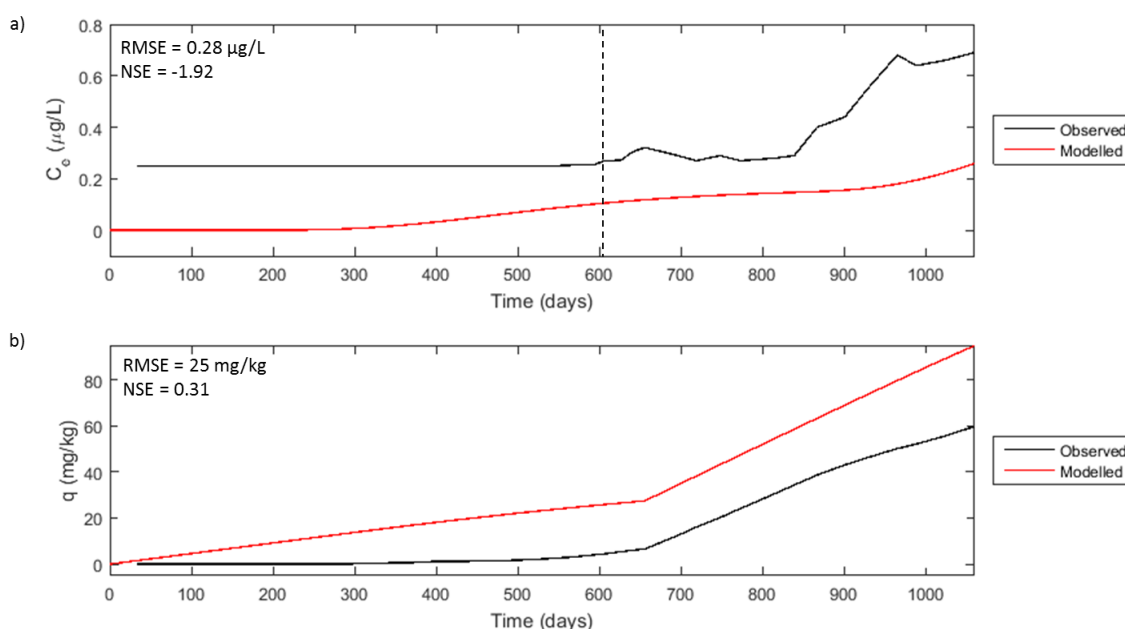


**Figure 4-7: Validation Model Results.** The observed (black) and pre-calibrated modelled (red) effluent concentration,  $C_e$ , of PFAS is compared in (a) and the quantity of PFAS adsorbed per kg of GAC is compared in (b).

Although the model results are questionable for the modelled PFAS concentration in the effluent, the results for PFAS adsorption to GAC are in the range of acceptable, providing confidence that the model can be used for its intended purpose. As a test, both E and R were altered using the validation data to see what the effect would be on the RMSE and NSE. When E was decreased to  $0.0002 \text{ m}^2/\text{s}$ , the RMSE and the NSE for  $C_e$  improved slightly ( $0.22 \mu\text{g/L}$  and -0.72), but not enough to render the model acceptable. When R was reduced in half to 23,500, both the RMSE and NSE improved substantially to  $0.12 \mu\text{g/L}$  and 0.48 respectively. In both cases, the RMSE for  $q$  only improved slightly ( $18.93 \text{ mg/kg}$  when adjusting R, and  $23.38 \text{ mg/kg}$  when adjusting E), and the NSE worsened slightly, but still remained above 0 indicating that even though the modelled PFAS concentrations are suspect, the modelled PFAS adsorption is somewhat consistent and more reliable.

### 4.3.3 Application of Model to Shipboard Scenario

The parameters that were input into the model for application to the ship scenario are listed in Table 4-4. To determine the volume of GAC required for all of the PFAS in 60 m<sup>3</sup> of AFFF + seawater, flowing at 1.5 m<sup>3</sup>/min, to adsorb to the GAC, both the time step and the distance step in the model had to be reduced (0.02 hrs and 0.0013 m). At a flow of 1.5 m<sup>3</sup>/min, 42 min are required to pump all 60 m<sup>3</sup> of AFFF + seawater through the GAC column. The remaining parameters, with the exception of the influent concentration of PFAS, which was determined to be 0.48 kg/m<sup>3</sup> (480,000 µg/L) in section 4.2.4, remained unaltered.

Table 4-4: Parameters input into the model for the shipboard application.

Parameter	Value	Units
Distance Step, $\Delta x$	0.0013	m
Time Step, $\Delta t$	0.02	hrs
Velocity, $u$	0.00238	m/s
Dispersion coefficient, $E$	0.0004	m <sup>2</sup> /s
Average influent concentration, $C_i$	0.48	kg/m <sup>3</sup>
Retardation factor, $R$	47 000	--

Results using the parameters determined for shipboard application of the model are shown in Figure 4-8. Breakthrough of PFAS occurs around minute 45 (Figure 4-8a), at which point adsorption of PFAS to GAC is approximately 1.8 g/kg. By comparison, Ochoa-Herrera and Sierra-Alvarez (2008) achieved adsorption of 225 g PFOS/kg GAC, 60 g PFOA/kg GAC and 50 g PFBS/kg GAC using Calgon F400 GAC with an influent concentration of 0.08 kg/m<sup>3</sup>. The volume of GAC based on the results presented in Figure 4-8 was calculated to be 0.42 m<sup>3</sup>, which equates to 265 kg of Calgon F600 GAC.

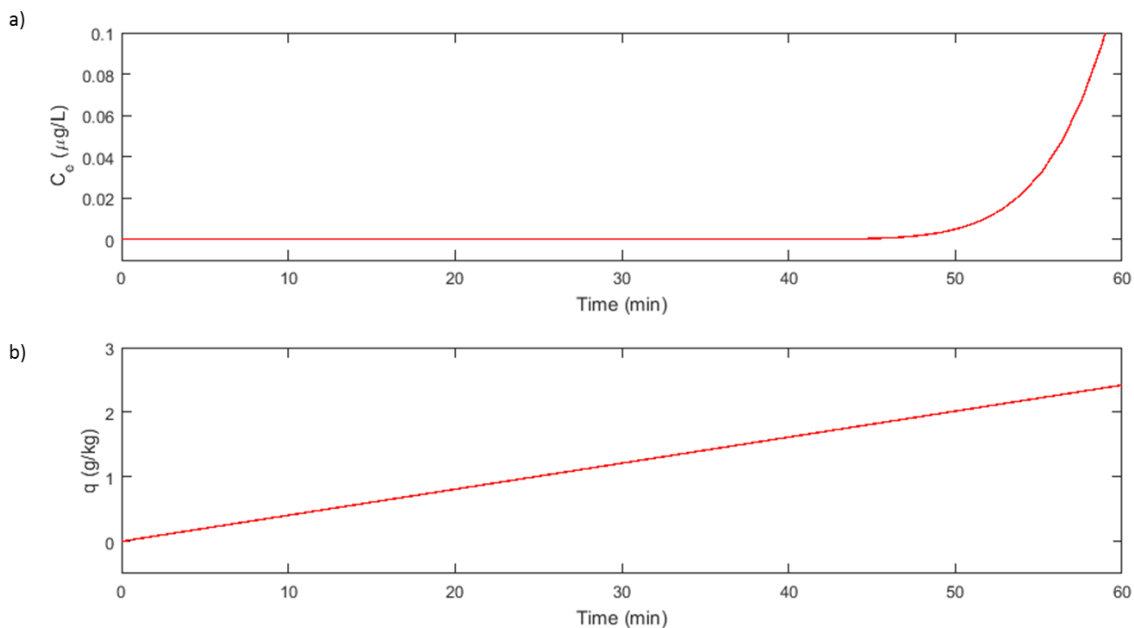




**Figure 4-8: Results of Applying Model to Shipboard Scenario.** The modelled effluent concentration,  $C_e$ , of PFAS from 3.6 m<sup>3</sup> of AFFF (a) and the quantity of PFAS adsorbed per kg of GAC (b) are shown for an input concentration of 0.48 kg/m<sup>3</sup>.

Since the RMSE and NSE suggest that the model provides only marginally acceptable results, and the modelled PFAS adsorption was approximately 2.7 times greater than the observed PFAS adsorption, a safety factor of 3 was considered when determining the amount of GAC required to achieve full adsorption with no breakthrough. After applying the safety factor, the volume of GAC required becomes 1.26 m<sup>3</sup>, and the corresponding mass of Calgon F600 GAC increases to 795 kg. A GAC column of this size and mass could physically fit onboard a ship.

#### **4.4 Summary and Conclusion**

A numerical model was developed to simulate PFAS adsorption to GAC. The calibrated model was applied to a shipboard scenario to estimate the quantity of GAC required for removing PFAS from used AFFF in a single event scenario. Validation of the model suggested that the model's ability to accurately predict PFAS breakthrough in the effluent is not reliable, however its prediction of the amount of PFAS adsorbed per unit mass of GAC is moderately acceptable. Due to the uncertainty of the model's output, a safety factor of 3 was considered when sizing the GAC column. The model results, including the safety factor, suggest that a GAC column holding 795 kg of GAC would be capable of removing all of the PFAS from the AFFF contained in the fitted system onboard a Halifax Class CPF. The corresponding volume of the GAC column required is 1.26 m<sup>3</sup>, which could physically fit onboard a ship. While the modelled results suggest that GAC could be a viable option for removal of PFAS from used AFFF onboard warships, the reliability of the model creates enough uncertainty that the feasibility of using this method cannot be thoroughly evaluated. Moving forward, bench scale studies to determine the adsorption rates of the specific types of PFAS contained in samples of AFFF could be useful in gaining data that could then be modelled. Data from actual application of GAC to remove PFAS from AFFF impacted water such as was done in Lac-Mégantic, could also prove useful, as there may be other organic matter present in AFFF that could compete with the PFAS for adsorption sites on the GAC. Model reliability might be improved by modelling PFAS adsorption to GAC as a sink instead of using a retardation factor, which seems to change depending on the influent concentration of PFAS.

## **Chapter 5 Principle Outcomes and Recommendations**

### **5.1 Summary of Main Objectives**

The objectives of this thesis were to: (1) identify where PFAS exists within the RCN, and in what quantities; (2) understand the quantities of PFAS entering the environment and their fate and transport as a result of AFFF sent into the ocean from RCN vessels; and (3) to investigate potential methods to reduce or eliminate PFAS from AFFF entering the ocean environment and the feasibility of implementing one of these methods.

### **5.2 Per- and Polyfluoroalkyl Substances in the Royal Canadian Navy**

A literature review presented in Chapter 1 revealed many studies related to environmental quantification, and fate and transport of PFAS from AFFF used by military installations at land based facilities, but not naval use of AFFF onboard warships. The extent that naval use of AFFF contributes to the overall quantification of PFAS in the environment, and the impact of the Navy's use of AFFF was not well understood. Furthermore, if the Navy's use of AFFF was found to impact the environment, options for reducing or eliminating PFAS release to the environment had not been explored.

In Chapter 2, types and quantities of PFAS in items used within the RCN were described, with a focus on the use of AFFF in warships. US military specification (MIL-F-24385F) AFFF, manufactured by Ansul, is used in 12 Halifax Class Canadian Patrol Frigates (CPFs), four Victoria Class Submarines and 12 Kingston Class Maritime Coastal Defence Vessels (MCDVs) (DNPS 6-2 2016). In total, these vessels carry 90 m<sup>3</sup> of undiluted AFFF (DND 2005; Babcock 2015; Gallant 2017; McNaughton 2017). A 6% AFFF meeting MIL-F-24385F contains between 4 and 8 kg/m<sup>3</sup> of 6:2 fluorotelomer thioamido sulfonates (Backe et al. 2013; Tyco 2015; Johnson 2017). Ten years of fire reports onboard RCN vessels revealed that the AFFF fitted system was used once in 64 reported fires (CFFM 2017). An account from an engine room fire onboard a vessel in the early 2000s indicated AFFF was released overboard, but the exact quantity was unknown. AFFF usage has resulted in quantities of PFOS and PFOA in groundwater that are several million times greater (550,000 ng/L and 220,000 ng/L) than the US EPA's combined health advisory limit of 70 ppt for PFOS and PFOA (Backe et al. 2013; Barzen-Hanson and Field 2015). Desorption studies estimate that PFAS impacted fire training sites will remain contaminated with PFAS for years, taking two years for 90 % of the fluorotelomers present to desorb and upwards of 82 years for 90 % of the PFOS to desorb (Baduel et al. 2015). Fish downstream from an accidental AFFF release were found to have elevated levels of PFOS up to ten years following the release (Awad et al. 2011).

The investigation into types and quantities of PFAS in the RCN presented in Chapter 2 suggest that given the quantities of AFFF carried onboard RCN vessels, combined with the number of reported fires and the fact that used AFFF has been sent overboard in the past, that there is reason to believe that RCN use of AFFF could potentially add to the PFAS burden in the environment. Research presented in Chapter 2 demonstrates that PFAS from AFFF that has entered the environment has had profound effects and could continue to impact the areas of release for several decades.

### **5.3 Fate and Transport of PFAS from AFFF in Halifax Harbour**

Research conducted in Chapter 2 revealed that the RCN's use of AFFF could potentially contribute PFAS to the environment when used AFFF is allowed to flow overboard into the ocean. However, the quantity of PFAS entering the marine environment following release of AFFF overboard compared to existing quantities of PFAS, and its fate and transport once released were unknown.

In Chapter 3, a hydrodynamic model was used to investigate the fate and transport of a tracer-like substance, representing PFAS from used AFFF, for a release into different areas both inside and outside of Halifax Harbour for differing wind and surface wave scenarios.

The results of the model simulation, described in Chapter 3, predicted that for 6 kg/m<sup>3</sup> of PFAS flowing into the Harbour at 0.006 m<sup>3</sup>/s for 10 minutes, initial quantities of PFAS will reach 6 orders of magnitude when measured in pg/L. For comparison, drinking water screening values provided by Health Canada for several perfluoroalkyl carboxylic acids and perfluoroalkyl sulfonic acids range from 0.2 up to 30 ug/L (200,000 to 3 x 10<sup>7</sup> pg/L). PFAS subjected to high winds and surface waves travelled further and more quickly than the PFAS released during calm weather and sea conditions. PFAS released in the Narrows impacted the shoreline within 1 hour at concentrations that were 5 x 10<sup>6</sup> pg/L. PFAS from all release locations within the Harbour were impacting the coastal areas regardless of wind and wave conditions within 12 hours. After 10 days, PFAS released during calm conditions remained at elevated levels in all areas of the Harbour ranging from 800 pg/L in the Outer Harbour to 60,000 pg/L in the Narrows. In comparison, background levels of PFAS off the coast of Rhode Island were determined to be 5800 pg/L by (Benskin et al. 2012). PFAS release outside of the Harbour was transported more quickly and was completely flushed out of the area after 10 days.

The results of the hydrodynamic model used to simulate fate and transport of PFAS from used AFFF released into the ocean in Halifax Harbour show that elevated levels of PFAS will remain with the Harbour for several days following the release, and that regardless of where the release was in the Harbour, that the shoreline will be impacted by the PFAS. Elevated wind and wave conditions will cause the PFAS to travel further and faster and thus could result in the coastal communities being impacted in a shorter time range than PFAS released during calm wind and wave conditions.

### **5.4 Sizing of a GAC Based PFAS Adsorption Column**

The hydrodynamic model results for PFAS fate and transport from AFFF released into a marine environment presented in Chapter 3 indicate that AFFF released overboard is likely to result in elevated levels of PFAS that could impact coastal areas. Granular activated carbon (GAC) was successfully used to remove PFAS from AFFF impacted water at the site of a train derailment in 2013, but its use for the removal of PFAS from AFFF impacted water onboard a marine vessel has not been investigated.

A numerical model was used to simulate PFAS adsorption to GAC in order to determine the quantity of GAC that would be required to remove all PFAS from 3.6 m<sup>3</sup> of AFFF, and to investigate the feasibility of using GAC onboard a warship. Both bulk flow and hydrodynamic dispersion were considered in one dimension, and adsorption of PFAS to GAC was represented

using a retardation factor. The model was calibrated and validated using data from a full scale setup that used GAC to remove PFAS from groundwater.

Validation of the model, using a separate set of data from the same full scale setup that was used to calibrate the model, indicated that the results for PFAS concentration in the effluent were outside of acceptable according to Nash-Sutcliffe Efficiency (NSE was -1.92). The NSE for the amount of PFAS adsorbed to GAC was within the range of acceptable at 0.31. Based on the model's predicted PFAS adsorption being 2.7 times greater than the observed PFAS adsorption when run using the validation data from Basin 2, a safety factor of 3 was applied to the model's estimate for the amount of GAC required for removal of 0.48 kg/m<sup>3</sup> of PFAS from 3.6 m<sup>3</sup> of AFFF. Including the safety factor, the model predicted that 1.26 m<sup>3</sup> of GAC was required, which corresponds to 795 kg of Calgon F600. The volume and corresponding mass of GAC required, including the safety factor, could physically fit onboard a ship, but the poor model performance made it impossible to decisively conclude whether or not it is a viable for use by the RCN.

## **5.5 Future Research and Recommendations**

While quantities of AFFF carried onboard RCN vessels were readily available, indications of AFFF released due to firefighting, maintenance or accidental release were unknown, as were quantities of AFFF that may have been released overboard. In the future, a reporting system within the RCN to capture quantities of AFFF deployed during firefighting, maintenance or accidental deployment, as well as estimated quantities, locations and weather conditions for any AFFF that might have been released overboard would be useful in determining whether or not RCN use of AFFF is likely impacting the surrounding environment.

Given the known types and quantities of PFAS in the AFFF used by the RCN, fate and transport modelling of PFAS from used AFFF sent overboard could be improved by considering partitioning to the atmosphere or sediments, as well as potential transformations due to reactions in the environment. Although certain types of PFAS have been shown to act as conservative tracers, the density of PFAS is greater than that of water, and future modelling work may be improved by accounting for this. A mass balance should be considered in order to account for any PFAS that might exit the modelling domain due to partitioning or flow through the boundary. As partitioning coefficients may not be available in the literature, lab scale experiments to determine these coefficients may be required. While some work has been undertaken to study the transformation of 6:2 FtTAoS in microcosms, further work to investigate potential transformation in seawater would be useful to help determine the fate of this type of PFAS when released into the ocean.

Methods of removing PFAS from AFFF impacted water onboard a ship should continue to be investigated. The use of GAC could still be a viable option. Given that the PFAS in AFFF used by the RCN is mostly 6:2 FtTAoS, bench scale studies to determine the adsorption rates of this specific PFAS could be useful in gaining data that could then be modelled. Likewise, data from actual application of GAC to remove PFAS from AFFF impacted water could also prove useful. Furthermore, model reliability might be improved by modelling PFAS adsorption to GAC as a sink instead of using a retardation factor.

## References

- 3M (1999a) "Perfluorooctane Sulfonate: Current Summary of Human Sera, Health and Toxicology Data." 14.
- 3M (1999b). The Science of Organic Fluorochemistry, US Environmental Protection Agency Washington, DC.
- 3M (2000b). 3M Phase Out Plan for POSF Based Products: 11.
- Ahrens, L. (2011). "Polyfluoroalkyl compounds in the aquatic environment: a review of their occurrence and fate." Journal of Environmental Monitoring **13**(1): 20-31.
- Ahrens, L., J. L. Barber, et al. (2009). "Longitudinal and Latitudinal Distribution of Perfluoroalkyl Compounds in the Surface Water of the Atlantic Ocean." Environmental Science & Technology **43**(9): 3122-3127.
- Ahrens, L., Z. Y. Xie, et al. (2010). "Distribution of perfluoroalkyl compounds in seawater from Northern Europe, Atlantic Ocean, and Southern Ocean." Chemosphere **78**(8): 1011-1016.
- Apelberg, B. J., L. R. Goldman, et al. (2007). "Determinants of fetal exposure to polyfluoroalkyl compounds in Baltimore, Maryland." Environmental Science & Technology **41**(11): 3891-3897.
- Appleman, T. D., E. R. V. Dickenson, et al. (2013). "Nanofiltration and granular activated carbon treatment of perfluoroalkyl acids." Journal of Hazardous Materials **260**: 740-746.
- Appleman, T. D., C. P. Higgins, et al. (2014). "Treatment of poly- and perfluoroalkyl substances in US full-scale water treatment systems." Water Research **51**: 246-255.
- Arias E, V. A., M. Mallavarapu, et al. (2015). "Identification of the source of PFOS and PFOA contamination at a military air base site." Environmental Monitoring and Assessment **187**(1).
- Ashall, L. M., R. P. Mulligan, et al. (2016). "Variability in suspended sediment concentration in the Minas Basin, Bay of Fundy, and implications for changes due to tidal power extraction." Coastal Engineering **107**: 102-115.
- Australian Government, D. o. D. (2007). Environmental Guidelines for Management of Fire Fighting Aqueous Film Forming Foam (AFFF) Products. D. o. Defence.
- Awad, E., X. M. Zhang, et al. (2011). "Long-Term Environmental Fate of Perfluorinated Compounds after Accidental Release at Toronto Airport." Environmental Science & Technology **45**(19): 8081-8089.
- Babcock, C. (2015). Baseline DC and FF Equip Layout (Draft).
- Backe, W. J., T. C. Day, et al. (2013). "Zwitterionic, Cationic, and Anionic Fluorinated Chemicals in Aqueous Film Forming Foam Formulations and Groundwater from US Military Bases by Nonaqueous Large-Volume Injection HPLC-MS/MS." Environmental Science & Technology **47**(10): 5226-5234.

- Baduel, C., C. J. Paxman, et al. (2015). "Perfluoroalkyl substances in a firefighting training ground (FTG), distribution and potential future release." Journal of Hazardous Materials **296**: 46-53.
- Barzen-Hanson, K. A. and J. A. Field (2015). "Discovery and Implications of C-2 and C-3 Perfluoroalkyl Sulfonates in Aqueous Film-Forming Foams and Groundwater." Environmental Science & Technology Letters **2**(4): 95-99.
- Barzen-Hanson, K. A., S. C. Roberts, et al. (2017). "Discovery of 40 Classes of Per- and Polyfluoroalkyl Substances in Historical Aqueous Film-Forming Foams (AFFFs) and AFFF-Impacted Groundwater." Environmental Science & Technology **51**(4): 2047-2057.
- Benskin, J. P., M. G. Ikonomidou, et al. (2012). "Observation of a Novel PFOS-Precursor, the Perfluorooctane Sulfonamido Ethanol-Based Phosphate (SAmPAP) Diester, in Marine Sediments." Environmental Science & Technology **46**(12): 6505-6514.
- Benskin, J. P., D. C. G. Muir, et al. (2012). "Perfluoroalkyl Acids in the Atlantic and Canadian Arctic Oceans." Environmental Science & Technology **46**(11): 5815-5823.
- Booij, N., R. Ris, et al. (1999). "A third-generation wave model for coastal regions: 1. Model description and validation." Journal of Geophysical Research: Oceans **104**(C4): 7649-7666.
- Bossi, R., K. Vorkamp, et al. (2016). "Concentrations of organochlorine pesticides, polybrominated diphenyl ethers and perfluorinated compounds in the atmosphere of North Greenland." Environmental Pollution **217**: 4-10.
- Brede, E., M. Wilhelm, et al. (2010). "Two-year follow-up biomonitoring pilot study of residents' and controls' PFC plasma levels after PFOA reduction in public water system in Arnsberg, Germany." International Journal of Hygiene and Environmental Health **213**(3): 217-223.
- Bromly, M., C. Hinz, et al. (2007). "Relation of dispersivity to properties of homogeneous saturated repacked soil columns." European journal of soil science **58**(1): 293-301.
- Brown, M. M., R. P. Mulligan, et al. (2014). "Modeling the transport of freshwater and dissolved organic carbon in the Neuse River Estuary, NC, USA following Hurricane Irene (2011)." Estuarine Coastal and Shelf Science **139**: 148-158.
- Brumovsky, M., P. Karaskova, et al. (2016). "Per- and polyfluoroalkyl substances in the Western Mediterranean Sea waters." Chemosphere **159**: 308-316.
- Buck, R. C., J. Franklin, et al. (2011). "Perfluoroalkyl and polyfluoroalkyl substances in the environment: Terminology, classification, and origins." Integrated Environmental Assessment and Management **7**(4): 513-541.
- Buckley, D. E. and G. V. Winters (1992). "Geochemical characteristics of contaminated surficial sediments in Halifax Harbour: impact of waste discharge." Canadian Journal of Earth Sciences **29**(12): 2617-2639.
- C8 Science Panel. (2017). "The Science Panel Website." Retrieved 22 September 2017, from <http://www.c8sciencepanel.org/panel.html>.

- Cai, M. H., H. Z. Yang, et al. (2012). "Per- and polyfluoroalkyl substances in snow, lake, surface runoff water and coastal seawater in Fildes Peninsula, King George Island, Antarctica." Journal of Hazardous Materials **209**: 335-342.
- CFFM, C. F. F. M. (2017). Incident Information Department of National Defence Canadian Forces 2007-01-01 to 2017-07-26.
- Chemours. (2017). "Facts on C-8 Litigation." Retrieved 29 August 2017, 2017, from [https://www.chemours.com/Chemours\\_Home/en\\_US/facts-on-C8-litigation.html](https://www.chemours.com/Chemours_Home/en_US/facts-on-C8-litigation.html).
- Crawford, A. (2014). Environmental characterization for the PISCES2 Trial, Defence Research and Development Canada - Atlantic Research Centre: 18.
- D'Agostino, L. A. and S. A. Mabury (2014). "Identification of Novel Fluorinated Surfactants in Aqueous Film Forming Foams and Commercial Surfactant Concentrates." Environmental Science & Technology **48**(1): 121-129.
- D'eon, J. C., M. D. Hurley, et al. (2006). "Atmospheric chemistry of N-methyl perfluorobutane sulfonamidoethanol, C<sub>4</sub>F<sub>9</sub>SO<sub>2</sub>N(CH<sub>3</sub>)CH<sub>2</sub>CH<sub>2</sub>OH: Kinetics and mechanism of reaction with OH." Environmental Science & Technology **40**(6): 1862-1868.
- Deltares (2014). Delft3D-FLOW User Manual. Simulation of multi-dimensional hydrodynamic flows and transport phenomena, including sediments. Delft, The Netherlands, Deltares.
- DeYoung, D. (1993). National Security and the US Naval Research Laboratory, Seventy Years of Science for the Navy and the Nation (1923-1993), DTIC Document.
- DHH, D. H. a. H. (2017). Canadian Armed Forces Dress Instructions. D. o. N. Defence.
- Dias, A. M. A., C. M. B. Gonçalves, et al. (2005). "Densities and Vapor Pressures of Highly Fluorinated Compounds." Journal of Chemical & Engineering Data **50**(4): 1328-1333.
- Dlugogorski, B., E. Kennedy, et al. (2002). "What properties matter in fire-fighting foams?" SCIENCE, TECHNOLOGY AND STANDARDS FOR FIRE SUPPRESSION SYSTEMS: 57-76.
- DND, C. F. (2005). HFX-D97-323-000-01 Fire Extinguishing System Diagram (AFFF). D. o. N. Defence.
- DNPS 6-2, D. (2016). C-97-323-000-TB-002 AFFF FIRE EXTINGUISHING SYSTEMS TECHNICAL BULLETIN (MARINE) ALL CLASSES. D. o. N. Defence: 27.
- Domingo, J. L. (2012). "Health risks of dietary exposure to perfluorinated compounds." Environment International **40**: 187-195.
- Douglas, A. (2017). "The Naval Service of Canada 1910-2010." Retrieved 2 October 2017, 2017, from <https://www.canada.ca/en/navy/services/history/naval-service-1910-2010.html>.
- ECCC, E. a. C. C. C. (2017) "<FEQG\_PFOS.pdf>." Federal Environmental Quality Guidelines Perfluorooctane Sulfonate (PFOS), 25.
- ECHA, E. C. A. (2017). Information on Chemicals.
- ECHA, E. C. A. (2017). "Registered Substances." Retrieved 25 August 2017, 2017, from <https://echa.europa.eu/registration-dossier/-/registered-dossier/6361/1>.

- Efsa Panel on food contact materials, e. f. and a. processing (2010). "Scientific Opinion on the safety evaluation of the substance perfluoro acetic acid,  $\alpha$ -substituted with the copolymer of perfluoro-1, 2-propylene glycol and perfluoro-1, 1-ethylene glycol, terminated with chlorohexafluoropropoxy groups, CAS No. 329238–24-6 for use in food contact materials." EFSA Journal **8**(2): 1519-n/a.
- Efsa Panel on food contact materials, e. f. and a. processing (2011). "Scientific Opinion on the safety evaluation of the substance, Perfluoro[(2-ethoxy-ethoxy)acetic acid], ammonium salt, CAS No. 908020-52-0, for use in food contact materials." EFSA Journal **9**(6): 2183-n/a.
- Elias, E., D. Walstra, et al. (2001). Hydrodynamic validation of Delft3D with field measurements at Egmond. Coastal Engineering **2000**: 2714-2727.
- Fader, G. B. (2007, 2007/10/09). "Halifax Harbour." Retrieved 13 December 2017, 2017, from <http://www.bedfordbasin.ca/halifaxharbour/DVD/fig1-eng.php>.
- Farley, J. P. and P. E. Scheffey (2016). A Historical Review of Fluorinated Foam Firefighting Agents, Performance Requirements/Environmental Safeguards Review, San Diego, CA.
- Gallant, T., CPO2 (2017). Seeking Information on AFFF in Frigates. L. M. Hodgkins, LCdr.
- Gannon, S. A., W. J. Fasano, et al. (2016). "Absorption, distribution, metabolism, excretion, and kinetics of 2,3,3,3-tetrafluoro-2-(heptafluoropropoxy)propanoic acid ammonium salt following a single dose in rat, mouse, and cynomolgus monkey." Toxicology **340**: 1-9.
- Giesy, J. P. and K. Kannan (2001). "Global Distribution of Perfluorooctane Sulfonate in Wildlife." Environmental Science & Technology **35**(7): 1339-1342.
- Gomis, M. I., Z. Y. Wang, et al. (2015). "A modeling assessment of the physicochemical properties and environmental fate of emerging and novel per- and polyfluoroalkyl substances." Science of the Total Environment **505**: 981-991.
- Gordon, S. C. (2011). "Toxicological evaluation of ammonium 4,8-dioxa-3H-perfluorononanoate, a new emulsifier to replace ammonium perfluorooctanoate in fluoropolymer manufacturing." Regulatory Toxicology and Pharmacology **59**(1): 64-80.
- Granum, B., L. S. Haug, et al. (2013). "Pre-natal exposure to perfluoroalkyl substances may be associated with altered vaccine antibody levels and immune-related health outcomes in early childhood." Journal of Immunotoxicology **10**(4): 373-379.
- Guelfo, J. L. and C. P. Higgins (2013). "Subsurface Transport Potential of Perfluoroalkyl Acids at Aqueous Film-Forming Foam (AFFF)-Impacted Sites." Environmental Science & Technology **47**(9): 4164-4171.
- Guy, W. S., D. R. Taves, et al. (1976). Organic Fluorocompounds in Human Plasma: Prevalence and Characterization. Biochemistry Involving Carbon-Fluorine Bonds, AMERICAN CHEMICAL SOCIETY. **28**: 117-134.
- Gyllenhammar, I., U. Berger, et al. (2015). "Influence of contaminated drinking water on perfluoroalkyl acid levels in human serum - A case study from Uppsala, Sweden." Environmental Research **140**: 673-683.



- Hanford, W. E. and J. R. M. Joyce (1948). Halogenated hydrocarbons and method for their preparation, Google Patents.
- Hannah, C. G., J. A. Shore, et al. (2001). "Seasonal circulation on the western and central Scotian Shelf." Journal of Physical Oceanography **31**(2): 591-615.
- Hansen, M. C., M. H. Borresen, et al. (2010). "Sorption of perfluorinated compounds from contaminated water to activated carbon." Journal of Soils and Sediments **10**(2): 179-185.
- Happonen, M., H. Koivusalo, et al. (2016). "Contamination risk of raw drinking water caused by PFOA sources along a river reach in south-western Finland." Science of the Total Environment **541**: 74-82.
- Harding-Marjanovic, K. C., E. F. Houtz, et al. (2015). "Aerobic Biotransformation of Fluorotelomer Thioether Amido Sulfonate (Lodyne) in AFFF-Amended Microcosms." Environmental Science & Technology **49**(13): 7666-7674.
- Harding-Marjanovic, K. C., S. Yi, et al. (2016). "Effects of Aqueous Film-Forming Foams (AFFFs) on Trichloroethene (TCE) Dechlorination by a Dehalococcoides mccartyi-Containing Microbial Community." Environmental Science & Technology **50**(7): 3352-3361.
- HC, H. C. (2016a) "Health Canada's Drinking Water Screening Values for Perfluoroalkylated Substances (PFAS)." Health Canada's Drinking Water Screening Values for Perfluoroalkyl Substances (PFAS), 2.
- HC, H. C. (2016b). Perfluorooctane Sulfonate (PFOS) in Drinking Water, Document for Public Consultation. H. Canada: 102.
- HC, H. C. (2016c). Perfluorooctanoic Acid (PFOA) in Drinking Water, Document for Public Consultation: 103.
- Higgins, C. P., J. A. Field, et al. (2005). "Quantitative determination of perfluorochemicals in sediments and domestic sludge." Environmental Science & Technology **39**(11): 3946-3956.
- Houtz, E. F., C. P. Higgins, et al. (2013). "Persistence of perfluoroalkyl acid precursors in AFFF-impacted groundwater and soil." Environmental Science and Technology **47**(15): 8187-8195.
- Johnson, J. C. (2017). Ansilite AFC-6MS 6% AFFF Concentrate Data Sheet.
- Kannan, K. (2011). "Perfluoroalkyl and polyfluoroalkyl substances: current and future perspectives." Environmental Chemistry **8**(4): 333-338.
- Kannan, K., J. C. Franon, et al. (2001). "Perfluorooctane Sulfonate in Fish-Eating Water Birds Including Bald Eagles and Albatrosses." Environmental Science & Technology **35**(15): 3065-3070.
- Kannan, K., J. Koistinen, et al. (2001). "Accumulation of perfluorooctane sulfonate in marine mammals." Environmental Science and Technology **35**(8): 1593-1598.

- Kempisty, D. M. (2014). "Adsorption of volatile and perfluorinated compounds from groundwaters using granular activated carbon."
- Knepper, T. P. and F. T. Lange (2011). Polyfluorinated chemicals and transformation products, Springer Science & Business Media.
- Kujath, J., LCdr (2017). Historical Usage of AFFF at the DC Schools. L. M. Hodgkins, LCdr.
- Lai, S. C., J. W. Song, et al. (2016). "Neutral polyfluoroalkyl substances in the atmosphere over the northern South China Sea." Environmental Pollution **214**: 449-455.
- Lang, J. R., B. M. Allred, et al. (2016). "Release of Per- and Polyfluoroalkyl Substances (PFASs) from Carpet and Clothing in Model Anaerobic Landfill Reactors." Environmental Science & Technology **50**(10): 5024-5032.
- Lassen, C., A. Brinch, et al. (2017). Sources of Perfluorobutane Sulfonic Acid (PFBS) in the Environment. Denmark, COWI A/S: 122.
- Lesser, G. R., J. A. Roelvink, et al. (2004). "Development and validation of a three-dimensional morphological model." Coastal Engineering **51**(8-9): 883-915.
- Li, Q. F., T. Y. Wang, et al. (2017). "Using hydrodynamic model to predict PFOS and PFOA transport in the Daling River and its tributary, a heavily polluted river into the Bohai Sea, China." Chemosphere **167**: 344-352.
- Liu, Z. Y., Y. L. Lu, et al. (2017). "Pollution pathways and release estimation of perfluorooctane sulfonate (PFOS) and perfluorooctanoic acid (PFOA) in central and eastern China." Science of the Total Environment **580**: 1247-1256.
- Lovanh, N., Y.-K. Zhang, et al. (2000). "Guidelines to determine site-specific parameters for modeling the fate and transport of monoaromatic hydrocarbons in groundwater." report submitted to the Iowa Comprehensive Petroleum Underground Storage Tank Fund Board, University of Iowa, Iowa City, Iowa.
- Martin, J. W., B. J. Asher, et al. (2010). PFOS or PreFOS? Are perfluorooctane sulfonate precursors (PreFOS) important determinants of human and environmental perfluorooctanesulfonate (PFOS) exposure?
- McNaughton, I., CPO2 (2017). AFFF in MCDVs. L. M. Hodgkins, LCdr.
- Mejia-Avendano, S., S. V. Duy, et al. (2016). "Generation of Perfluoroalkyl Acids from Aerobic Biotransformation of Quaternary Ammonium Polyfluoroalkyl Surfactants." Environmental Science & Technology **50**(18): 9923-9932.
- Miyake, Y., T. Kobayashi, et al. (2014). "Comparison study on observed and estimated concentrations of perfluorooctane sulfonate using a fate model in Tokyo Bay of Japan." Journal of Environmental Science and Health Part a-Toxic/Hazardous Substances & Environmental Engineering **49**(7): 770-776.
- Moilanen, L. H., B. D. Bagley, et al. (2015). "A Combined 28-Day Oral Toxicity Study of HFPO-Amidol (CASRN 75888-49-2) With Reproductive/Developmental Toxicity Screening Test in Wistar Han Rats." International Journal of Toxicology **34**(6): 514-533.

- Moody, C. A. and J. A. Field (1999). "Determination of perfluorocarboxylates in groundwater impacted by fire-fighting activity." Environmental Science and Technology **33**(16): 2800-2806.
- Moriasi, D. N., J. G. Arnold, et al. (2007). "Model evaluation guidelines for systematic quantification of accuracy in watershed simulations." Transactions of the ASABE **50**(3): 885-900.
- Mulligan, R. P., A. J. Bowen, et al. (2008). "Whitecapping and wave field evolution in a coastal bay." Journal of Geophysical Research-Oceans **113**(C3).
- Mulligan, R. P., A. E. Hay, et al. (2008). "Wave-driven circulation in a coastal bay during the landfall of a hurricane." Journal of Geophysical Research-Oceans **113**(C5).
- Munoz, G., M. Desrosiers, et al. (2017). "Environmental Occurrence of Perfluoroalkyl Acids and Novel Fluorotelomer Surfactants in the Freshwater Fish *Catostomus commersonii* and Sediments Following Firefighting Foam Deployment at the Lac-Mégantic Railway Accident." Environmental Science & Technology **51**(3): 1231-1240.
- Ochoa-Herrera, V. and R. Sierra-Alvarez (2008). "Removal of perfluorinated surfactants by sorption onto granular activated carbon, zeolite and sludge." Chemosphere **72**(10): 1588-1593.
- Olsen, G. W., J. M. Burris, et al. (1999). "Serum perfluorooctane sulfonate and hepatic and lipid clinical chemistry tests in fluorochemical production employees." Journal of Occupational and Environmental Medicine **41**(9): 799-806.
- Ouellette, R., J. P. Farley, et al. (2013). Comparison of Commercial Grade Heptane with Unleaded, Ethanol-Free Gasoline as Fuels for AFFF Qualification Testing under the MIL-F-24385 Protocol - Final Report, Naval Research Laboratory.
- Pabon, M. and J. M. Corpart (2002). "Fluorinated surfactants: synthesis, properties, effluent treatment." Journal of Fluorine Chemistry **114**(2): 149-156.
- Paquin, J. (2014). Treatment of the Contaminated Water after the Lac-Mégantic Disaster. Remediation Technologies Symposium, Banff, Alberta, Canada.
- Pereira, L. A. M., L. F. G. Martins, et al. (2014). "Diffusion Coefficients of Fluorinated Surfactants in Water: Experimental Results and Prediction by Computer Simulation." Journal of Chemical and Engineering Data **59**(10): 3151-3159.
- Perez, F., M. Nadal, et al. (2013). "Accumulation of perfluoroalkyl substances in human tissues." Environment International **59**: 354-362.
- Place, B. J. and J. A. Field (2012). "Identification of Novel Fluorochemicals in Aqueous Film-Forming Foams (AFFF) Used by the US Military." Environmental Science & Technology **46**(13): 7120-7127.
- Place, B. J. and J. A. Field (2012). "Identification of novel fluorochemicals in aqueous film-forming foams used by the US military." Environmental Science and Technology **46**(13): 7120-7127.

- Prevedouros, K., I. T. Cousins, et al. (2006). "Sources, fate and transport of perfluorocarboxylates." *Environmental Science & Technology* **40**(1): 32-44.
- RCN, R. C. N. (2013). "Structure of the RCN." Retrieved 2 October 2017, 2017, from <http://www.navy-marine.forces.gc.ca/en/about/structure-home.page>.
- RCN, R. C. N. (2017). RCN Fleet Poster, Government of Canada.
- Rotander, A., L. M. L. Toms, et al. (2015). "Elevated levels of PFOS and PFHxS in firefighters exposed to aqueous film forming foam (AFFF)." *Environment International* **82**: 28-34.
- Sarty, R. (2017). "Toward a Canadian Naval Service (1867-1914)." Retrieved 2 October 2017, 2017, from <https://www.canada.ca/en/navy/services/history/naval-service-1910-2010/toward.html>.
- Schaefer, T. H., B. Z. Dlugogorski, et al. (2008). "Sealability properties of fluorine-free fire-fighting foams (FfreeF)." *Fire Technology* **44**(3): 297-309.
- Schlummer, M., L. Gruber, et al. (2013). "Detection of fluorotelomer alcohols in indoor environments and their relevance for human exposure." *Environment International* **57-58**: 42-49.
- Seals, R., S. M. Bartell, et al. (2011). "Accumulation and clearance of perfluorooctanoic acid (PFOA) in current and former residents of an exposed community." *Environ Health Perspect* **119**(1): 119-124.
- Shan, S. L. and J. Y. Sheng (2012). "Examination of circulation, flushing time and dispersion in Halifax Harbour of Nova Scotia." *Water Quality Research Journal of Canada* **47**(3-4): 353-374.
- Shan, S. L., J. Y. Sheng, et al. (2011). "Simulating the three-dimensional circulation and hydrography of Halifax Harbour using a multi-nested coastal ocean circulation model." *Ocean Dynamics* **61**(7): 951-976.
- Sherbondy, J. and J. Mickler (2017) "What is Activated Carbon?".
- Thomsen, C., L. S. Haug, et al. (2010). "Changes in Concentrations of Perfluorinated Compounds, Polybrominated Biphenyl Ethers, and Polychlorinated Biphenyls in Norwegian Breast-Milk during Twelve Months of Lactation." *Environmental Science & Technology* **44**(24): 9550-9556.
- Tyco, T. F. P. P. (2015). Ansulite 6% AFFF (AFC-6MS) Safety Data Sheet.
- US EPA, U. S. E. P. A. (2016a). Health Effects Support Document for Perfluorooctane Sulfonate (PFOS). Washington, DC: 245.
- US EPA, U. S. E. P. A. (2016b). Health Effects Support Document for Perfluorooctanoic Acid (PFOA). Washington, DC: 322.
- US EPA, U. S. E. P. A. (2016c). Fact Sheet PFOA and PFOS Drinking Water Health Advisories. U. S. E. P. A. US EPA.

- US EPA, U. S. E. P. A. (2017). "Fact Sheet: 2010/2015 PFOA Stewardship Program." Retrieved 5 September 2017, 2017, from <https://www.epa.gov/assessing-and-managing-chemicals-under-tsca/fact-sheet-20102015-pfoa-stewardship-program>.
- Van Genuchten, M. T. and W. Alves (1982). Analytical solutions of the one-dimensional convective-dispersive solute transport equation, United States Department of Agriculture, Economic Research Service.
- Wang, S. W., J. Huang, et al. (2013). "First Report of a Chinese PFOS Alternative Overlooked for 30 Years: Its Toxicity, Persistence, and Presence in the Environment." Environmental Science & Technology **47**(18): 10163-10170.
- Wang, Z. Y., I. T. Cousins, et al. (2014). "Global emission inventories for C-4-C-14 perfluoroalkyl carboxylic acid (PFCA) homologues from 1951 to 2030, Part I: production and emissions from quantifiable sources." Environment International **70**: 62-75.
- Wang, Z. Y., I. T. Cousins, et al. (2013). "Fluorinated alternatives to long-chain perfluoroalkyl carboxylic acids (PFCAs), perfluoroalkane sulfonic acids (PFSAs) and their potential precursors." Environment International **60**: 242-248.
- Weber, C. C., A. F. Masters, et al. (2013). "Structural features of ionic liquids: consequences for material preparation and organic reactivity." Green Chemistry **15**(10): 2655-2679.
- White, N. D., L. Balthis, et al. (2015). "Elevated levels of perfluoroalkyl substances in estuarine sediments of Charleston, SC." Science of the Total Environment **521**: 79-89.
- Williams, B., T. Murray, et al. (2011). Extinguishment and Burnback Tests of Fluorinated and Fluorine-free Firefighting Foams with and without Film Formation. Suppression, Detection and Signaling Research and Applications - A Technical Working Conference (SUPDET 2011) 22 - 25 March 2011. Orlando, FL.
- Xu, F. M. and W. Perrie (2012). "Extreme Waves and Wave Run-up in Halifax Harbour under Climate Change Scenarios." Atmosphere-Ocean **50**(4): 407-420.
- Yamashita, N., S. Taniyasu, et al. (2008). "Perfluorinated acids as novel chemical tracers of global circulation of ocean waters." Chemosphere **70**(7): 1247-1255.
- Yang, X., J. Huang, et al. (2014). "Stability of 6:2 fluorotelomer sulfonate in advanced oxidation processes: degradation kinetics and pathway." Environmental Science and Pollution Research **21**(6): 4634-4642.
- Yu, J., J. Y. Hu, et al. (2009). "Perfluorooctane sulfonate (PFOS) and perfluorooctanoic acid (PFOA) in sewage treatment plants." Water Research **43**(9): 2399-2408.
- Yu, J., L. Lv, et al. (2012). "Effect of effluent organic matter on the adsorption of perfluorinated compounds onto activated carbon." Journal of Hazardous Materials **225**: 99-106.
- Yu, Q., R. Q. Zhang, et al. (2009). "Sorption of perfluorooctane sulfonate and perfluorooctanoate on activated carbons and resin: Kinetic and isotherm study." Water Research **43**(4): 1150-1158.

Zhang, Y. F., S. Beesoon, et al. (2013). "Biomonitoring of Perfluoroalkyl Acids in Human Urine and Estimates of Biological Half-Life." Environmental Science & Technology **47**(18): 10619-10627.